

# Inside-out cross-covariance for spatial multivariate data

Michele Peruzzi\*

## Abstract

As the spatial features of multivariate data are increasingly central in researchers' applied problems, there is a growing demand for novel spatially-aware methods that are flexible, easily interpretable, and scalable to large data. We develop inside-out cross-covariance (IOX) models for multivariate spatial likelihood-based inference. IOX leads to valid cross-covariance matrix functions which we interpret as inducing spatial dependence on independent replicates of a correlated random vector. The resulting sample cross-covariance matrices are “inside-out” relative to the ubiquitous linear model of coregionalization (LMC). However, unlike LMCs, our methods offer direct marginal inference, easy prior elicitation of covariance parameters, the ability to model outcomes with unequal smoothness, and flexible dimension reduction. As a covariance model for a  $q$ -variate Gaussian process, IOX leads to scalable models for noisy vector data as well as flexible latent models. For large  $n$  cases, IOX complements Vecchia approximations and related process-based methods based on sparse graphical models. We demonstrate superior performance of IOX on synthetic datasets as well as on colorectal cancer proteomics data. An R package implementing the proposed methods is available at [github.com/mkln/spiox](https://github.com/mkln/spiox).

*Keywords:* Gaussian process, co-kriging, dimension reduction, coregionalization, Bayesian hierarchical models.

## 1 Introduction

Multivariate data with spatial dependence are increasingly common in fields such as ecology, environmental science, remote sensing, epidemiology, with growing interest in applying spatially-aware methods to ‘omics’ data, such as proteomics and genomics. Researchers aim to understand how the joint dependence across multiple variables changes as a function of

---

\*Department of Biostatistics, University of Michigan–Ann Arbor.

space. For example, in community ecology, joint species distribution models assume that species interactions are influenced by both their spatial context and the colocation with other species. Similarly, cancer development impacts the spatial arrangement of cells of different types within the tumor microenvironment. In these contexts, we expect multivariate spatial models to uncover deeper insights than univariate or non-spatial multivariate models, but their increased computational cost often limits their practical utility. In fact, any method for multivariate spatial data must balance between flexibility and interpretability with scalability and parsimony. Achieving this balance is particularly difficult when we have a large number of spatially-resolved variables (e.g.,  $q > 10$ ) observed at many spatial sites ( $n$  in the thousands). In such cases, fully flexible methods struggle to scale, whereas dimension reduction techniques can lead to interpretability or performance issues relative to univariate or non-spatial models.

These challenges can be addressed in principle by modeling spatial dependence across multiple variables via a  $q$ -variate Gaussian process (GP). The GP is a flexible probabilistic framework for modeling spatial dependence of vector-valued outcomes. It can also act as a prior process in a Bayesian hierarchical regression for inferring spatial and cross-variable dependence, estimation of exposure effects, and predictions at unobserved locations. A GP is fully specified by its mean and cross-covariance matrix functions. The mean can typically be assumed to be zero or modeled as a separate component of the Bayesian hierarchy, if necessary. Cross-covariance matrix functions vary in terms of parsimony, interpretability, modeling flexibility, parameter identifiability, and computational feasibility, especially in “large  $n$ , large  $q$ ” settings on which we focus. The choice of cross-covariance matrix function thus reflects the challenges we mentioned above. Let  $\mathbf{M}_{q \times q}$  be the set of  $q \times q$  real-valued matrices and  $\mathcal{D} \subset \mathfrak{R}^d$  the spatial domain of dimension  $d$ , then a cross-

covariance matrix function is  $\mathbf{C} : \mathcal{D} \times \mathcal{D} \rightarrow \mathbf{M}_{q \times q}$  such that  $\mathbf{C}(\boldsymbol{\ell}, \boldsymbol{\ell}') = \mathbf{C}(\boldsymbol{\ell}', \boldsymbol{\ell})^\top$  and  $\sum_{i=1}^n \sum_{j=1}^n \mathbf{x}_i^\top \mathbf{C}(\boldsymbol{\ell}_i, \boldsymbol{\ell}_j) \mathbf{x}_j > 0$  for any integer  $n$ , any finite set  $\{\boldsymbol{\ell}_1, \boldsymbol{\ell}_2, \dots, \boldsymbol{\ell}_n\}$ , and for all  $\mathbf{x}_i, \mathbf{x}_j \in \mathbb{R}^q \setminus \{\mathbf{0}\}$ . Then, if  $\{\mathbf{y}(\boldsymbol{\ell}), \boldsymbol{\ell} \in \mathcal{D}\}$  is a  $q$ -variate GP with cross-covariance matrix function  $\mathbf{C}(\cdot, \cdot)$ , the  $(i, j)$ th entry of  $\mathbf{C}(\boldsymbol{\ell}, \boldsymbol{\ell}')$  evaluates to  $C_{ij}(\boldsymbol{\ell}, \boldsymbol{\ell}') = \text{cov}(y_i(\boldsymbol{\ell}), y_j(\boldsymbol{\ell}'))$ . Following [Genton & Kleiber \(2015\)](#), we call  $C_{ii}(\cdot, \cdot)$  the marginal covariance and  $C_{ij}(\cdot, \cdot), i \neq j$  as the cross-covariance functions. Building a cross-covariance matrix function boils down to specifying  $q(q+1)/2$  distinct covariance and cross-covariance functions and establishing the validity of the overall model; both tasks are increasingly difficult as  $q$  grows.

The linear model of coregionalization (LMC, [Matheron 1982](#), [Wackernagel 2003](#), [Schmidt & Gelfand 2003](#), see also [Alie et al. 2024](#)) writes  $C_{ij}(\cdot, \cdot)$  as a linear combination of  $k \leq q \ll q(q+1)/2$  univariate correlation functions, i.e.,  $C_{ij}(\boldsymbol{\ell}, \boldsymbol{\ell}') = \sum_{r=1}^k a_{ir} a_{rj} \rho_r(\boldsymbol{\ell}, \boldsymbol{\ell}')$ . If  $k < q$ , we refer to the LMC as a spatial factor model. The LMC is the most popular cross-covariance model for multivariate data due to its computational tractability: it can be extended to model non-stationarity ([Gelfand et al. 2004](#)), spatially-varying regression coefficients ([Gelfand et al. 2003](#) and [Reich et al. 2010](#), both assuming separability), space-time data ([Berrocal et al. 2010](#), [De Iaco et al. 2019](#)); it can be included as a latent process in Bayesian hierarchies for non-Gaussian data ([Peruzzi & Dunson 2024](#)), used as a dimension reduction tool in the large  $n$ , large  $q$  setting by letting  $k \ll q$  ([Taylor-Rodriguez et al. 2019](#), [Zhang & Banerjee 2022](#)). LMCs and methods based on linear combinations of independent GPs are very popular in many fields (see, e.g., [Teh et al. 2005](#), [Finley et al. 2008](#), [Álvarez & Lawrence 2011](#), [Fricker et al. 2013](#), [Moreno-Muñoz et al. 2018](#), [Liu et al. 2022](#), [Townes & Engelhardt 2023](#)). Statistical software packages for multivariate spatial data typically implement LMCs ([Pebesma 2004](#), [Finley et al. 2015](#), [Tikhonov et al. 2020](#), [Finazzi & Fassò 2014](#), [Krainski et al. 2019](#), [Peruzzi 2022](#)).

The LMC has several major limitations. First, it is inadequate in modeling outcomes with different smoothness because the smoothness of outcome  $j$  is always equal to the smoothness of the roughest of the  $k$  correlation functions (Genton & Kleiber 2015). Second, it is difficult to interpret and assign priors to its parameters, e.g., the spatial range of outcome  $j$  is a non-linear function of all the  $k$  spatial range parameters (Schmidt & Gelfand 2003, Section 3.4). Third, the LMC is inadequate as a model of responses measured with independent measurement errors; “nugget” effects in the constituent processes are linearly combined into correlated noise. One must then use LMCs as priors for latent effects, leading to slower computations even when using scalable alternatives to GPs (Finley et al. 2019). Fourth, LMCs link the number of constituent spatial processes  $k$  to the rank of  $\mathbf{A}\mathbf{A}^\top = \mathbf{C}(\boldsymbol{\ell}, \boldsymbol{\ell})$ ; this is inflexible for outcomes in a community structure that also have distinct spatial features. Further, because LMCs define both  $C_{ii}(\cdot, \cdot)$  and  $C_{ij}(\cdot, \cdot)$ ,  $i \neq j$ , based on the same set of  $k$  functions, a reduction in  $k$  reduces flexibility and expressiveness of both cross- and marginal covariances. Finally, the infill asymptotics of LMCs are poorly understood—it is likely LMCs inherit some inconsistencies of univariate Matérn models (Zhang 2007, Section 6, also see Velandia et al. 2017). In univariate models, we know the functional form of the microergodic parameter, which can be estimated consistently (Stein 1990, Zhang 2004); this option is unavailable to LMCs, leading to possibly large variance of parameter estimates or inefficient posterior sampling in finite samples (Peruzzi et al. 2021). The issues we mentioned greatly reduce the inferential usefulness of LMCs, as one may have to rely on potentially inefficient estimation of parameters with intricate interpretations.

Alternative methods that solve some of the limitations of the LMC include the multivariate Matérn model (Gneiting et al. 2010, see also Apanasovich et al. 2012, Emery et al. 2022, Yarger et al. 2024), approaches based on latent dimensions (Apanasovich & Genton

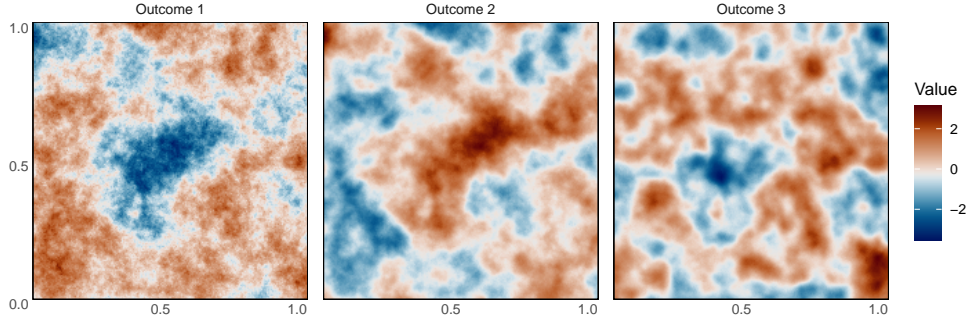


Figure 1: Three spatially correlated outcomes generated via GP-IOX at  $n = 40,000$  gridded locations.

We let  $\sigma_{ii} = 1$  for  $i \in \{1, 2, 3\}$  and  $\sigma_{12} = -0.9, \sigma_{13} = 0.7, \sigma_{23} = -0.5$  and choose  $\rho_i(\cdot, \cdot)$  as Matérn (Vecchia-approximated with  $m = 50$  neighbors) with range  $1/5, 1/15, 1/30$  and smoothness  $0.5, 1.2, 1.9$ , respectively.

2010), and convolution methods (Gaspari & Cohn 1999, Majumdar & Gelfand 2007). However, these methods are only suitable to very small  $q$  as they do not lead to exploitable structure in the sample covariance or facilitate dimension reduction, or require numerical integration for computing  $C_{ij}(\cdot, \cdot)$ . The Appendix includes a more detailed discussion on the multivariate Matérn model. When  $q$  is large, process-level conditional independence may ease the computational burden only when not requiring stochastic exploration of unknown sparse graphs (Dey et al. 2022), and local assumptions on conditional independence across outcomes may be overly restrictive (Peruzzi & Dunson 2022).

In this article, we introduce the Inside-Out Cross-covariance (IOX) model for large  $n$ , large  $q$  data. IOX leads to parsimonious cross-covariance matrix functions defined on the basis of  $q$  univariate correlation functions and a covariance matrix  $\Sigma$ . Dimension reduction using IOX may proceed by clustering the outcomes or via a low-rank assumption on  $\Sigma$ . Intuitively, IOX induces spatial dependence on the margins of a correlated random vector. Our model resolves several major flaws of LMCs: in IOX, there is a 1:1 link between the marginal covariance of the  $j$ th variable and the  $j$ th univariate correlation function used to define it, facilitating prior elicitation and interpretable process-based inference.

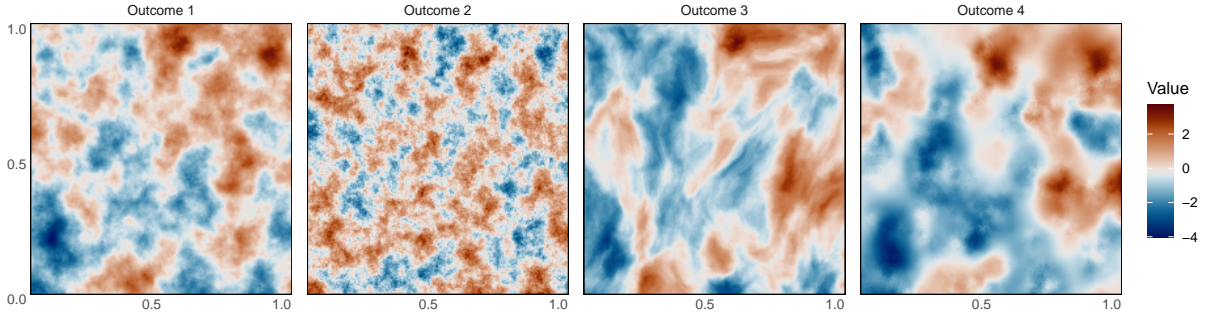


Figure 2: Four spatially correlated outcomes generated via GP-IOX at  $n = 40,000$  gridded locations. Outcomes 1 and 2 have stationary marginal covariances, whereas 3 and 4 are non-stationary.

Furthermore, IOX is flexible in allowing different smoothness, “nugget” effects, or non-stationarity of one or more outcomes. Figure 1 shows a realization of a noise-free GP-IOX where three Matérn outcomes have different smoothness. In Figure 2, we generate four spatially correlated outcomes via IOX; one of them is non-stationary via deformation of the spatial domain as in [Sampson & Guttorp \(1992\)](#), another has a spatially-varying sill. More details about Figure 2 are in the Appendix. Relative to multivariate Matérns, IOX is more flexible in allowing the marginal covariances to be defined freely (e.g., not Matérn), and more scalable because it results in sample covariance matrices whose structure we can exploit for likelihood-based inference in the “large  $n$ , large  $q$ ” scenario. When building IOX using  $q$  stationary Matérn covariances, IOX is more flexible than a parsimonious multivariate Matérn ([Gneiting et al. 2010](#)) because it allows the marginal ranges to be defined freely, and more parsimonious than a general multivariate Matérn because IOX does not directly parametrize the cross-covariances.

Our definition of IOX requires the specification of a fixed set of *reference* locations  $\mathcal{S}$ . As a consequence, our model is non-stationary even when built using  $q$  stationary correlation functions. However, this has minimal practical impact, as IOX is no more complex than other cross-covariance models when  $n$  is large. In these settings, GPs scale poorly and

they must be replaced with scalable alternatives. Vecchia approximations (Vecchia 1988) and related methods based on sparse directed acyclic graphs (DAGs; see, e.g., Datta et al. 2016, Shirota et al. 2019, Quiroz et al. 2021, Peruzzi et al. 2022) have desirable theoretical properties and excellent practical performance (Zhu et al. 2024, Schäfer et al. 2024, Heaton et al. 2019). Several other scalable GPs can be cast as “sparse DAG” methods (Banerjee et al. 2008, 2010, Finley et al. 2009, Katzfuss 2017, Katzfuss & Gong 2019). The main advantage of sparse DAG methods is that they enable process-based inference and can thus be seamlessly embedded into Bayesian hierarchies for added flexibility. Process-based inference using sparse DAGs *always* leads to nonstationary GPs, as one must specify a set  $\mathcal{S}$  when implementing any sparse DAG GP. IOX can simply use the same  $\mathcal{S}$ . As is standard practice in implementing Vecchia-related methods, we choose  $\mathcal{S}$  as the set of observed locations in all our applications.

We outline IOX in Section 2 and prove its validity. We develop the GP-IOX in Section 3 and the related posterior sampling algorithms in Section 4. We show how IOX can be exploited for scalable operations in the “large  $n$ , large  $q$ ” settings of interest in Sections 5 and 6. We conclude with applications and a discussion. Proofs, as well as additional details and comparisons, are available in the Appendix. Software for fitting Bayesian spatial regression models using IOX is available at [github.com/mkln/spiox](https://github.com/mkln/spiox).

## 2 Inside-out cross-covariance

Let the spatial domain  $\mathcal{D} \subset \mathbb{R}^d$  be of dimension  $d$ , typically  $d = 2$  for longitude and latitude or x,y coordinates on an image. Introduce  $q$  univariate correlation functions  $\rho_j(\cdot, \cdot) : \mathcal{D} \times \mathcal{D} \rightarrow \mathbb{R}$ . For example, we may let  $\rho_j(\boldsymbol{\ell}, \boldsymbol{\ell}') = \exp\{-\phi_j \|\boldsymbol{\ell} - \boldsymbol{\ell}'\|\}$  or a more complex Matérn correlation parametrized by vector  $\boldsymbol{\theta}_j$ . Letting  $\boldsymbol{\theta}_j = (\phi_j, \nu_j)$ , the Matérn correlation

function is  $\mathcal{M}_{\nu_j}(\boldsymbol{\ell}, \boldsymbol{\ell}'; \phi_j) = \frac{2^{1-\nu_j}}{\Gamma(\nu_j)} \phi_j^{\nu_j} \|\boldsymbol{\ell} - \boldsymbol{\ell}'\|^{\nu_j} K_{\nu_j}(\phi_j \|\boldsymbol{\ell} - \boldsymbol{\ell}'\|)$  where  $K_{\nu_j}$  is the modified Bessel function of the second kind of order  $\nu_j$ . The inclusion of nuggets is possible, as we discuss later. Suppose  $\mathcal{A} = \{\mathbf{a}_1, \dots, \mathbf{a}_{n_A}\} \subset \mathcal{D}$  and  $\mathcal{B} = \{\mathbf{b}_1, \dots, \mathbf{b}_{n_B}\} \subset \mathcal{D}$ , then we denote as  $\rho_h(\mathcal{A}, \mathcal{B})$  the a  $n_A \times n_B$  matrix whose  $(i, j)$  element is  $\rho_h(\mathbf{a}_i, \mathbf{b}_j)$ , and let  $\rho_h(\mathcal{A}) := \rho_h(\mathcal{A}, \mathcal{A})$  and  $\rho_h(\boldsymbol{\ell}, \mathcal{A}) := \rho_h(\{\boldsymbol{\ell}\}, \mathcal{A})$ . Choose a set of *reference* locations  $\mathcal{S} = \{\boldsymbol{\ell}_1, \dots, \boldsymbol{\ell}_n\} \subset \mathcal{D}$ . In applications, we choose  $\mathcal{S}$  as the sample locations. The set of non-reference locations  $\mathcal{S}^c = \mathcal{D} \setminus \mathcal{S}$  may be thought of as a superset of the prediction locations. We do not make any distributional assumption in this section. After defining our cross-covariance model, we study its properties and prove the validity of the resulting cross-covariance matrix function. All proofs and derivations are in the Appendix.

**Definition 1** (Inside-out cross-covariance). *Let  $\boldsymbol{\Sigma} = (\sigma_{ij})_{i,j=1}^q$  be a non-negative definite matrix,  $\rho_i(\cdot, \cdot)$  for  $i = 1, \dots, q$  and  $\mathcal{S}$  as above. We define the IOX cross-covariance as:*

$$C_{ij}(\boldsymbol{\ell}, \boldsymbol{\ell}') = \sigma_{ij} [\mathbf{h}_i(\boldsymbol{\ell}) \mathbf{L}_i \mathbf{L}_j^\top \mathbf{h}_j(\boldsymbol{\ell}')^\top + \varepsilon(\boldsymbol{\ell}, \boldsymbol{\ell}')], \quad (1)$$

where  $\mathbf{h}_i(\boldsymbol{\ell}) = \rho_i(\boldsymbol{\ell}, \mathcal{S}) \rho_i(\mathcal{S})^{-1}$ ,  $\mathbf{L}_i$  is the lower Cholesky factor of  $\rho_i(\mathcal{S})$ , i.e. it is lower triangular and such that  $\mathbf{L}_i \mathbf{L}_i^\top = \rho_i(\mathcal{S})$ ,  $\varepsilon(\boldsymbol{\ell}, \boldsymbol{\ell}') = \mathbb{1}_{\{\boldsymbol{\ell}=\boldsymbol{\ell}'\}} \sqrt{r_i(\boldsymbol{\ell}) r_j(\boldsymbol{\ell})}$ , and  $r_i(\boldsymbol{\ell}) = \rho_i(\boldsymbol{\ell}, \boldsymbol{\ell}) - \mathbf{h}_i(\boldsymbol{\ell}) \rho_i(\mathcal{S}, \boldsymbol{\ell})$ . We let  $\mathbb{1}_{\{c\}} = 1$  if  $c$  is true, 0 otherwise.

Next, we show that IOX leads to easily interpretable inference and prior elicitation of marginal covariance parameters.

**Proposition 2** (Marginal covariance).

$$C_{ii}(\boldsymbol{\ell}, \boldsymbol{\ell}') = \begin{cases} \sigma_{ii} \rho_i(\boldsymbol{\ell}, \boldsymbol{\ell}') & \text{if } \boldsymbol{\ell} \in \mathcal{S} \text{ or } \boldsymbol{\ell}' \in \mathcal{S} \text{ or } \boldsymbol{\ell} = \boldsymbol{\ell}', \\ \sigma_{ii} \rho_i(\boldsymbol{\ell}, \mathcal{S}) \rho_i(\mathcal{S})^{-1} \rho_i(\mathcal{S}, \boldsymbol{\ell}') & \text{if } \boldsymbol{\ell}, \boldsymbol{\ell}' \in \mathcal{S}^c \text{ and } \boldsymbol{\ell} \neq \boldsymbol{\ell}'. \end{cases}$$

The first case ( $\boldsymbol{\ell} \in \mathcal{S}$  or  $\boldsymbol{\ell}' \in \mathcal{S}$  or  $\boldsymbol{\ell} = \boldsymbol{\ell}'$ ) is the most relevant in practice and motivates our choice of  $\mathcal{S}$  as the observed locations. In fact, by letting  $\mathcal{S}$  correspond to the observed



locations, the tasks of parameter estimation and prediction at new locations will both solely depend on the cross-covariance model when at least one of  $\ell$  or  $\ell'$  are in  $\mathcal{S}$ . In this key scenario, Proposition 2 shows that IOX retains  $\rho_i(\ell, \ell')$  as the marginal covariance for outcome  $i$ . In the residual case  $\ell, \ell' \in \mathcal{S}^c$ , the marginal covariance takes the form of the predictive process (PP) covariance on  $\rho_i(\cdot, \cdot)$  with knots  $\mathcal{S}$  (Banerjee et al. 2008), which is known to approximate  $\rho_i(\cdot, \cdot)$  increasingly well as the size of  $\mathcal{S}$  increases. In any event, for all  $\ell, \ell' \in \mathcal{D}$ ,  $C_{ii}(\cdot, \cdot)$  is a function of  $\rho_i(\cdot, \cdot)$  only, leading to direct interpretation of its parameters. From a Bayesian perspective, Proposition 2 simplifies prior elicitation, as one can take advantage of exploratory tools like variograms to build informative priors.

Next, we study the role of  $\sigma_{ij}$  for  $i \neq j$  and show that two variables have a cross-covariance of  $\sigma_{ij}$  at zero distance if their marginal correlations functions are the same. Otherwise,  $\sigma_{ij}$  bounds the cross-covariance  $C_{ij}(\ell, \ell')$  from above—this behavior also occurs in the multivariate Matérn model due to the necessary validity conditions (refer to the Appendix for more details).

**Proposition 3** (Cross-covariance and  $\sigma_{ij}$ ). *For all  $\ell, \ell' \in \mathcal{D}$  and all  $i, j = 1, \dots, q$ , the cross-covariance is  $C_{ij}(\ell, \ell') \leq \sigma_{ij}$ . If  $\rho_i(\cdot, \cdot) = \rho_j(\cdot, \cdot)$ , then  $C_{ij}(\ell, \ell) = \sigma_{ij}$ .*

$C_{ij}(\cdot, \cdot)$  is non-stationary even when each of the  $\rho_i(\cdot, \cdot)$  are stationary and isotropic due to its dependence on  $\mathcal{S}$ . We showed in Proposition 2 that we can rely on  $\rho_i(\cdot, \cdot)$  and its parameters to interpret  $C_{ii}(\cdot, \cdot)$ . For  $i \neq j$ , we can easily draw interpretable covariance curves by averaging the values of  $C_{ij}(\cdot, \cdot)$  across the spatial domain. In Figure 3, we compute and visualize the scaling factor, i.e.,  $C_{ij}(\cdot, \cdot)/\sigma_{ij}$ , when  $\rho_i(\cdot, \cdot)$  and  $\rho_j(\cdot, \cdot)$  are Matérn. More details are in the Appendix.

We now outline two equivalent definitions of the cross-covariance matrix function of IOX. The first does not involve  $nq \times nq$  matrices, whereas the second facilitates likelihood

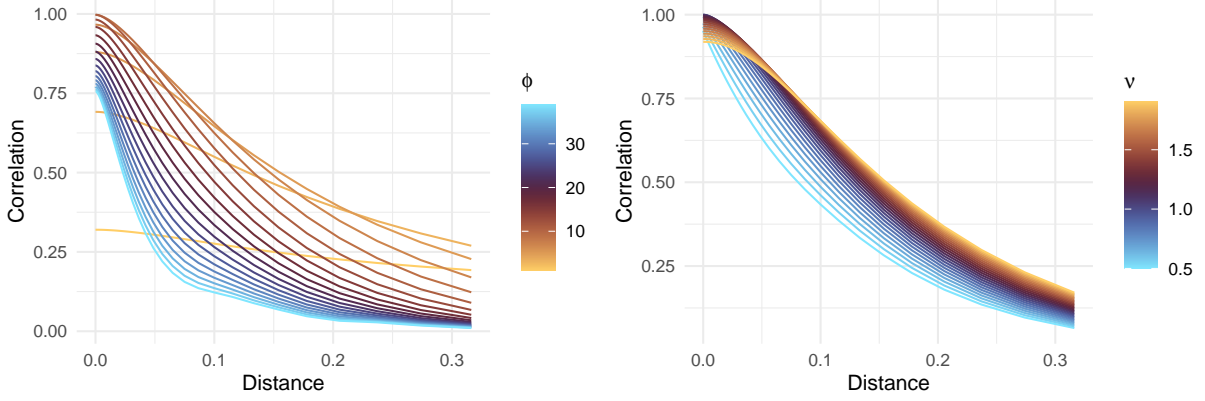


Figure 3: We plot  $C_{ij}(\boldsymbol{\ell}, \boldsymbol{\ell} + \mathbf{h})/\sigma_{ij} = \mathbf{h}_i(\boldsymbol{\ell})\mathbf{L}_i\mathbf{L}_j^\top\mathbf{h}_j(\boldsymbol{\ell} + \mathbf{h})$  for different distance values  $\mathbf{h}$  and taking  $\rho_i(\cdot, \cdot)$  as a Matérn correlation with  $\nu = 1$ ,  $\phi = 10$  and  $\rho_j(\cdot, \cdot)$  as a Matérn with  $\nu = 1$  and varying the values of  $\phi$  (left), or with  $\phi = 10$  and varying the values of  $\nu$  (right), averaged across  $\mathcal{D}$ .

inference. We prove the validity of this cross-covariance matrix function in Proposition 6.

**Proposition 4** (IOX cross-covariance matrix function). *Let  $\boldsymbol{\ell}, \boldsymbol{\ell}' \in \mathcal{S}$ .*

$$\begin{aligned} \mathbf{C}(\boldsymbol{\ell}, \boldsymbol{\ell}') &= \boldsymbol{\Sigma} \odot [\mathbf{K}(\boldsymbol{\ell}, \boldsymbol{\ell}') + \mathbf{d}(\boldsymbol{\ell}, \boldsymbol{\ell}')\mathbf{d}(\boldsymbol{\ell}, \boldsymbol{\ell}')^\top] \\ &= \{\oplus \mathbf{h}_i(\boldsymbol{\ell})\mathbf{L}_i\}(\boldsymbol{\Sigma} \otimes \mathbf{I}_n)\{\oplus \mathbf{L}_i^\top \mathbf{h}_i(\boldsymbol{\ell}')^\top\} + \mathbf{D}(\boldsymbol{\ell}, \boldsymbol{\ell}')\boldsymbol{\Sigma}\mathbf{D}(\boldsymbol{\ell}, \boldsymbol{\ell}'), \end{aligned} \quad (2)$$

where  $\mathbf{K}(\boldsymbol{\ell}, \boldsymbol{\ell}')$  is the  $q \times q$  matrix whose  $i, j$  element is  $\mathbf{h}_i(\boldsymbol{\ell})\mathbf{L}_i\mathbf{L}_j^\top\mathbf{h}_j(\boldsymbol{\ell}')^\top$ ,  $\mathbf{d}(\boldsymbol{\ell}, \boldsymbol{\ell}')$  is a vector of dimension  $q$  whose  $i$ th element is  $\mathbb{1}_{\{\boldsymbol{\ell}=\boldsymbol{\ell}'\}}\sqrt{r_i(\boldsymbol{\ell})}$ ,  $\mathbf{D}(\boldsymbol{\ell}, \boldsymbol{\ell}') = \text{diag}\{\mathbf{d}(\boldsymbol{\ell}, \boldsymbol{\ell}')\}$ , “ $\oplus$ ” is the direct sum operator and we denote  $\{\oplus \mathbf{h}_i(\boldsymbol{\ell})\mathbf{L}_i\}$  as the  $q \times nq$  block-diagonal matrix with  $\mathbf{h}_i(\boldsymbol{\ell})\mathbf{L}_i$  as its  $i$ th block, and “ $\odot$ ” is the Hadamard element-by-element product.

The following corollary specifies the structure of IOX at locations in  $\mathcal{S}$ .

**Corollary 5.** *If  $\boldsymbol{\ell} \in \mathcal{S}$  then  $\mathbf{h}_i(\boldsymbol{\ell})\mathbf{L}_i = \mathbf{L}_i[\boldsymbol{\ell}, :]$ , the row of  $\mathbf{L}_i$  corresponding to  $\boldsymbol{\ell}$ . Then,*

$$\mathbf{C}(\mathcal{S}) = (\boldsymbol{\Sigma} \otimes \mathbf{1}_{n,n}) \odot \mathbf{K} = \{\oplus \mathbf{L}_i\}(\boldsymbol{\Sigma} \otimes \mathbf{I}_n)\{\oplus \mathbf{L}_i^\top\}, \quad (3)$$

where  $\mathbf{K}$  is the  $nq \times nq$  matrix whose  $(i, j)$ th block is  $\mathbf{L}_i\mathbf{L}_j^\top$ ;  $\mathbf{1}_{n,n}$  is the  $n \times n$  matrix of 1s.

A LMC corresponds to  $\mathbf{C}(\mathcal{S}) = (\mathbf{\Lambda} \otimes \mathbf{I}_n)\{\oplus \rho_i(\mathcal{S})\}(\mathbf{\Lambda}^\top \otimes \mathbf{I}_n)$ , where  $\mathbf{\Lambda}\mathbf{\Lambda}^\top = \mathbf{\Sigma}$ . We call our cross-covariance model “inside-out” because it rearranges the way in which spatial and cross-outcome dependence appear in  $\mathbf{C}(\mathcal{S})$  relative to LMCs.

**Proposition 6.**  *$\mathbf{C}(\boldsymbol{\ell}, \boldsymbol{\ell}')$  is a valid cross-covariance matrix function.*

The main take-away of Proposition 6 is that IOX can be built upon any off-the-shelf univariate correlation functions without additional conditions or constraints. This yields flexibility in modeling outcome-specific features such as non-stationarities (as in Figure 2) or covariate dependence. The lack of additional restrictions distinguishes IOX from multivariate Matérns. We provide a more detailed comparison in the Appendix.

We establish a connection between IOX and LMCs in the separable or intrinsic specification, i.e.  $\rho_i(\cdot, \cdot) = \rho(\cdot, \cdot)$  for all  $i$ . Separability is restrictive in forcing all outcomes to be modeled via a the same spatial covariance (with the same range and smoothness).

**Proposition 7.** *In the separable specification, i.e.,  $\rho_i(\cdot, \cdot) = \rho(\cdot, \cdot)$  for all  $i$ , IOX and LMC coincide at  $\mathcal{S}$ .*

Finally, define  $\mathcal{T} = \mathcal{S} \cup \{\boldsymbol{\ell}, \boldsymbol{\ell}'\}$  with  $\boldsymbol{\ell} \neq \boldsymbol{\ell}'$ . The following proposition shows that the Schur complement of  $\mathbf{C}(\mathcal{S})$  in  $\mathbf{C}(\mathcal{T})$  is the zero matrix. If we assume a joint Gaussian distribution for all variables in  $\mathcal{T}$ , then this proposition implies that the observation vectors at  $\boldsymbol{\ell}$  and  $\boldsymbol{\ell}'$  are conditionally independent given their values at  $\mathcal{S}$ .

**Proposition 8.** *Suppose  $\boldsymbol{\ell}, \boldsymbol{\ell}' \in \mathcal{S}^c$ ,  $\boldsymbol{\ell} \neq \boldsymbol{\ell}'$ . Then,  $\mathbf{C}(\boldsymbol{\ell}, \boldsymbol{\ell}') - \mathbf{C}(\boldsymbol{\ell}, \mathcal{S})\mathbf{C}(\mathcal{S})^{-1}\mathbf{C}(\mathcal{S}, \boldsymbol{\ell}') = \mathbf{0}$ .*

Finally, IOX allows outcome-specific nuggets without impacting the validity of the resulting cross-covariance matrix function. We refer to the nugget as the variance of spatially uncorrelated measurement error. Because the measurement error process may be unrelated

to the underlying multivariate spatial process, we seek flexibility in modeling nugget effects independently from other model components. Suppose for each  $j = 1, \dots, q$  we let  $\rho_j(\boldsymbol{\ell}, \boldsymbol{\ell}') = \rho_j^*(\boldsymbol{\ell}, \boldsymbol{\ell}') + \tau_j^2 \mathbb{1}_{\{\boldsymbol{\ell}=\boldsymbol{\ell}'\}}$ . Then, if  $\boldsymbol{\ell} = \boldsymbol{\ell}'$  then  $C_{jj}(\boldsymbol{\ell}, \boldsymbol{\ell}) = \sigma_{jj} + \sigma_{jj}\tau_j^2$ , therefore we directly interpret  $\sigma_{jj}\tau_j^2$  as the nugget term for the  $j$ th variable. The fact that we are defining  $\rho_j(\cdot, \cdot)$  as a covariance function rather than a correlation function has no impact on the validity of the resulting IOX model; in the Appendix, we show that IOX can be defined on the basis of  $q$  univariate covariance functions without compromising the validity of the approach. Because IOX allows outcome-specific nuggets, it is more flexible than a LMC. In a LMC, nuggets are linearly combined into correlated measurement error for the outcomes. In fact, the LMC can be expressed as  $\mathbf{y}(\boldsymbol{\ell}) = \mathbf{A}(\mathbf{v}(\boldsymbol{\ell}) + \boldsymbol{\nu}(\boldsymbol{\ell}))$  where  $\mathbf{v}(\boldsymbol{\ell})$  is the  $k$ -variate spatial GP and  $\boldsymbol{\nu}(\boldsymbol{\ell}) \stackrel{iid}{\sim} N(\mathbf{0}, \mathbf{D}_\nu)$ . Then,  $\mathbf{y}(\boldsymbol{\ell}) = \mathbf{A}\mathbf{v}(\boldsymbol{\ell}) + \mathbf{A}\boldsymbol{\nu}(\boldsymbol{\ell})$  implies that the measurement error has covariance  $\mathbf{A}\mathbf{D}_\nu\mathbf{A}^\top$ , resulting in considerable inflexibility due to its dependence on  $\mathbf{A}$ . A LMC cross-covariance for a prior process in a latent model resolves this problem, but that leads to added computational complexity due to the presence of high-dimensional latent variables.

We have shown that IOX is a valid cross-covariance matrix function. We can define a GP based on it, which we call the GP-IOX. The next section details properties and develops models based on GP-IOX.

### 3 IOX Gaussian process models

We build models for a  $q$ -variate response, either as a GP-IOX, or by letting a GP-IOX be the prior process for latent effects in a Bayesian hierarchical regression. We outline general algorithms for prior and posterior sampling of the models we present, as well as analyze posterior predictive distributions. Throughout this section, we choose  $\mathcal{S} = \{\boldsymbol{\ell}_1, \dots, \boldsymbol{\ell}_n\}$  as

the set of observed locations, and let  $\mathbf{y}_j$  be the  $n \times 1$  vector whose  $i$ th element is  $y_j(\ell_i)$ . We assume the outcomes are aligned and  $\mathbf{Y}$  is a  $n \times q$  matrix with  $(i, j)$  entry  $y_j(\ell_i)$ . We let  $\mathbf{y}_j = (y_j(\ell_1), \dots, y_j(\ell_n))^\top$ ,  $\mathbf{y}(\ell_i) = (y_1(\ell_i), \dots, y_q(\ell_i))^\top$ ,  $\mathbf{y} = \text{vec}(\mathbf{Y}) = (\mathbf{y}_1^\top, \dots, \mathbf{y}_q^\top)^\top$ . Unless otherwise specified, we assume  $\mathbf{y}$  has mean zero for ease of exposition. More in general, we can simply condition on  $\boldsymbol{\beta}$  and work with  $\tilde{\mathbf{y}} = \mathbf{y} - \mathbf{X}_q \boldsymbol{\beta}$ , where after letting  $\mathbf{X}$  be the  $n \times p$  matrix of predictors at the  $n$  observed locations, we denote  $\mathbf{X}_q = \mathbf{I}_q \otimes \mathbf{X}$ . Throughout the article, we denote  $\mathbf{Q} = \boldsymbol{\Sigma}^{-1}$ ,  $\mathbf{v}_j = \mathbf{L}_j^{-1} \mathbf{y}_j$ , and let  $\mathbf{V}$  be the  $n \times q$  matrix whose  $j$ th column is  $\mathbf{v}_j$ .

**Proposition 9** (Log-likelihood of GP-IOX).

$$\log p(\mathbf{y} \mid \boldsymbol{\theta}, \mathbf{Q}) = \text{const} + \frac{n}{2} \log \det(\mathbf{Q}) \sum_{ij} \mathbf{L}_i^{-1}[j, j] - \frac{1}{2} \text{Tr}(\mathbf{V} \mathbf{Q} \mathbf{V}^\top), \quad (4)$$

where  $\mathbf{L}_i^{-1}[j, j]$  is the  $j$ th diagonal element of  $\mathbf{L}_i^{-1}$ .

A consequence of Proposition 9 is that the scalability of IOX to large  $n$  depends on the complexity of computing  $\mathbf{V}$ : for a given  $\mathbf{V}$  and without additional assumptions on  $\mathbf{Q}$ , evaluating (4) scales as  $O(nq^2)$ . Section 5 details how to scalably compute  $\mathbf{V}$ .

IOX also leads to easy-to-evaluate conditional densities  $p(\mathbf{y}_j \mid \mathbf{y}_{j^c}, \boldsymbol{\theta}, \mathbf{Q})$ , where  $j^c = \{1, \dots, q\} \setminus \{j\}$ . We use the following result to develop efficient posterior sampling algorithms in Sections 4.1 and 4.2.

**Proposition 10** (Conditional density).  $p(\mathbf{y}_j \mid \mathbf{y}_{j^c}, \boldsymbol{\theta}, \mathbf{Q}) = N(\mathbf{y}_j; \mathbf{m}_j, \mathbf{M}_j)$ , where  $\mathbf{m}_j = -\mathbf{L}_j \sum_{r \in j^c} \frac{Q_{jr}}{Q_{jj}} \mathbf{v}_r$  and  $\mathbf{M}_j^{-1} = Q_{jj} \rho_j(\mathcal{S})^{-1}$ . Then, we evaluate  $N(\mathbf{y}_j; \mathbf{m}_j, \mathbf{M}_j)$  as:

$$N(\mathbf{y}_j; \mathbf{m}_j, \mathbf{M}_j) \propto \sqrt{|Q_{jj} \rho_j(\mathcal{S})^{-1}|} \exp \left\{ -\frac{1}{2Q_{jj}} \mathbf{Q}_j \cdot \mathbf{V}^\top \mathbf{V} \mathbf{Q}_j^\top \right\}, \quad (5)$$

where  $Q_{jr}$  is the  $(j, r)$ th element and  $\mathbf{Q}_j \cdot$  is the  $j$ th row of  $\mathbf{Q}$ .

### 3.1 Multivariate response model

A response model lets  $\mathbf{y}(\cdot) \sim GP(\mathbf{x}(\ell)^\top \boldsymbol{\beta}, \mathbf{C}(\cdot, \cdot))$ , where  $\mathbf{C}(\cdot, \cdot) = \mathbf{C}(\cdot, \cdot; \boldsymbol{\Sigma}, \boldsymbol{\theta})$  is the IOX cross-covariance matrix function, whose dependence on  $\boldsymbol{\Sigma}, \boldsymbol{\theta}$  we will omit from notation for simplicity. Solely for the purpose of outlining a complete model, we assume a single correlation function equipped with outcome-specific parameters, i.e.  $\rho_i(\cdot, \cdot) = \rho(\cdot, \cdot; \theta_i)$ ,  $i = 1, \dots, q$ , and  $\boldsymbol{\theta} = (\theta_1^\top, \dots, \theta_q^\top)^\top$ . We let  $\mathbf{x}(\ell)$  be a  $pq \times 1$  vector of predictors at  $\ell$  and  $\boldsymbol{\beta}$  the corresponding  $pq \times 1$  vector of linear effects. We assume all outcomes share a common set of  $p$  predictors; the generalization to outcome-specific sets of predictors is straightforward and beyond the scope of this article. The observed data are such that

$$\mathbf{y} \sim N(\mathbf{X}_q \boldsymbol{\beta}, \mathbf{C}), \quad \mathbf{C} = \{\oplus \mathbf{L}_i\}(\boldsymbol{\Sigma} \otimes \mathbf{I}_n)\{\oplus \mathbf{L}_i^\top\}. \quad (6)$$

We specify the prior distributions  $\boldsymbol{\theta} \sim p(\boldsymbol{\theta})$ ,  $\boldsymbol{\Sigma} \sim \mathcal{W}^{-1}(\nu_\Sigma, \boldsymbol{\Psi}^{-1})$ —the inverse Wishart distribution with scale matrix  $\boldsymbol{\Psi}^{-1}$  and  $\nu_\Sigma$  degrees of freedom,  $\boldsymbol{\beta} \sim N(\mathbf{m}_\beta, \mathbf{M}_\beta)$ .

### 3.2 Latent model

Defining  $\mathbf{w}$  as the  $nq \times 1$  vector of latent effects corresponding to  $\mathbf{y}$  and assuming  $\mathbf{w}(\cdot) \sim GP$ -IOX, a latent model for Gaussian data measured with spatially uncorrelated errors is:

$$\begin{aligned} \mathbf{y} &= \mathbf{X}_q \boldsymbol{\beta} + \mathbf{w} + \boldsymbol{\varepsilon}, & \boldsymbol{\varepsilon} &\sim N(\mathbf{0}, \boldsymbol{\Delta} \otimes \mathbf{I}_n), \\ \mathbf{w} &\sim N(\mathbf{0}, \mathbf{C}), & \mathbf{C} &= \{\oplus \mathbf{L}_i\}(\boldsymbol{\Sigma} \otimes \mathbf{I}_n)\{\oplus \mathbf{L}_i^\top\}, \end{aligned} \quad (7)$$

where all parameters that appear in both (6) and (7) can be assigned the same prior distributions, whereas  $\boldsymbol{\Delta}$  is a  $q \times q$  measurement error covariance matrix with  $q(q+1)/2$  free parameters  $\delta_{ij}$ ,  $j = 1, \dots, i$  and  $i = 1, \dots, q$ . Model (7) is more flexible and less parsimonious than a response model, whose nugget is defined on  $q$  terms. To simplify, we assume  $\boldsymbol{\Delta}$  is diagonal, hence  $\mathbf{w}$  captures all cross-outcome dependence as a  $q$ -variate

noise-free GP-IOX. We let the  $i$ th diagonal element of  $\mathbf{\Delta}$  have the prior  $\delta_{ii} \sim \text{inv.G}(a_d, b_d)$ . The latent model can be extended further: in the Appendix, we propose a latent factor model which assumes  $\mathbf{\Sigma}$  is low-rank.

Although (7) has a Gaussian first stage, we can straightforwardly generalize to binomial and negative-binomial data via data augmentation schemes (Albert & Chib 1993, Polson et al. 2013). The discussion above remains useful in more general settings: efficient Hamiltonian Monte Carlo methods that use second order information about the target density have connections with Gibbs sampling of Gaussian models (see Girolami & Calderhead 2011, or Peruzzi & Dunson 2024 for the multivariate spatial setting).

### 3.3 Predictions at new locations

Having chosen  $\mathcal{S}$  as the set of observed locations, let  $\mathcal{T} = \{\mathbf{t}_1, \dots, \mathbf{t}_N\}$  be the test set and denote the  $Nq$ -dimensional vector of predictions as  $\mathbf{y}_{\mathcal{T}}$ . For any multivariate GP with cross-covariance matrix function  $\mathbf{K}(\cdot, \cdot)$ , the conditional distribution of  $\mathbf{y}_{\mathcal{T}}$  given the data  $\mathbf{y}$  and fixing all unknowns is Gaussian, with mean  $\mathbf{K}(\mathcal{T}, \mathcal{S})\mathbf{K}(\mathcal{S})^{-1}\mathbf{y}$  and covariance  $\mathbf{K}(\mathcal{T}) - \mathbf{K}(\mathcal{T}, \mathcal{S})\mathbf{K}(\mathcal{S})^{-1}\mathbf{K}(\mathcal{S}, \mathcal{T})$ . In GP-IOX, Proposition 8 implies that  $\text{cov}(\mathbf{y}(\mathbf{t}_r), \mathbf{y}(\mathbf{t}_s) \mid \mathbf{y}) = 0$  if  $\mathbf{t}_r \neq \mathbf{t}_s$ , i.e.,  $\mathbf{y}(\mathbf{t}_r)$  and  $\mathbf{y}(\mathbf{t}_s)$  are conditionally independent given the data; therefore, we can focus on marginal predictions of the outcome vector at individual locations.

For a new location  $\mathbf{t}$ , let  $\mathbf{H}(\mathbf{t}) = \mathbf{C}(\mathbf{t}, \mathcal{S})\mathbf{C}(\mathcal{S})^{-1}$  and  $\mathbf{R}(\mathbf{t}) = \mathbf{C}(\mathbf{t}) - \mathbf{H}(\mathbf{t})\mathbf{C}(\mathcal{S}, \mathbf{t})$ . Then, in the response model, for every posterior sample of  $\mathbf{\Sigma}, \boldsymbol{\beta}, \boldsymbol{\theta}$  we draw from  $p(\mathbf{y}(\mathbf{t}) \mid \mathbf{y}, \boldsymbol{\beta}, \mathbf{\Sigma}, \boldsymbol{\theta}) = N(\mathbf{m}_y(\mathbf{t}), \mathbf{R}(\mathbf{t}))$  for each  $\mathbf{t} \in \mathcal{T}$ , where  $\mathbf{m}_y(\mathbf{t}) = \mathbf{x}(\mathbf{t})^\top \boldsymbol{\beta} + \mathbf{H}(\mathbf{t})(\mathbf{y} - \mathbf{X}_q \boldsymbol{\beta})$ . In the latent model, for every posterior sample of  $\boldsymbol{\beta}, \mathbf{w}, \mathbf{\Sigma}, \boldsymbol{\theta}, \mathbf{\Delta}$  we sample  $\mathbf{w}_{\mathcal{T}}$  from  $p(\mathbf{w}(\mathbf{t}) \mid \mathbf{w}, \mathbf{\Sigma}) = N(\mathbf{m}_w(\mathbf{t}), \mathbf{R}(\mathbf{t}))$ , where  $\mathbf{m}_w(\mathbf{t}) = \mathbf{H}(\mathbf{t})\mathbf{w}$ , then let  $\mathbf{y}(\mathbf{t}) = \mathbf{x}^\top(\mathbf{t})\boldsymbol{\beta} + \mathbf{w}(\mathbf{t}) + \mathbf{\Delta}^{\frac{1}{2}}\mathbf{u}$  where  $\mathbf{u} \sim N(\mathbf{0}, \mathbf{I}_q)$ . The following proposition clarifies that IOX maintains for predictions

the same marginal structure we outlined in Proposition 2; spatial cross-variable dependence in predictions is induced by the off-diagonal elements of  $\mathbf{R}(\mathbf{t})$ .

**Proposition 11.**  $\mathbf{H}(\mathbf{t}) = \{\oplus \mathbf{h}_i(\mathbf{t})\}$  and  $\mathbf{R}(\mathbf{t}) = \mathbf{D}(\mathbf{t}, \mathbf{t})\boldsymbol{\Sigma}\mathbf{D}(\mathbf{t}, \mathbf{t})$ . Therefore, marginal predictions for outcome  $i$  only depend on  $\rho_i(\cdot, \cdot)$  at  $\mathcal{S}$ , and  $\sigma_{ii}$ .

We now consider a setting in which the test set includes partly observed locations. Suppose  $m \subset \{1, \dots, q\}$  is the set of outcomes that are missing at  $\mathbf{t}$ , and  $o$  (for *observed*) its complement. We predict the missing outcomes at  $\mathbf{t}$  by computing  $p(\mathbf{y}_m(\mathbf{t}) \mid \mathbf{y}_o(\mathbf{t}), \mathbf{y})$ .

**Proposition 12.**  $p(\mathbf{y}_m(\mathbf{t}) \mid \mathbf{y}_o(\mathbf{t}), \mathbf{y}) = N(\mathbf{y}_m(\mathbf{t}); \mathbf{h}_{m|o}, \mathbf{R}_{m|o}(\mathbf{t}))$ , where  $\mathbf{h}_{m|o} = \mathbf{H}_m(\mathbf{t})\mathbf{y} + \mathbf{H}_{m|o}(\mathbf{t})(\mathbf{y}_o(\mathbf{t}) - \mathbf{H}_o(\mathbf{t})\mathbf{y})$ ,  $\mathbf{H}_o(\mathbf{t})$  is the submatrix of  $\mathbf{H}(\mathbf{t})$  where we take the rows corresponding to  $o$  (similarly  $\mathbf{H}_m(\mathbf{t})$  with rows  $m$ ), and

$$\mathbf{H}_{m|o}(\mathbf{t}) = \mathbf{D}_m(\mathbf{t}, \mathbf{t})\boldsymbol{\Sigma}_{m,o}\boldsymbol{\Sigma}_o^{-1}\mathbf{D}_o^{-1}(\mathbf{t}, \mathbf{t}) = -\mathbf{D}_m(\mathbf{t}, \mathbf{t})\mathbf{Q}_m^{-1}\mathbf{Q}_{m,o}\mathbf{D}_o^{-1}(\mathbf{t}, \mathbf{t})$$

$$\mathbf{R}_{m|o}(\mathbf{t}) = \mathbf{D}_m(\mathbf{t}, \mathbf{t})(\boldsymbol{\Sigma}_m - \boldsymbol{\Sigma}_{m,o}\boldsymbol{\Sigma}_o^{-1}\boldsymbol{\Sigma}_{o,m})\mathbf{D}_m(\mathbf{t}, \mathbf{t}) = \mathbf{D}_m(\mathbf{t}, \mathbf{t})\mathbf{Q}_m^{-1}\mathbf{D}_m(\mathbf{t}, \mathbf{t}),$$

where  $\boldsymbol{\Sigma}_{m,o}$  subsets  $\boldsymbol{\Sigma}$  to its  $m$  rows and  $o$  columns, and similarly for  $\mathbf{Q}$ .

In particular, if  $m = \{j\}$ ,  $\mathbf{R}_{m|o}(\mathbf{t}) = \frac{r_j(\mathbf{t})}{Q_{jj}}$ . In other terms, the predictive variance at an unobserved location when conditioning on all outcomes except  $j$  decreases if  $\mathbf{t}$  is close to  $\mathcal{S}$  based on  $\rho_j(\cdot, \cdot)$ , or when the other variables “explain” the  $j$ th variable (large  $Q_{jj}$ ).

## 4 Computations with GP-IOX models

We outline the key details of posterior sampling for GP-IOX. Additional details, as well as methods for prior sampling of GP-IOX, are in the Appendix.



## 4.1 Posterior sampling of the multivariate response model

We target the posterior distribution  $p(\boldsymbol{\Sigma}, \boldsymbol{\beta}, \boldsymbol{\theta} \mid \mathbf{y}) \propto p(\mathbf{y} \mid \boldsymbol{\Sigma}, \boldsymbol{\beta}, \boldsymbol{\theta})p(\boldsymbol{\Sigma})p(\boldsymbol{\theta})p(\boldsymbol{\beta})$ . The sampling algorithm detailed in the Appendix is straightforward:  $p(\boldsymbol{\beta} \mid \mathbf{y}, \boldsymbol{\Sigma}, \boldsymbol{\theta})$  is Gaussian;  $p(\boldsymbol{\Sigma} \mid \mathbf{y}, \boldsymbol{\beta}, \boldsymbol{\theta})$  is inverse Wishart;  $\boldsymbol{\theta}$  is updated via Metropolis-Hastings. There is a computational bottleneck in updating  $\boldsymbol{\theta}$ . A joint update targets  $p(\boldsymbol{\theta} \mid \mathbf{y}, \boldsymbol{\beta}, \boldsymbol{\Sigma}) \propto p(\mathbf{y} \mid \boldsymbol{\theta}, \boldsymbol{\beta}, \boldsymbol{\Sigma})p(\boldsymbol{\theta})$ , which we can evaluate using Proposition 9. A block update of  $\boldsymbol{\theta}_j$ —the marginal correlation parameters for outcome  $j$ —targets  $p(\boldsymbol{\theta}_j \mid \boldsymbol{\theta}_{j^c}, \mathbf{y})$ . We assume independent prior  $p(\boldsymbol{\theta}) = \prod_j p(\boldsymbol{\theta}_j)$ , then (omitting other model parameters for simplicity) we find

$$p(\boldsymbol{\theta}_j \mid \boldsymbol{\theta}_{j^c}, \mathbf{y}) \propto p(\mathbf{y} \mid \boldsymbol{\theta}_j, \boldsymbol{\theta}_{j^c})p(\boldsymbol{\theta}_j \mid \boldsymbol{\theta}_{j^c}) = p(\mathbf{y}_j \mid \mathbf{y}_{j^c}, \boldsymbol{\theta})p(\mathbf{y}_{j^c} \mid \boldsymbol{\theta})p(\boldsymbol{\theta}_j) \propto p(\mathbf{y}_j \mid \mathbf{y}_{j^c}, \boldsymbol{\theta})p(\boldsymbol{\theta}_j),$$

where we evaluate  $p(\mathbf{y}_j \mid \mathbf{y}_{j^c}, \boldsymbol{\theta})$  via Proposition 10. We use joint updates of  $\boldsymbol{\theta}$  when using dimension reduction via clustering or when  $q$  is small (Sections 6 and 7.1, respectively), and block updates in all other settings.

## 4.2 Posterior sampling of the latent model

We sample from the joint posterior  $p(\mathbf{w}, \boldsymbol{\beta}, \boldsymbol{\Sigma}, \boldsymbol{\Delta}, \boldsymbol{\theta} \mid \mathbf{y})$  by iterating through all full conditional distributions. In particular, the full conditional posterior distribution of  $\mathbf{w}$  is  $p(\mathbf{w} \mid \mathbf{y}, \boldsymbol{\beta}, \boldsymbol{\Sigma}, \boldsymbol{\Delta}, \boldsymbol{\theta}) = N(\mathbf{m}_{w|y}, \mathbf{M}_{w|y})$ , where

$$\mathbf{M}_{w|y}^{-1} = \mathbf{C}^{-1} + (\boldsymbol{\Delta}^{-1} \otimes \mathbf{I}_n) \quad \text{and} \quad \mathbf{M}_{w|y}^{-1} \mathbf{m}_{w|y} = (\boldsymbol{\Delta}^{-1} \otimes \mathbf{I}_n)(\mathbf{y} - \mathbf{X}_q \boldsymbol{\beta}),$$

which requires to solve a linear system on  $\mathbf{M}_{w|y}^{-1}$  to compute  $\mathbf{m}_{w|y}$ ; this operation is costly since  $\mathbf{M}_{w|y}^{-1}$  has dimension  $nq \times nq$ . Alternatively, we can update  $\mathbf{w}_j$  given  $\mathbf{w}_{j^c}$  and the data for a sequential single-outcome sampler: we write the hierarchical model as

$$\mathbf{w}_j \mid \mathbf{w}_{j^c} \sim N(\mathbf{m}_j, \mathbf{M}_j), \quad \mathbf{y}_j = \mathbf{X} \boldsymbol{\beta}_j + \mathbf{w}_j + \boldsymbol{\varepsilon}_j, \quad \boldsymbol{\varepsilon}_j \sim N(\mathbf{0}, \delta_{jj} \mathbf{I}_n),$$

where  $\mathbf{M}_j$  and  $\mathbf{m}_j$  are the same as in Proposition 10, except we replace  $\mathbf{y}$  with  $\mathbf{w}$ . Then, we update  $\mathbf{w}_j$  via its conditional posterior  $N(\mathbf{w}_j; \mathbf{m}_{w_j|y_j}, \mathbf{M}_{w_j|y_j})$ , where  $\mathbf{M}_{w_j|y_j} = (\mathbf{M}_j^{-1} + \frac{1}{\delta_{jj}} \mathbf{I}_n)^{-1}$  and  $\mathbf{M}_{w_j|y_j}^{-1} \mathbf{m}_{w_j|y_j} = \mathbf{M}_j^{-1} \mathbf{m}_j + \frac{1}{\delta_{jj}} (\mathbf{y}_j - \mathbf{X} \boldsymbol{\beta}_j)$ . We compute  $\mathbf{M}_j^{-1} \mathbf{m}_j$  directly as

$$\mathbf{M}_j^{-1} \mathbf{m}_j = \mathbf{Q}_{jj} \mathbf{L}_j^{-\top} \widetilde{\mathbf{W}}_{j^c} \boldsymbol{\Sigma}_{j^c}^{-1} \boldsymbol{\Sigma}_{j^c, j} = -\mathbf{L}_j^{-\top} \widetilde{\mathbf{W}}_{j^c} \mathbf{Q}_{j^c, j},$$

where  $\widetilde{\mathbf{W}}_{j^c}$  is the  $n \times q - 1$  matrix such that  $\text{vec}\{\widetilde{\mathbf{W}}_{j^c}\} = \{\oplus_{j^c} \mathbf{L}_r^{-1}\} \mathbf{w}_{j^c}$ . The bottleneck here is computing the conditional covariances  $\mathbf{M}_{w_j|y_j}$  (i.e., solving the linear system  $\mathbf{M}_{w_j|y_j}^{-1} \mathbf{x} = \mathbf{b}$ ), but each of them can be computed efficiently in parallel – for large  $n$ , we use the methods of Section 5. The sequential portion of the algorithm is the computation of  $\mathbf{M}_j^{-1} \mathbf{m}_j$  and subsequent sampling of  $\mathbf{w}_j$ . The remainder of our posterior sampling algorithm requires to sample  $\boldsymbol{\beta}$  from its Gaussian full conditional posterior distribution, whereas  $\boldsymbol{\Sigma}$  is conditionally sampled from an inverse Wishart distribution and the diagonal elements of  $\boldsymbol{\Delta}$  from an inverse Gamma distribution. Updating  $\boldsymbol{\theta}$  proceeds like in the response model after replacing  $\mathbf{y}$  with  $\mathbf{w}$ . Additional details are in the Appendix, which also includes the single-site sampler for updating  $\mathbf{w}(\ell_i)$  given  $\mathbf{w}(\mathcal{S} \setminus \{\ell_i\})$ .

## 5 Scaling IOX to large $n$

Computing  $\mathbf{L}_i$  or  $\mathbf{L}_i^{-1}$  for each  $i = 1, \dots, q$  from  $\rho_i(\mathcal{S})$  is prohibitively costly when  $n$  is in the thousands and we have dozens of outcomes. We construct GP-IOX methods based on Vecchia approximations and sparse DAGs, resulting in fast likelihood-based inference.

Suppose  $p(\mathbf{z})$  is the joint density of a  $n \times 1$  vector  $\mathbf{z}$  at locations  $\mathcal{S} = \{\ell_1, \dots, \ell_n\}$ . Vecchia (1988) proposed the approximation  $p(\mathbf{z}) \approx \prod_i p(z_i | \mathbf{z}_{N_m(i)})$ , where  $\mathbf{z}_{N_m(i)}$  is the subset of  $\mathbf{z}$  at the  $m$  locations closest to  $\ell_i$  within the set  $\{\ell_1, \dots, \ell_{i-1}\}$ . This approximation yields a valid standalone stochastic process that satisfies Kolmogorov’s consistency

conditions by assuming conditional independence at all other locations (Datta et al. 2016). More in general, we can define new scalable GPs based on sparsity assumptions of an underlying directed acyclic graph (DAG)—there are several ways to do so (see, e.g., Katzfuss & Guinness 2021, Peruzzi et al. 2022, Zheng et al. 2023, Jin et al. 2024). We can understand these scalable GPs in two manners. First, they are approximations of a parent GP with correlation function  $\rho(\cdot, \cdot)$ . Equivalently, they are exact GPs with correlation function  $\tilde{\rho}(\cdot, \cdot)$ . Since each  $\tilde{\rho}_i(\cdot, \cdot)$  is a valid correlation function, we can build IOX and the corresponding GP-IOX using  $\tilde{\rho}_i(\cdot, \cdot)$ . By Proposition 6, the resulting IOX cross-covariance matrix function inherits its validity from the validity of each  $\tilde{\rho}(\cdot, \cdot)$ .

By construction, the Vecchia correlation function  $\tilde{\rho}(\cdot, \cdot)$  leads to  $\tilde{\rho}(\mathcal{S}) = \tilde{\mathbf{L}}\tilde{\mathbf{L}}^\top = (\mathbf{I}_n - \mathbf{H})^{-1}\mathbf{R}^{\frac{1}{2}}\mathbf{R}^{\frac{1}{2}}(\mathbf{I}_n - \mathbf{H})^{-\top}$ , where  $\mathbf{H}$  is a lower triangular  $n \times n$  matrix with zero diagonal whose  $(i, j)$  entry is nonzero if and only if  $j \rightarrow i$  in the DAG. Letting  $[i]$  be the set of indices of the non-zero columns of  $\mathbf{H}$  at row  $i$ , the nonzeros at row  $i$  are  $\mathbf{h}_i = \rho(\boldsymbol{\ell}_i, \boldsymbol{\ell}_{[i]})\rho(\boldsymbol{\ell}_{[i]})^{-1}$ , i.e., the value of  $\mathbf{H}$  at  $(i, [i]_r)$  is the  $r$ th element of  $\mathbf{h}_i$ . Building  $\mathbf{H}$  and  $\tilde{\mathbf{L}}^{-1} = \mathbf{R}^{-\frac{1}{2}}(\mathbf{I}_n - \mathbf{H})$  requires  $O(nm^3)$  flops. The posterior sampling algorithms we outlined in Sections 3.1 and 3.2 only involve  $\mathbf{L}_i^{-1}$  for  $i = 1, \dots, q$ , therefore they scale to large  $n$  when using  $\tilde{\mathbf{L}}_i^{-1}$ . Both response and latent models benefit from these methods in evaluating the likelihood for updating  $\boldsymbol{\theta}$  (either the joint of (4) or the conditional of (5)). As for sampling  $\mathbf{w}$ , we can take advantage of the sparse DAG and the resulting small Markov blankets of its nodes to develop a single-site sampler (available in the Appendix).

Finally, if some outcomes require conditioning sets that include locations farther in space (Stein et al. 2004), one just needs to choose the appropriate outcome-specific DAG and build  $\tilde{\mathbf{L}}_i$  accordingly for each  $i = 1, \dots, q$ . Doing so in LMCs is not as straightforward because a factor-specific DAG does not translate to the same DAG for any of the outcomes.

## 6 Clusters of correlation functions for the large $q$ case

If  $q$  is large, computing and storing  $\mathbf{L}_i$  for each  $i = 1, \dots, q$  becomes computationally intensive, even with scalable sparse DAG methods as in Section 5. Additionally, the dimension of  $\boldsymbol{\theta}$  increases with  $q$  and joint updates of  $\boldsymbol{\theta}$  (say, for an adaptive Metropolis step) become increasingly complex, with likely loss of efficiency. We propose a method of dimension reduction for IOX models. Suppose we choose the parameters of each correlation function from a small set of options, i.e., let  $\Theta_{k_1} = \{\boldsymbol{\theta}_1, \dots, \boldsymbol{\theta}_{k_1}\}$  and  $\rho_i(\cdot, \cdot) = \rho(\cdot, \cdot; \boldsymbol{\theta}_{\pi(i)})$  where  $\pi(i) \in \{1, \dots, k_1\}$  maps each outcome with a correlation function. Outcomes are thus clustered into groups based on whether or not they share the same marginal correlation function. A priori, we may assume independent uniform priors for each cluster assignment  $\pi(i)$ . The GP-IOX of Section 3.1 expands into a hierarchy

$$\begin{aligned} \boldsymbol{\theta}_j &\propto p(\boldsymbol{\theta}_j), \quad j = 1, \dots, k_1, & \mathbf{\Pi} &= \{\pi(1), \dots, \pi(q)\}, & p(\mathbf{\Pi}) &\propto 1, \\ \mathbf{y} &\sim N(\mathbf{X}_q \boldsymbol{\beta}, \mathbf{C}_\pi) \quad \text{where} \quad \mathbf{C}_\pi &= \{\oplus \mathbf{L}_{\pi(i)}\} (\boldsymbol{\Sigma} \otimes \mathbf{I}_n) \{\oplus \mathbf{L}_{\pi(i)}^\top\}. \end{aligned} \tag{8}$$

Gibbs updates for  $\boldsymbol{\Sigma}$ ,  $\boldsymbol{\beta}$  are unchanged from Section 3.1. Conditional on  $\mathbf{\Pi}$ , the update for  $\boldsymbol{\theta}$  has the same target density but simplifies due to the dimension reduction from  $q$  to  $k_1$ . Updating  $\mathbf{\Pi}$  proceeds sequentially element-by-element via Gibbs steps: we update  $\pi(j)$  conditional on the other cluster assignments  $\mathbf{\Pi}_{-j} = \mathbf{\Pi} \setminus \{\pi(j)\}$  by evaluating the conditional posterior at each of the  $k_1$  options in  $\Theta$ , then sample from the resulting discrete probability mass function. With this approach, one only ever needs to build  $k_1$  inverse Cholesky factors, rather than  $q$ . We label this method as *IOX Cluster* in Section 7.

An even simpler option for (8) is to fix  $\boldsymbol{\theta}_j$ ,  $j = 1, \dots, k_1$  (i.e., assign  $\boldsymbol{\theta}_j$  a discrete prior with known hyperparameters). Intuitively, each outcome is associated to one of  $k_1$  possible values from a fixed “menu” or grid of options. Even if  $k_1$  is large, we compute all possible  $\mathbf{L}_i$  (or  $\mathbf{L}_i^{-1}$ ) only once, rather than at each MCMC iteration, yielding substantial compu-

tational savings. Choosing the correlation hyperparameters from a fixed grid is common in cross-validated approaches, see, e.g., [Shirota et al. \(2019\)](#), [Zhang et al. \(2021\)](#), [Zhang & Banerjee \(2022\)](#). Translating (8) for the latent model of Section 3.2 is straightforward. We refer to this method as *IOX Grid* in Section 7.

## 7 Applications

We test the performance of GP-IOX in three settings: first, we consider simulated datasets with  $q = 3$  outcomes to compare IOX to state-of-the-art methods for fitting multivariate Matérn models. Then, we increase the number of outcomes to  $q = 24$  in order to showcase the performance of IOX and related dimension reduction methods in higher dimensional settings. Finally, we analyze a spatial proteomics dataset collected as part of a colorectal cancer study.

### 7.1 Toy examples on trivariate data

We analyze two scenarios. First, we sample from GP-IOX with Matérn margins, whereas in the second, we sample from a GP with multivariate Matérn cross-covariance. When we build IOX with univariate Matérn margins, the marginal covariance parameters of both IOX and multivariate Matérn models have the same interpretations. Therefore, we can cross-test the performance of IOX in estimating marginal parameters of multivariate Matérns, and, viceversa, the performance of a multivariate Matérn model in estimating marginal parameters of a IOX with Matérn margins. We include a LMC for completeness.

We repeat the same analysis on 60 datasets for each scenario, for a total of 120 datasets. Each dataset measures three outcomes at a different set of 2,500 spatial locations which are sampled uniformly on  $[0, 1]^2$ . In all 120 datasets, we let  $\Sigma$  be a correlation matrix

with off-diagonal entries  $\sigma_{12} = -0.9, \sigma_{13} = 0.7, \sigma_{23} = -0.5$ . The decay, smoothness, and nugget parameters of the three outcomes are set as  $\phi_1 = \phi_2 = \phi_3 = 30, \nu_1 = 0.5, \nu_2 = 0.8, \nu_3 = 1.2$ , and  $\tau_1^2 = \tau_2^2 = \tau_3^2 = 10^{-3}$ . No other parameters are necessary for IOX datasets. For the multivariate Matérn, we let the cross-variable decay be fixed at  $\phi_{ij} = 30$  and the smoothness as  $\nu_{ij} = \frac{\nu_i + \nu_j}{2}$  for all  $i, j$  and we fix the cross-variable nuggets at  $\tau_{ij}^2 = 10^{-3}$  for all  $i, j$ , resulting in a parsimonious Matérn specification as in [Gneiting et al. \(2010\)](#). We evaluate the performance in estimating the marginal parameters as well as the cross-correlations at zero distance  $\rho_{ij}$ , which are computed in the multivariate Matérn cases as  $\rho_{ij} = \sigma_{ij} \frac{\sqrt{\Gamma(\nu_i+1)}}{\sqrt{\Gamma(\nu_i)}} \frac{\sqrt{\Gamma(\nu_j+1)}}{\sqrt{\Gamma(\nu_j)}} \frac{\Gamma(\nu_i/2 + \nu_j/2)}{\Gamma(\nu_i/2 + \nu_j/2 + 1)}$ , whereas in the IOX cases we average the values of  $C_{ij}(\mathbf{0})$  at each observed location to compute the resulting scaling factor (the Appendix details this procedure for interpreting  $C_{ij}$ ). In LMCs the cross-correlation at zero is  $\mathbf{D}_S^{-1} \boldsymbol{\Sigma} \mathbf{D}_S^{-1}$ , where  $\boldsymbol{\Sigma} = \mathbf{A} \mathbf{A}^\top + \mathbf{I}_q$ ,  $\mathbf{D}_s = \text{diag}\{\sqrt{\boldsymbol{\Sigma}_{jj}}\}$ , and  $\mathbf{A}$  is the loadings matrix.

We fit a IOX response model with joint updates of  $\boldsymbol{\theta}$  (Section 4.1) and test both the single-outcome sampler (Section 4.2) and single-site sampler (Appendix) for the latent model in Section 3.2. All IOX models use a Vecchia approximation with  $m = 15$  neighbors for scalability. A Vecchia-approximated ( $m = 15$ ) multivariate Matérn model, as in [Emery et al. \(2022\)](#), is fit via maximum likelihood using `GpGpm` v0.4.0 ([Fahmy & Guinness 2022](#)), available on Github. Posterior sampling for the LMC is performed with the `meshed` R package ([Peruzzi 2022](#)), available on CRAN. Table 1 reports the root mean squared error (RMSE) for parameter estimation (averaged across datasets) and average wall clock time for model fitting. Timing refers to maximum likelihood for the Matérn model and a 10,000-iteration MCMC chain for all others. The LMC model does not estimate outcome-specific spatial decay or smoothness, leaving those table cells blank.

Models based on GP-IOX outperform others in the estimation of all parameters in

IOX data	$\rho_{21}$	$\rho_{31}$	$\rho_{32}$	$\nu_1$	$\nu_2$	$\nu_3$	$\phi_1$	$\phi_2$	$\phi_3$	$\tau_1^2$	$\tau_2^2$	$\tau_3^2$	Time
IOX Response	<b>0.0045</b>	0.0208	0.0188	0.1100	0.0335	<b>0.0474</b>	<b>2.89</b>	<b>2.01</b>	<b>2.28</b>	0.0089	0.0007	<b>0.0005</b>	12
IOX Latent Sequential single-site	0.0065	<b>0.0198</b>	0.0187	0.0803	0.0293	0.0836	3.25	2.11	3.90	0.0013	<b>0.0004</b>	<b>0.0005</b>	22
IOX Latent Sequential single-outcome	0.0058	0.0197	<b>0.0184</b>	<b>0.0763</b>	<b>0.0285</b>	0.0842	3.36	2.13	3.87	<b>0.0006</b>	0.0005	<b>0.0005</b>	41
Mult. Matérn	0.0098	0.0246	0.0226	0.1170	0.0620	0.0616	7.53	3.31	2.32	0.0209	0.0026	0.0006	3
LMC	0.0936	0.3510	0.4020							0.0252	0.0025	0.0020	13

Mult. Matérn data	$\rho_{21}$	$\rho_{31}$	$\rho_{32}$	$\nu_1$	$\nu_2$	$\nu_3$	$\phi_1$	$\phi_2$	$\phi_3$	$\tau_1^2$	$\tau_2^2$	$\tau_3^2$	Time
IOX Response	0.0228	0.0533	0.0506	0.1030	0.0465	0.0539	<b>2.84</b>	<b>2.23</b>	2.21	0.0219	0.0016	0.0009	11
IOX Latent Sequential single-site	0.0100	0.0431	0.0440	0.0351	0.0462	0.0998	3.92	2.34	3.45	0.0056	0.0002	<b>0.0004</b>	21
IOX Latent Sequential single-outcome	0.0129	0.0452	0.0454	<b>0.0258</b>	0.0551	0.1050	4.29	2.53	3.43	<b>0.0037</b>	<b>0.0001</b>	<b>0.0004</b>	40
Mult. Matérn	<b>0.0074</b>	<b>0.0180</b>	<b>0.0234</b>	0.0527	<b>0.0436</b>	<b>0.0473</b>	4.03	2.92	<b>2.10</b>	0.0109	0.0013	<b>0.0004</b>	3
LMC	0.0643	0.3450	0.3920							0.0269	0.0032	0.0024	12

Table 1: Average RMSE and time in minutes for estimating model parameters across 60 IOX-generated datasets (top) and 60 multivariate Matérn-generated datasets (bottom). Lowest RMSEs in bold.

the IOX data scenario and are competitive in the multivariate Matérn scenario, achieving very similar when not better performance than the correctly specified multivariate Matérn model. The LMC lacks the flexibility in modeling these data, resulting in inferior performance in estimating the cross-correlation at zero.

## 7.2 Comparisons on spatial data with 24 outcomes

We move to the much more challenging problem of fitting multivariate models on data with  $q = 24$  spatially correlated outcomes. We simulate 40 datasets, each of which includes synthetic data at a different set of  $n = 2,500$  spatial locations distributed uniformly on  $[0, 1]^2$ . The effective dimension of each dataset is  $nq = 60,000$ . Of the 40 datasets, we generate 20 by sampling from a GP-IOX such that the  $j$ th variable has Matérn marginal correlation with range  $\phi_j = 30$ , nugget parameter  $\tau_j^2 = 10^{-3}$ ; we sample  $\nu_j$  independently

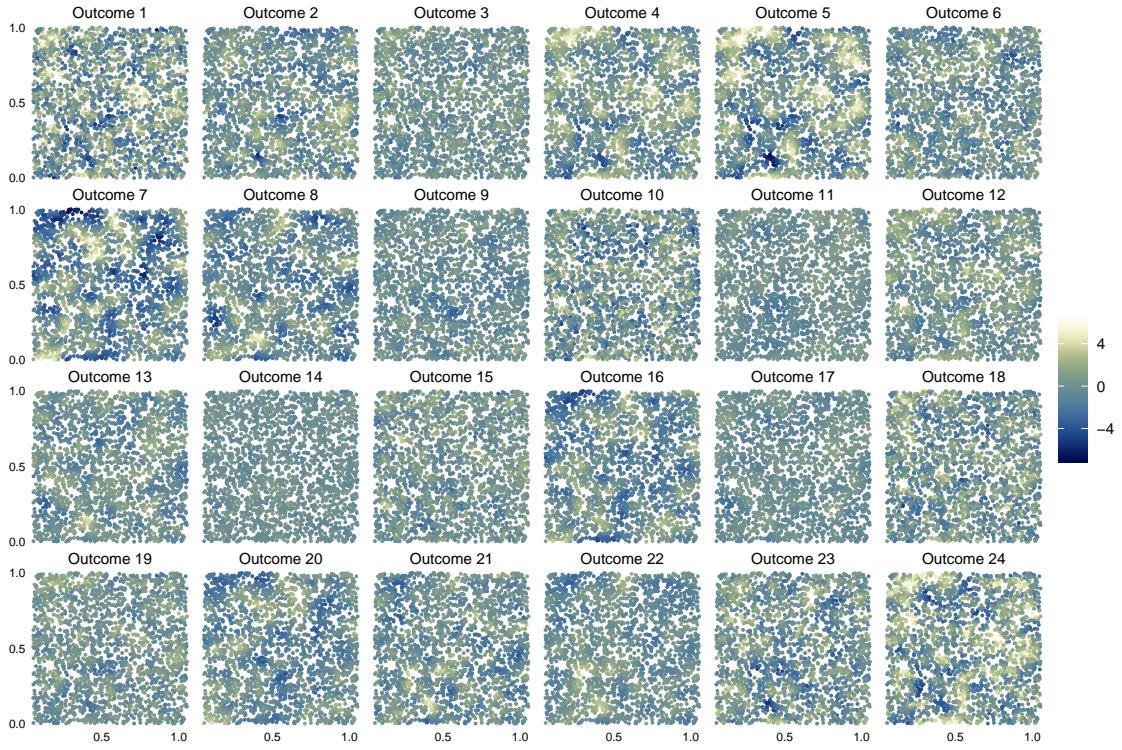


Figure 4: The first of 20 datasets sampled from GP-IOX for the comparison of Section 7.2.

from a discrete uniform prior on  $\{0.5, 0.8, 1.1, 1.4, 1.7, 2.0\}$  and  $\Sigma \sim \mathcal{W}_{q+1}^{-1}(\frac{1}{2}\mathbf{I}_q)$ . Figure 4 shows one of the IOX synthetic datasets. The other 20 datasets are generated as GPs with LMC cross-covariance with rank  $k = 8$  such that each of the 8 constituent processes is Matérn with smoothness  $\nu_j = 1$ , no nugget term, and spatial range  $\phi_j$  sampled uniformly for each  $j = 1, \dots, 8$  from a discrete distribution on a sequence of length 10 starting from 5 and ending at 20 with equal spacing. We generate the  $24 \times 8$  loading matrix  $\mathbf{A}$  by independently sampling each of its elements as  $a_{ij} \sim N(0, 1)$ . Finally, we add independent Gaussian measurement error with unit variance to each of the outcomes.

In both scenarios, we target the estimation of the cross-correlation between the 24 outcomes at zero spatial distance, as well as predictions at a test set of 400 locations located on a  $20 \times 20$  grid (the same across all 40 datasets). We compare models based on RMSE in estimating the zero-distance correlations  $\rho_{ij}, i < j$ , averaged across datasets, as



Method	IOX data					LMC data			
	$\rho_{ij}$	$\nu_j$	Predictions (full)	Predictions (partial)	Time	$\rho_{ij}$	Predictions (full)	Predictions (partial)	Time
IOX Full	<b>0.0167</b>	<b>0.0692</b>	<b>0.482</b>	<b>0.123</b>	40	0.162	1.22	1.15	66
IOX Grid	0.0250	0.169	0.490	0.140	4.1	0.234	1.45	1.46	11
IOX Cluster	0.0191	0.250	0.493	0.138	12	0.163	1.23	1.16	20
LMC	0.270		0.685	0.631	15	0.312	<b>1.15</b>	<b>1.08</b>	34
NNGP Indep. univariate	0.106	0.124	0.483		76	0.123	1.21		55
Non-spatial model	0.0610			0.386	3	<b>0.0921</b>		1.27	3

Table 2: RMSE in estimating  $\rho_{ij}, i < j$ , RMSPE in predicting  $\mathbf{y}(\cdot)$  at 400 new locations (full vector or a random set of 4 variables, given the others), and wall clock time (in minutes) in two data scenarios, averaged across outcomes and 20 datasets for each of the two scenarios. Lowest RMSE or RMSPE in bold.

well as the marginal smoothness in the IOX-generated data. We split the prediction task into two subtasks. In the first (labeled “full”), we perform predictions of the entire vector of 24 outcomes. In the second (“partial”), we make predictions for 4 outcomes (randomly selected at each location in the test set) using data about the other 20. In both subtasks, none of the data in the test set is used to train any of the models; we compare models via root mean square prediction error (RMSPE), averaged across datasets and variables.

We test estimation and prediction performance of several variants of the GP-IOX response model: *IOX Full* estimates  $\phi_j, \nu_j, \tau_j^2$  in the IOX-generated data, whereas fixes  $\nu_j = 1$  in the LMC-generated data, using Metropolis-within-Gibbs updates of  $\boldsymbol{\theta}$  as described in Section 4.1; *IOX Grid* fixes  $\phi_j = 30, \tau^2 = 10^{-3}$  for all  $j$  in the IOX-generated data scenario, and assumes a uniform prior on  $\nu_j$  on a sequence of 30 equally-spaced numbers starting at 0.5 and ending at 2; *IOX Cluster* fixes  $\phi_j = 30, \tau^2 = 10^{-3}$  but implements the clustering method of Section 6, fixing the number of clusters at 6. We fit a scalable LMC with R package `meshed`, fixing  $k = 6$  in the IOX-generated data and  $k = 8$  for LMC-generated

data. Finally, we compare with spatial univariate methods and non-spatial multivariate methods. For the former, we fit 24 independent univariate NNGP models to each of the 40 datasets using R package `spNNGP` (Finley et al. 2020): in IOX-generated datasets, we fix  $\phi_j = 30$  for all  $j$  and estimate smoothness, nugget, and variance. In LMC-generated datasets, we fix  $\nu_j = 1$  for all  $j$  and estimate decay, nugget, and variance. We compute  $\rho_{ij}$  for the NNGP models as the correlation between samples from the posterior predictive distributions. The nonspatial multivariate method simply assumes  $\mathbf{y}(\boldsymbol{\ell}) \stackrel{iid}{\sim} N(\mathbf{0}, \boldsymbol{\Sigma})$ . Timing for all methods is calculated as model fitting plus prediction time. Model fitting for all methods involves MCMC for 10,000 iterations, discarding the first half as burn-in.

Table 2 summarises the result of this comparison. In the IOX data scenario, *IOX Full* outperforms all other methods and the LMC offers inferior performance to both spatial univariate and nonspatial multivariate methods. This result confirms the theoretical finding that LMCs are a poor fit for variables with different smoothness. In the LMC scenario, IOX-based models outperform the LMC in estimating zero-distance correlations; however, the non-spatial model is associated with the smallest average RMSE. In the prediction tasks, *IOX Full* exhibits similar performance to the LMC, demonstrating the flexibility of our proposed approach in diverse scenarios. In terms of compute time, the *IOX Full* model is comparable to a set of independent univariate models, demonstrating that IOX scales to large data settings in practice. The *IOX Cluster* method was associated with only a slight deterioration of performance but a sizeable reduction in compute time. The *IOX Grid* is computationally inexpensive but exhibits inferior overall performance relative to *Full*; therefore, it could be used as an exploratory tool in practice.

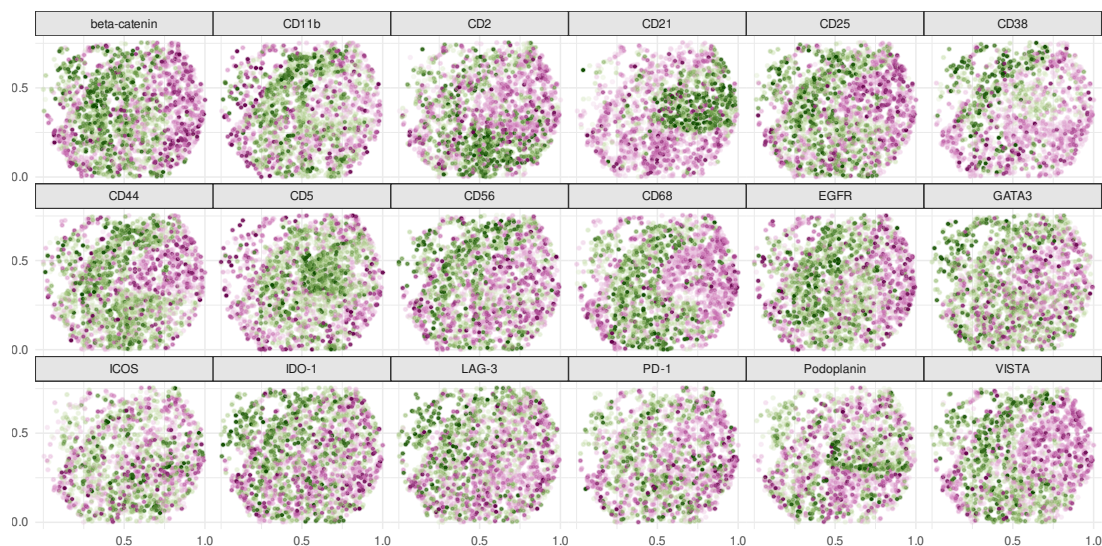


Figure 5: CRC CODEX data on 18 protein markers of a CRC patient. Green color corresponds to higher log-intensity of the marker.

### 7.3 Cancer proteomics CODEX data

We consider a colorectal cancer dataset previously analyzed in [Schürch et al. \(2020\)](#). This dataset was generated using co-detection by indexing (CODEX) technology optimized for formalin-fixed, paraffin-embedded tissue and tissue microarrays, leading to immunofluorescence imaging of the immune tumor microenvironment on 140 tissue regions of 35 advanced-stage colorectal cancer (CRC) patients. We restrict our analysis to a single tissue image (spot *55A*) from patient 28, and consider the 18 most common protein markers in this tissue. At each spatial location, the data include the intensity of expression of each of the 18 protein markers. After log-transforming the data, we obtain an aligned dataset of 18 continuous variables at 2,873 spatial locations, for a total dimension of 51,714. [Figure 5](#) visualizes the dataset.

We estimate  $\phi_j, \nu_j, \tau_j^2$  for all  $j$  by fitting IOX using Metropolis-within-Gibbs updates of  $\theta$  as described in [Section 4.1 \(IOX Full\)](#) as well as the clustering method of [Section 6](#), fixing the number of clusters at 6 (*IOX Cluster*). We validate our approaches by comparing

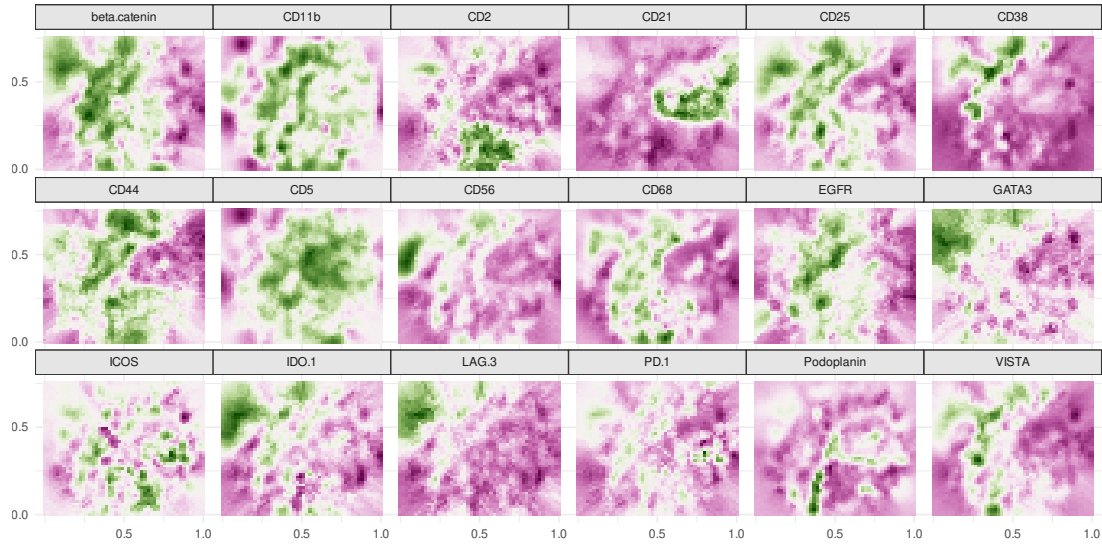


Figure 6: Intensity maps of the 18 protein markers from CRC CODEX data obtained via IOX (*Full* variant) by predicting the entire vector of variables at 2500 equally-spaced locations. Green color corresponds to higher log-intensity of the marker.

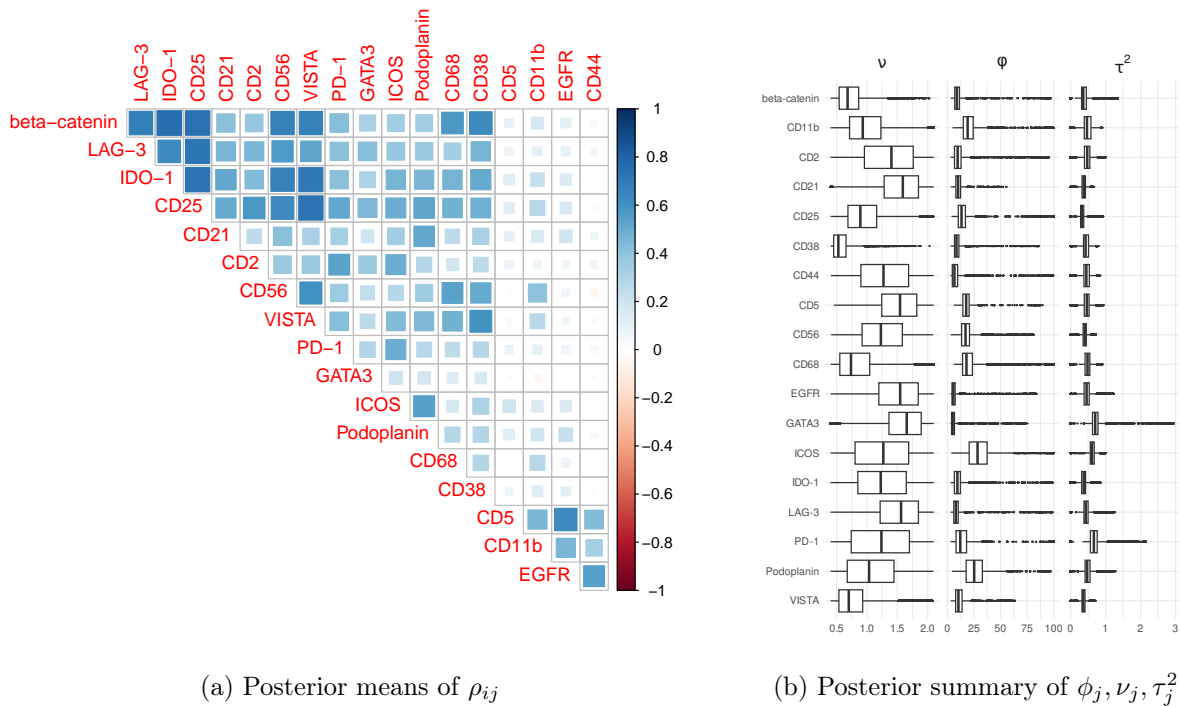


Figure 7: Posterior summaries for IOX parameters in the CODEX CRC analysis.

Method	APE	Time(s)
IOX Full	0.0639	47
IOX Cluster	<b>0.0638</b>	22
LMC $k = 6$	0.0704	37
LMC $k = 8$	0.0679	52
Non-spatial model	0.0687	1

Table 3: Predictive performance and runtime in seconds of IOX, LMCs, and a non-spatial model, on the CODEX CRC data analysis.

their predictive performance to LMCs (with 6 or 8 factors) and a nonspatial multivariate model. We use a test set  $\mathcal{L}_{\text{test}}$  of 400 locations which we built by removing 2 randomly selected outcomes from the data at each of the locations in  $\mathcal{L}_{\text{test}}$ . Therefore, we predict the unobserved part of  $\mathbf{y}(\ell)$  at each  $\ell \in \mathcal{L}_{\text{test}}$ . Table 3 summarizes our findings: IOX outperformed other tested methods in out-of-sample predictions while demonstrating scalability to large data settings. In particular, dimension reduction using IOX (the *Cluster* variant) resulted in a three-fold reduction of compute time at no cost of predictive performance. Dimension reduction using LMCs resulted in a deterioration of predictive performance that led to worse predictive performance relative to a non-spatial model.

## 8 Discussion

We have introduced IOX as a novel flexible class of cross-covariance functions for modeling spatial data in the “large  $n$ , large  $q$ ” setting. IOX leads to direct marginal inference and provides multiple avenues for flexible likelihood-based modeling and dimension reduction. In prioritizing inference of marginal covariances as well as overall parsimony, our method restricts  $C_{ij}(\cdot, \cdot)$  through a product of the marginal Cholesky factors. Similar restrictions are common; see, e.g., [Emery et al. 2022](#) for the multivariate Matérn. Extending IOX to more flexible parametrizations of  $C_{ij}(\cdot, \cdot)$  is possible, as we show in the Appendix. We have outlined clustering methods for dimension reduction, but more flexible hierarchical

priors may offer better performance in some settings—this is an interesting area for future research. Another possible future direction is the exploration of spatial extensions of recent factor models which have shown promising performance (Chandra et al. 2022, Chattopadhyay et al. 2024).

Non-stationarities and covariate-dependence can be introduced into IOX by choosing appropriate univariate correlations functions. Alternatively, one can directly take advantage of the structure of IOX. For example, if  $\mathbf{w}(\cdot)$  is a  $q$ -variate GP,  $\mathbf{w}_i$  the vector of values of the  $i$ th margin of  $\mathbf{w}(\cdot)$ , and  $\mathbf{D}_{w_i} = \text{diag}(\mathbf{w}_i)$ , then we can model  $q$  outcomes via  $C_{ij}(\boldsymbol{\ell}, \boldsymbol{\ell}') = \sigma_{ij} w_i(\boldsymbol{\ell}) w_j(\boldsymbol{\ell}') (\mathbf{h}_i(\boldsymbol{\ell}) \mathbf{L}_i \mathbf{L}_j^\top \mathbf{h}_j(\boldsymbol{\ell}') + \varepsilon(\boldsymbol{\ell}, \boldsymbol{\ell}'))$ , leading to  $\mathbf{C}(\mathcal{S}) = \{\oplus \mathbf{L}_i \mathbf{D}_{w_i}\} (\boldsymbol{\Sigma} \otimes \mathbf{I}_n) \{\oplus \mathbf{D}_{w_i} \mathbf{L}_i^\top\}$ , in which case  $\mathbf{w}_i^2$  models the spatially-varying sill of outcome  $i$ . IOX may also facilitate fitting multivariate extensions of the deformation method of Sampson & Guttorp (1992) by assuming multiple outcomes share the same latent input space, which is realistic with “omics” data.

We can also think of novel ways to model spatial time series data using IOX. Rather than  $q$  outcomes, we consider a single spatial outcome measured at  $T$  discrete time points and  $n$  sites. At each  $t = 1, \dots, T$ , we can let  $\rho_t(\cdot, \cdot)$  evolve with  $t$  according to some dynamics, as well as model  $\mathbf{Q} = \boldsymbol{\Sigma}^{-1}$ , e.g., by imposing Markovian assumptions leading to a sparse and banded  $\mathbf{Q}$ . For multivariate spatial time series, we may model the temporal evolution of cross-dependence via a time-varying precision matrix  $\mathbf{Q}_t$ .

## Acknowledgements

We thank D. Dunson and B. Jin for helpful comments and suggestions.

## APPENDIX

### A Proofs

**Proposition 2** (Marginal covariance).

$$C_{ii}(\boldsymbol{\ell}, \boldsymbol{\ell}') = \begin{cases} \sigma_{ii}\rho_i(\boldsymbol{\ell}, \boldsymbol{\ell}') & \text{if } \boldsymbol{\ell} \in \mathcal{S} \text{ or } \boldsymbol{\ell}' \in \mathcal{S} \text{ or } \boldsymbol{\ell} = \boldsymbol{\ell}', \\ \sigma_{ii}\rho_i(\boldsymbol{\ell}, \mathcal{S})\rho_i(\mathcal{S})^{-1}\rho_i(\mathcal{S}, \boldsymbol{\ell}') & \text{if } \boldsymbol{\ell}, \boldsymbol{\ell}' \in \mathcal{S}^c \text{ and } \boldsymbol{\ell} \neq \boldsymbol{\ell}'. \end{cases}$$

*Proof of Proposition 2.* Letting  $i = j$  we write (1) as

$$\begin{aligned} C_{ii}(\boldsymbol{\ell}, \boldsymbol{\ell}') &= \sigma_{ii} [\mathbf{h}_i(\boldsymbol{\ell})\rho_i(\mathcal{S})\mathbf{h}_i(\boldsymbol{\ell}') + \mathbb{1}_{\{\boldsymbol{\ell}=\boldsymbol{\ell}'\}}r_i(\boldsymbol{\ell})] \\ &= \sigma_{ii} [\rho_i(\boldsymbol{\ell}, \mathcal{S})\rho_i(\mathcal{S})^{-1}\rho_i(\mathcal{S}, \boldsymbol{\ell}') + \mathbb{1}_{\{\boldsymbol{\ell}=\boldsymbol{\ell}'\}}(\rho_i(\boldsymbol{\ell}, \boldsymbol{\ell}) - \rho_i(\boldsymbol{\ell}, \mathcal{S})\rho_i(\mathcal{S})^{-1}\rho_i(\mathcal{S}, \boldsymbol{\ell}))]. \end{aligned}$$

We immediately notice that if  $\boldsymbol{\ell} = \boldsymbol{\ell}'$  then  $C_{ii}(\boldsymbol{\ell}, \boldsymbol{\ell}) = \sigma_{ii}\rho_i(\boldsymbol{\ell}, \boldsymbol{\ell}) = \sigma_{ii}$ . If  $\boldsymbol{\ell} \neq \boldsymbol{\ell}'$  and  $\boldsymbol{\ell}, \boldsymbol{\ell}' \in \mathcal{S}^c$  then we obtain the stated result by just dropping the indicator term. Finally, suppose  $\boldsymbol{\ell} \in \mathcal{S}$  (the case  $\boldsymbol{\ell}' \in \mathcal{S}$  is analogous). This means there is  $r \in \{1, \dots, n\}$  such that  $\boldsymbol{\ell} = \boldsymbol{\ell}_r$ , which implies the vector  $\mathbf{h}_i(\boldsymbol{\ell}) = \mathbf{e}_\ell = (e_1, \dots, e_n)^\top$  has  $e_r = 1$  and  $e_h = 0$  for  $h \neq r$ . We see this e.g. by letting  $\mathbf{x} = (x_1, \dots, x_n)^\top$ ,  $E[\mathbf{x}] = 0$ , and  $\text{cov}(\mathbf{x}, \mathbf{x}) = \rho_i(\mathcal{S})$ . Then,  $\mathbf{h}_i(\boldsymbol{\ell})\mathbf{x} = E[x_r | \mathbf{x}] = x_r$ . In other words, if  $\boldsymbol{\ell} = \boldsymbol{\ell}_r \in \mathcal{S}$  then  $\mathbf{h}_i(\boldsymbol{\ell})$  selects the  $r$ th row from the matrix to which it is premultiplied. Therefore, we select the  $r$ th row of  $\rho_i(\mathcal{S}, \boldsymbol{\ell}')$ , which is equal to  $\rho_i(\boldsymbol{\ell}_r, \boldsymbol{\ell}') = \rho_i(\boldsymbol{\ell}, \boldsymbol{\ell}')$ .  $\square$

**Proposition 3** (Cross-covariance and  $\sigma_{ij}$ ). *For all  $\boldsymbol{\ell}, \boldsymbol{\ell}' \in \mathcal{D}$  and all  $i, j = 1, \dots, q$ , the cross-covariance is  $C_{ij}(\boldsymbol{\ell}, \boldsymbol{\ell}') \leq \sigma_{ij}$ . If  $\rho_i(\cdot, \cdot) = \rho_j(\cdot, \cdot)$ , then  $C_{ij}(\boldsymbol{\ell}, \boldsymbol{\ell}) = \sigma_{ij}$ .*

*Proof of Proposition 3.* We start by proving that  $\|\mathbf{h}_i(\boldsymbol{\ell})\mathbf{L}_i\| \leq 1$ . Because  $\rho_i(\cdot, \cdot)$  is a correlation function, then  $r_i(\boldsymbol{\ell}) = \rho_i(\boldsymbol{\ell}, \boldsymbol{\ell}) - \rho(\boldsymbol{\ell}, \mathcal{S})\rho_i(\mathcal{S})^{-1}\rho_i(\mathcal{S}, \boldsymbol{\ell}) = 1 - \mathbf{h}_i(\boldsymbol{\ell})\rho_i(\mathcal{S})\mathbf{h}_i(\boldsymbol{\ell})^\top \geq 0$  which implies  $\mathbf{h}_i(\boldsymbol{\ell})\rho_i(\mathcal{S})\mathbf{h}_i(\boldsymbol{\ell})^\top = \mathbf{h}_i(\boldsymbol{\ell})\mathbf{L}_i\mathbf{L}_i^\top\mathbf{h}_i(\boldsymbol{\ell}) = \|\mathbf{h}_i(\boldsymbol{\ell})\mathbf{L}_i\|^2 \leq 1$ .

Let  $\mathbf{a}^\top = \mathbf{h}_i(\boldsymbol{\ell})\mathbf{L}_i$  and  $\mathbf{b}^\top = \mathbf{h}_j(\boldsymbol{\ell}')\mathbf{L}_j$ . We showed above that  $\|\mathbf{a}\| \leq 1$  and  $\|\mathbf{b}\| \leq 1$ .

Then

$$\begin{aligned} C_{ij}(\boldsymbol{\ell}, \boldsymbol{\ell}') &= \sigma_{ij} \left[ \mathbf{h}_i(\boldsymbol{\ell})\mathbf{L}_i\mathbf{L}_j^\top\mathbf{h}_j(\boldsymbol{\ell}') + \sqrt{r_i(\boldsymbol{\ell})r_j(\boldsymbol{\ell}')} \right] \\ &= \sigma_{ij} \left[ \mathbf{a}^\top\mathbf{b} + \sqrt{(1 - \mathbf{a}^\top\mathbf{a})(1 - \mathbf{b}^\top\mathbf{b})} \right] \\ &\leq \sigma_{ij} \left[ \|\mathbf{a}\|\|\mathbf{b}\| + \sqrt{(1 - \|\mathbf{a}\|^2)(1 - \|\mathbf{b}\|^2)} \right] \leq \sigma_{ij}. \end{aligned}$$

In particular, consider the case  $\boldsymbol{\ell} = \boldsymbol{\ell}'$ . If  $\rho_i(\cdot, \cdot) = \rho_j(\cdot, \cdot)$  then we obtain  $C_{ij}(\boldsymbol{\ell}, \boldsymbol{\ell}') = \sigma_{ij}$ , which implies that  $\sigma_{ij}$  is the zero-distance correlation between variables with the same marginal correlation.  $\square$

**Proposition 4** (IOX cross-covariance matrix function). *Let  $\boldsymbol{\ell}, \boldsymbol{\ell}' \in \mathcal{S}$ .*

$$\begin{aligned} \mathbf{C}(\boldsymbol{\ell}, \boldsymbol{\ell}') &= \boldsymbol{\Sigma} \odot [\mathbf{K}(\boldsymbol{\ell}, \boldsymbol{\ell}') + \mathbf{d}(\boldsymbol{\ell}, \boldsymbol{\ell}')\mathbf{d}(\boldsymbol{\ell}, \boldsymbol{\ell}')^\top] \\ &= \{\oplus\mathbf{h}_i(\boldsymbol{\ell})\mathbf{L}_i\}(\boldsymbol{\Sigma} \otimes \mathbf{I}_n)\{\oplus\mathbf{L}_i^\top\mathbf{h}_i(\boldsymbol{\ell}')^\top\} + \mathbf{D}(\boldsymbol{\ell}, \boldsymbol{\ell}')\boldsymbol{\Sigma}\mathbf{D}(\boldsymbol{\ell}, \boldsymbol{\ell}'), \end{aligned} \tag{2}$$

where  $\mathbf{K}(\boldsymbol{\ell}, \boldsymbol{\ell}')$  is the  $q \times q$  matrix whose  $i, j$  element is  $\mathbf{h}_i(\boldsymbol{\ell})\mathbf{L}_i\mathbf{L}_j^\top\mathbf{h}_j(\boldsymbol{\ell}')^\top$ ,  $\mathbf{d}(\boldsymbol{\ell}, \boldsymbol{\ell}')$  is a vector of dimension  $q$  whose  $i$ th element is  $\mathbb{1}_{\{\boldsymbol{\ell}=\boldsymbol{\ell}'\}}\sqrt{r_i(\boldsymbol{\ell})}$ ,  $\mathbf{D}(\boldsymbol{\ell}, \boldsymbol{\ell}') = \text{diag}\{\mathbf{d}(\boldsymbol{\ell}, \boldsymbol{\ell}')\}$ , “ $\oplus$ ” is the direct sum operator and we denote  $\{\oplus\mathbf{h}_i(\boldsymbol{\ell})\mathbf{L}_i\}$  as the  $q \times nq$  block-diagonal matrix with  $\mathbf{h}_i(\boldsymbol{\ell})\mathbf{L}_i$  as its  $i$ th block, and “ $\odot$ ” is the Hadamard element-by-element product.

*Proof of Proposition 4.* Let  $\boldsymbol{\ell} \neq \boldsymbol{\ell}'$ . Then

$$\begin{aligned} \mathbf{C}(\boldsymbol{\ell}, \boldsymbol{\ell}') &= \left[ C_{ij}(\boldsymbol{\ell}, \boldsymbol{\ell}') \right]_{i,j=1,\dots,q} \\ &= \left[ \sigma_{ij}\mathbf{h}_i(\boldsymbol{\ell})\mathbf{L}_i\mathbf{L}_j^\top\mathbf{h}_j(\boldsymbol{\ell}')^\top \right]_{i,j=1,\dots,q} = \boldsymbol{\Sigma} \odot \left[ \mathbf{h}_i(\boldsymbol{\ell})\mathbf{L}_i\mathbf{L}_j^\top\mathbf{h}_j(\boldsymbol{\ell}')^\top \right]_{i,j=1,\dots,q} \\ &= \begin{bmatrix} \sigma_{11}\mathbf{h}_1(\boldsymbol{\ell})\mathbf{L}_1\mathbf{L}_1^\top\mathbf{h}_1(\boldsymbol{\ell}')^\top & \cdots & \sigma_{1q}\mathbf{h}_1(\boldsymbol{\ell})\mathbf{L}_1\mathbf{L}_q^\top\mathbf{h}_q(\boldsymbol{\ell}')^\top \\ & \ddots & \\ \sigma_{q1}\mathbf{h}_q(\boldsymbol{\ell})\mathbf{L}_q\mathbf{L}_1^\top\mathbf{h}_1(\boldsymbol{\ell}')^\top & & \sigma_{qq}\mathbf{h}_q(\boldsymbol{\ell})\mathbf{L}_q\mathbf{L}_q^\top\mathbf{h}_q(\boldsymbol{\ell}')^\top \end{bmatrix} \end{aligned}$$



$$\begin{aligned}
&= \begin{bmatrix} \sigma_{11}\mathbf{h}_1(\boldsymbol{\ell})\mathbf{L}_1 & \cdots & \sigma_{1q}\mathbf{h}_1(\boldsymbol{\ell})\mathbf{L}_1 \\ & \ddots & \\ \sigma_{q1}\mathbf{h}_q(\boldsymbol{\ell})\mathbf{L}_q & & \sigma_{qq}\mathbf{h}_q(\boldsymbol{\ell})\mathbf{L}_q \end{bmatrix} \begin{bmatrix} \mathbf{L}_1^\top \mathbf{h}_1(\boldsymbol{\ell}')^\top & & \\ & \ddots & \\ & & \mathbf{L}_q^\top \mathbf{h}_q(\boldsymbol{\ell}')^\top \end{bmatrix} \\
&= \begin{bmatrix} \mathbf{h}_1(\boldsymbol{\ell})\mathbf{L}_1 & & \\ & \ddots & \\ & & \mathbf{h}_q(\boldsymbol{\ell})\mathbf{L}_q \end{bmatrix} \begin{bmatrix} \sigma_{11}\mathbf{I}_n & \cdots & \sigma_{1q}\mathbf{I}_n \\ \vdots & \ddots & \vdots \\ \sigma_{q1}\mathbf{I}_n & \cdots & \sigma_{qq}\mathbf{I}_n \end{bmatrix} \begin{bmatrix} \mathbf{L}_1^\top \mathbf{h}_1(\boldsymbol{\ell}')^\top & & \\ & \ddots & \\ & & \mathbf{L}_q^\top \mathbf{h}_q(\boldsymbol{\ell}')^\top \end{bmatrix} \\
&= \{\oplus \mathbf{h}_i(\boldsymbol{\ell})\mathbf{L}_i\}(\boldsymbol{\Sigma} \otimes \mathbf{I}_n)\{\oplus \mathbf{L}_i^\top \mathbf{h}_i(\boldsymbol{\ell}')^\top\}.
\end{aligned}$$

If  $\boldsymbol{\ell} = \boldsymbol{\ell}'$  then we need to add  $\sqrt{r_i(\boldsymbol{\ell})r_j(\boldsymbol{\ell})}$  to the  $(i, j)$ th element of  $\mathbf{C}(\boldsymbol{\ell}, \boldsymbol{\ell}')$ , which is the purpose of  $\mathbf{d}(\boldsymbol{\ell}, \boldsymbol{\ell}')\mathbf{d}(\boldsymbol{\ell}, \boldsymbol{\ell}')^\top$  by construction. We conclude by noting that  $\boldsymbol{\Sigma} \odot (\mathbf{d}(\boldsymbol{\ell}, \boldsymbol{\ell}')\mathbf{d}(\boldsymbol{\ell}, \boldsymbol{\ell}')^\top) = \mathbf{D}(\boldsymbol{\ell}, \boldsymbol{\ell}')\boldsymbol{\Sigma}\mathbf{D}(\boldsymbol{\ell}, \boldsymbol{\ell}')$ .  $\square$

**Corollary 5.** *If  $\boldsymbol{\ell} \in \mathcal{S}$  then  $\mathbf{h}_i(\boldsymbol{\ell})\mathbf{L}_i = \mathbf{L}_i[\boldsymbol{\ell}, :]$ , the row of  $\mathbf{L}_i$  corresponding to  $\boldsymbol{\ell}$ . Then,*

$$\mathbf{C}(\mathcal{S}) = (\boldsymbol{\Sigma} \otimes \mathbf{1}_{n,n}) \odot \mathbf{K} = \{\oplus \mathbf{L}_i\}(\boldsymbol{\Sigma} \otimes \mathbf{I}_n)\{\oplus \mathbf{L}_i^\top\}, \quad (3)$$

where  $\mathbf{K}$  is the  $nq \times nq$  matrix whose  $(i, j)$ th block is  $\mathbf{L}_i\mathbf{L}_j^\top$ ;  $\mathbf{1}_{n,n}$  is the  $n \times n$  matrix of 1s.

*Proof of Corollary 5.* If  $\boldsymbol{\ell} = \boldsymbol{\ell}_r$  for some  $r \in \{1, \dots, n\}$ , then  $\mathbf{h}_i(\boldsymbol{\ell}) = \mathbf{e}_\ell = (e_1, \dots, e_n)^\top$  has  $e_r = 1$  and  $e_h = 0$  for  $h \neq r$ . We see this e.g. by letting  $\mathbf{x} = (x_1, \dots, x_n)^\top$ ,  $E[\mathbf{x}] = \mathbf{0}$ , and  $\text{cov}(\mathbf{x}, \mathbf{x}) = \rho_i(\mathcal{S})$ . Then,  $\mathbf{h}_i(\boldsymbol{\ell})\mathbf{x} = E[x_r | \mathbf{x}] = x_r$ . In other words, if  $\boldsymbol{\ell} = \boldsymbol{\ell}_r \in \mathcal{S}$  then  $\mathbf{h}_i(\boldsymbol{\ell})$  selects the  $r$ th row from the matrix to which it is premultiplied. Similarly, if  $\boldsymbol{\ell} \in \mathcal{S}$  then  $r_i(\boldsymbol{\ell}) = 0$  for all  $i = 1, \dots, q$ . The rest follows.  $\square$

**Proposition 6.**  *$\mathbf{C}(\boldsymbol{\ell}, \boldsymbol{\ell}')$  is a valid cross-covariance matrix function.*

*Proof of Proposition 6.* The conditions stated in the introduction can be expressed as follows. Suppose  $\mathbf{Z}$  is a  $m \times q$  random matrix whose  $i$ th row is  $\mathbf{z}(\boldsymbol{\ell}_i)^\top$ ,  $\boldsymbol{\ell}_i \in \mathcal{T} = \{\mathbf{t}_1, \dots, \mathbf{t}_m\}$  and  $j$ th column  $\mathbf{z}_j$ . Then, a cross-covariance matrix function must be such that the assumed

covariance matrix of  $\mathbf{z} = \text{vec}\{\mathbf{Z}\}$  (or, equivalently, of  $\text{vec}\{\mathbf{Z}^\top\}$ ) is symmetric non-negative definite for any  $\mathcal{T}$  and any  $m$  (Genton & Kleiber 2015). Because our assumption is that  $\text{cov}(\mathbf{z}) = \mathbf{C}(\mathcal{T})$ , we need to show that  $\mathbf{C}(\mathcal{T})$  is symmetric non-negative definite. If  $\ell \neq \ell'$ ,

$$\begin{aligned} \mathbf{C}(\ell, \ell') &= \boldsymbol{\Sigma} \odot (\mathbf{K}(\ell, \ell') + \mathbf{D}(\ell, \ell')) \\ &= \boldsymbol{\Sigma} \odot \left[ \mathbf{h}_i(\ell) \mathbf{L}_i \mathbf{L}_j^\top \mathbf{h}_j(\ell')^\top \right]_{i,j=1,\dots,q} \\ &= \boldsymbol{\Sigma} \odot \left[ \mathbf{h}_i(\ell') \mathbf{L}_i \mathbf{L}_j^\top \mathbf{h}_j(\ell)^\top \right]_{i,j=1,\dots,q}^\top \\ &= \boldsymbol{\Sigma} \odot \mathbf{K}(\ell', \ell)^\top = \mathbf{C}(\ell', \ell)^\top. \end{aligned}$$

The additional term  $\mathbf{D}(\ell, \ell')$  (defined in Proposition 4) is zero if  $\ell \neq \ell'$ ; otherwise,

$$\mathbf{D}(\ell, \ell) = \begin{bmatrix} \sqrt{r_1(\ell)} \\ \vdots \\ \sqrt{r_q(\ell)} \end{bmatrix} \begin{bmatrix} \sqrt{r_1(\ell)} & \cdots & \sqrt{r_q(\ell)} \end{bmatrix},$$

which is symmetric by construction. As for non-negative definiteness, define  $\mathbf{H}_i(\mathcal{T}) = \rho_i(\mathcal{T}, \mathcal{S}) \rho_i(\mathcal{S})^{-1}$ , i.e. the  $m \times n$  matrix whose  $i$ th row is  $\mathbf{h}_i(\mathbf{t}_i)$  and assume  $\boldsymbol{\Sigma} = \mathbf{A} \mathbf{A}^\top$  where  $\mathbf{A}$  is a  $q \times k$  matrix of rank  $k \leq q$ . Then,

$$\begin{aligned} \mathbf{C}(\mathcal{T}) &= \{\oplus \mathbf{H}_i(\mathcal{T}) \mathbf{L}_i\} (\boldsymbol{\Sigma} \otimes \mathbf{I}_n) \{\oplus \mathbf{L}_i^\top \mathbf{H}_i(\mathcal{T})^\top\} + (\boldsymbol{\Sigma} \otimes \mathbf{1}_{m,m}) \odot \mathbf{D}_T \\ &= \{\oplus \mathbf{H}_i(\mathcal{T}) \mathbf{L}_i\} (\mathbf{A} \otimes \mathbf{I}_n) (\mathbf{A}^\top \otimes \mathbf{I}_n) \{\oplus \mathbf{L}_i^\top \mathbf{H}_i(\mathcal{T})^\top\} + (\boldsymbol{\Sigma} \otimes \mathbf{1}_{m,m}) \odot \mathbf{D}_T \\ &= \mathbf{G} \mathbf{G}^\top + (\boldsymbol{\Sigma} \otimes \mathbf{1}_{m,m}) \odot \mathbf{D}_T, \end{aligned}$$

where  $\mathbf{G} = \{\oplus \mathbf{H}_i(\mathcal{T}) \mathbf{L}_i\} (\mathbf{A} \otimes \mathbf{I}_n)$  and  $\mathbf{D}_T$  is a  $mq \times mq$  block matrix whose  $(i, j)$ th block of dimension  $m \times m$  is a diagonal matrix whose diagonal entries are  $\sqrt{r_i(\ell_h) r_j(\ell_h)}$  for  $h = 1, \dots, m$ . The first term is non-negative definite because  $\mathbf{x}^\top \mathbf{G} \mathbf{G}^\top \mathbf{x} = \tilde{\mathbf{x}}^\top \tilde{\mathbf{x}} \geq 0$ . As for the second term,  $(\boldsymbol{\Sigma} \otimes \mathbf{1}_{m,m})$  is non-negative definite because  $\boldsymbol{\Sigma}$  is assumed to be. Finally, suppose  $\mathbf{P}$  is a permutation matrix that rearranges rows and columns of  $\mathbf{D}_T$  so

that  $\mathbf{P}\mathbf{D}_T\mathbf{P}^\top$  is a block diagonal matrix with  $\mathbf{D}(\boldsymbol{\ell}_i, \boldsymbol{\ell}_i)$  as its  $i$ th diagonal block, with  $i = 1, \dots, m$ .  $\mathbf{D}(\boldsymbol{\ell}_i, \boldsymbol{\ell}_i)$  is non-negative definite rank 1. Therefore,  $\mathbf{P}\mathbf{D}_T\mathbf{P}^\top$  is non-negative definite of rank  $m$ , and so is  $\mathbf{D}_T$ . Hadamard product and matrix sum retain non-negative definiteness.  $\square$

**Proposition 7.** *In the separable specification, i.e.,  $\rho_i(\cdot, \cdot) = \rho(\cdot, \cdot)$  for all  $i$ , IOX and LMC coincide at  $\mathcal{S}$ .*

*Proof of Proposition 7.* For IOX,

$$\begin{aligned} \mathbf{C}(\mathcal{S}) &= \{\oplus \mathbf{L}_i\}(\boldsymbol{\Sigma} \otimes \mathbf{I}_n)\{\oplus \mathbf{L}_i^\top\} \\ &= (\mathbf{I}_q \otimes \mathbf{L})(\boldsymbol{\Sigma} \otimes \mathbf{I}_n)(\mathbf{I}_q \otimes \mathbf{L}^\top) \\ &= \boldsymbol{\Sigma} \otimes \mathbf{L}\mathbf{L}^\top = \boldsymbol{\Sigma} \otimes \rho(\mathcal{S}). \end{aligned}$$

For LMC,

$$\begin{aligned} \mathbf{C}(\mathcal{S}) &= (\mathbf{A} \otimes \mathbf{I}_n)\{\oplus \rho_i(\mathcal{S})\}(\mathbf{A}^\top \otimes \mathbf{I}_n) \\ &= (\mathbf{A} \otimes \mathbf{I}_n)(\mathbf{I}_q \otimes \rho(\mathcal{S}))(\mathbf{A}^\top \otimes \mathbf{I}_n) \\ &= \mathbf{A}\mathbf{A}^\top \otimes \rho(\mathcal{S}) = \boldsymbol{\Sigma} \otimes \rho(\mathcal{S}). \end{aligned}$$

$\square$

**Proposition 8.** *Suppose  $\boldsymbol{\ell}, \boldsymbol{\ell}' \in \mathcal{S}^c$ ,  $\boldsymbol{\ell} \neq \boldsymbol{\ell}'$ . Then,  $\mathbf{C}(\boldsymbol{\ell}, \boldsymbol{\ell}') - \mathbf{C}(\boldsymbol{\ell}, \mathcal{S})\mathbf{C}(\mathcal{S})^{-1}\mathbf{C}(\mathcal{S}, \boldsymbol{\ell}') = \mathbf{0}$ .*

*Proof of Proposition 8.* We have  $\mathbf{C}(\boldsymbol{\ell}, \mathcal{S}) = \{\oplus \mathbf{h}_i(\boldsymbol{\ell})\mathbf{L}_i\}(\boldsymbol{\Sigma} \otimes \mathbf{I}_n)\{\oplus \mathbf{L}_i^\top\}$  and  $\mathbf{C}(\mathcal{S})^{-1} = \{\oplus \mathbf{L}_i^{-\top}\}(\boldsymbol{\Sigma}^{-1} \otimes \mathbf{I}_n)\{\oplus \mathbf{L}_i^{-1}\}$ . Together, these imply:

$$\mathbf{C}(\boldsymbol{\ell}, \mathcal{S})\mathbf{C}(\mathcal{S})^{-1}\mathbf{C}(\mathcal{S}, \boldsymbol{\ell}') = \{\oplus \mathbf{h}_i(\boldsymbol{\ell})\mathbf{L}_i\}(\boldsymbol{\Sigma} \otimes \mathbf{I}_n)\{\oplus \mathbf{L}_i^\top \mathbf{h}_i(\boldsymbol{\ell}')^\top\} = \mathbf{C}(\boldsymbol{\ell}, \boldsymbol{\ell}'). \quad \square$$

**Proposition 9** (Log-likelihood of GP-IOX).

$$\log p(\mathbf{y} \mid \boldsymbol{\theta}, \mathbf{Q}) = \text{const} + \frac{n}{2} \log \det(\mathbf{Q}) \sum_{ij} \mathbf{L}_i^{-1}[j, j] - \frac{1}{2} \text{Tr}(\mathbf{V}\mathbf{Q}\mathbf{V}^\top), \quad (4)$$

where  $\mathbf{L}_i^{-1}[j, j]$  is the  $j$ th diagonal element of  $\mathbf{L}_i^{-1}$ .

*Proof of Proposition 9.* We start by noting that

$$\mathbf{C}^{-1} = \{\oplus \mathbf{L}_i^{-\top}\}(\boldsymbol{\Sigma}^{-1} \otimes \mathbf{I}_n)\{\oplus \mathbf{L}_i^{-1}\} = \{\oplus \mathbf{L}_i^{-\top}\}(\mathbf{Q}^{-1} \otimes \mathbf{I}_n)\{\oplus \mathbf{L}_i^{-1}\},$$

and because  $\det(\mathbf{L}_i^{-1}) = \prod_j \mathbf{L}_i^{-1}[j, j]$ , we get  $-\frac{1}{2} \log \det(\mathbf{C}) = \frac{n}{2} \log \det(\mathbf{Q}) \sum_{ij} \mathbf{L}_i^{-1}[j, j]$ .

Then,

$$\begin{aligned} \log p(\mathbf{y} \mid \boldsymbol{\theta}, \boldsymbol{\beta}, \boldsymbol{\Sigma}) &= \text{const} - \frac{1}{2} \log \det(\mathbf{C}) - \frac{1}{2} \mathbf{y}^\top \mathbf{C}^{-1} \mathbf{y} \\ &= \text{const} + \frac{n}{2} \log \det(\mathbf{Q}) \sum_{ij} \mathbf{L}_i^{-1}[j, j] - \frac{1}{2} \mathbf{y}^\top \{\oplus \mathbf{L}_i^{-\top}\}(\mathbf{Q} \otimes \mathbf{I}_n)\{\oplus \mathbf{L}_i^{-1}\} \mathbf{y} \\ &= \text{const} + \frac{n}{2} \log \det(\mathbf{Q}) \sum_{ij} \mathbf{L}_i^{-1}[j, j] - \frac{1}{2} \text{vec}\{\mathbf{V}\}^\top (\mathbf{Q} \otimes \mathbf{I}_n) \text{vec}\{\mathbf{V}\} \\ &= \text{const} + \frac{n}{2} \log \det(\mathbf{Q}) \sum_{ij} \mathbf{L}_i^{-1}[j, j] - \frac{1}{2} \text{Tr}(\mathbf{V}^\top \mathbf{Q} \mathbf{V}). \end{aligned}$$

□

**Proposition 10** (Conditional density).  $p(\mathbf{y}_j \mid \mathbf{y}_{j^c}, \boldsymbol{\theta}, \mathbf{Q}) = N(\mathbf{y}_j; \mathbf{m}_j, \mathbf{M}_j)$ , where  $\mathbf{m}_j = -\mathbf{L}_j \sum_{r \in j^c} \frac{Q_{jr}}{Q_{jj}} \mathbf{y}_r$  and  $\mathbf{M}_j^{-1} = Q_{jj} \rho_j(\mathcal{S})^{-1}$ . Then, we evaluate  $N(\mathbf{y}_j; \mathbf{m}_j, \mathbf{M}_j)$  as:

$$N(\mathbf{y}_j; \mathbf{m}_j, \mathbf{M}_j) \propto \sqrt{|Q_{jj} \rho_j(\mathcal{S})^{-1}|} \exp \left\{ -\frac{1}{2Q_{jj}} \mathbf{Q}_j \cdot \mathbf{V}^\top \mathbf{V} \mathbf{Q}_j^\top \right\}, \quad (5)$$

where  $Q_{jr}$  is the  $(j, r)$ th element and  $\mathbf{Q}_j \cdot$  is the  $j$ th row of  $\mathbf{Q}$ .

*Proof of Proposition 10.* Because the joint distribution of  $\mathbf{y}$  is Gaussian, we have  $p(\mathbf{y}_j \mid \mathbf{y}_{j^c}, \boldsymbol{\theta}, \mathbf{Q}) = N(\mathbf{y}_j; \mathbf{m}_j, \mathbf{M}_j)$ , where  $\mathbf{M}_j^{-1}$  is the  $(j, j)$ th block of the precision matrix  $\mathbf{C}^{-1} = \{\oplus \mathbf{L}_j^{-\top}\}(\mathbf{Q} \otimes \mathbf{I}_n)\{\oplus \mathbf{L}_j^{-1}\}$ . Therefore, we find  $\mathbf{M}_j^{-1} = Q_{jj} \rho_j(\mathcal{S})^{-1}$  following the same steps as in Proposition 2. Again because the joint is Gaussian, the conditional mean is  $\mathbf{m}_j = \mathbf{C}_{j, j^c} \mathbf{C}_{j^c, j^c}^{-1} \mathbf{y}_{j^c}$ , which becomes

$$\begin{aligned} \mathbf{m}_j &= \mathbf{L}_j (\boldsymbol{\Sigma}_{j, j^c} \boldsymbol{\Sigma}_{j^c, j^c}^{-1} \otimes \mathbf{I}_n) \{\oplus_{j^c} \mathbf{L}_r^{-1}\} \mathbf{y}_{j^c} = -\mathbf{L}_j \left( \frac{\mathbf{Q}_{j, j^c}}{Q_{jj}} \otimes \mathbf{I}_n \right) \{\oplus_{j^c} \mathbf{L}_r^{-1}\} \mathbf{y}_{j^c} \\ &= -\mathbf{L}_j \sum_{r \in j^c} \frac{Q_{jr}}{Q_{jj}} \mathbf{L}_r^{-1} \mathbf{y}_r, \end{aligned}$$

where  $\mathbf{Q}_{j,j^c}$  is the  $1 \times q - 1$  vector obtained from the  $j$ th row and  $j^c$  columns of  $\mathbf{Q}$  and we denote with “ $\oplus_{j^c}$ ” the direct sum operator over  $j^c$  indices. As for evaluating the joint density,

$$\begin{aligned}
N(\mathbf{y}_j; \mathbf{m}_j, \mathbf{M}_j) &\propto |\mathbf{M}_j|^{-\frac{1}{2}} \exp\left\{-\frac{1}{2}(\mathbf{y}_j - \mathbf{m}_j)^\top \mathbf{M}_j^{-1}(\mathbf{y}_j - \mathbf{m}_j)\right\} \\
&= |\mathbf{M}_j|^{-\frac{1}{2}} \exp\left\{-\frac{Q_{jj}}{2}(\mathbf{y}_j - \mathbf{m}_j)^\top \mathbf{L}_j^{-\top} \mathbf{L}_j^{-1}(\mathbf{y}_j - \mathbf{m}_j)\right\} \\
(\star) \quad &= \sqrt{|Q_{jj}\rho_j(\mathcal{S})^{-1}|} \exp\left\{-\frac{1}{2Q_{jj}} \left(\sum_{r=1}^q Q_{jr}\mathbf{v}_r\right)^\top \left(\sum_{r=1}^q Q_{jr}\mathbf{v}_r\right)\right\} \\
&= \sqrt{|Q_{jj}\rho_j(\mathcal{S})^{-1}|} \exp\left\{-\frac{1}{2Q_{jj}} \mathbf{Q}_j \mathbf{V}^\top \mathbf{V} \mathbf{Q}_j^\top\right\}.
\end{aligned}$$

where for  $(\star)$  we use the following:

$$\begin{aligned}
\mathbf{L}_j^{-1}(\mathbf{y}_j - \mathbf{m}_j) &= \mathbf{L}_j^{-1}\mathbf{y}_j - \mathbf{L}_j^{-1}\mathbf{m}_j = \mathbf{L}_j^{-1}\mathbf{y}_j - \mathbf{L}_j^{-1}\mathbf{m}_j \\
&= \mathbf{L}_j^{-1}\mathbf{y}_j + \left(\frac{Q_{j,j^c}}{Q_{jj}} \otimes \mathbf{I}_n\right) \{\oplus_{j^c} \mathbf{L}_r^{-1}\}\mathbf{y}_{j^c} = \mathbf{L}_j^{-1}\mathbf{y}_j + \sum_{r \in j^c} \frac{Q_{jr}}{Q_{jj}} \mathbf{L}_r^{-1}\mathbf{y}_r \\
&= \sum_{r=1}^q \frac{Q_{jr}}{Q_{jj}} \mathbf{L}_r^{-1}\mathbf{y}_r = \sum_{r=1}^q \frac{Q_{jr}}{Q_{jj}} \mathbf{v}_r.
\end{aligned}$$

□

**Proposition 11.**  $\mathbf{H}(\mathbf{t}) = \{\oplus \mathbf{h}_i(\mathbf{t})\}$  and  $\mathbf{R}(\mathbf{t}) = \mathbf{D}(\mathbf{t}, \mathbf{t})\boldsymbol{\Sigma}\mathbf{D}(\mathbf{t}, \mathbf{t})$ . Therefore, marginal predictions for outcome  $i$  only depend on  $\rho_i(\cdot, \cdot)$  at  $\mathcal{S}$ , and  $\sigma_{ii}$ .

*Proof of Proposition 11.*

$$\begin{aligned}
\mathbf{H}(\mathbf{t}) &= \mathbf{C}(\mathbf{t}, \mathcal{S})\mathbf{C}(\mathcal{S})^{-1} \\
&= \{\oplus \mathbf{h}_i(\mathbf{t})\mathbf{L}_i\}(\boldsymbol{\Sigma} \otimes \mathbf{I}_n)\{\oplus \mathbf{L}_i^\top\}\{\oplus \mathbf{L}_i^{-\top}\}(\boldsymbol{\Sigma}^{-1} \otimes \mathbf{I}_n)\{\oplus \mathbf{L}_i^{-1}\} \\
&= \{\oplus \mathbf{h}_i(\mathbf{t})\mathbf{L}_i\}\{\oplus \mathbf{L}_i^{-1}\} = \{\oplus \mathbf{h}_i(\mathbf{t})\}
\end{aligned}$$

$$\mathbf{R}(\mathbf{t}) = \mathbf{C}(\mathbf{t}) - \mathbf{H}(\mathbf{t})\mathbf{C}(\mathcal{S}, \mathbf{t})$$

$$\begin{aligned}
&= \{\oplus \mathbf{h}_i(\mathbf{t}) \mathbf{L}_i\}(\boldsymbol{\Sigma} \otimes \mathbf{I}_n) \{\oplus \mathbf{L}_i^\top \mathbf{h}_i(\mathbf{t})^\top\} + \mathbf{D}(\mathbf{t}, \mathbf{t}) \boldsymbol{\Sigma} \mathbf{D}(\mathbf{t}, \mathbf{t}) - \\
&\quad - \{\oplus \mathbf{h}_i(\mathbf{t})\} \{\oplus \mathbf{L}_i\}(\boldsymbol{\Sigma} \otimes \mathbf{I}_n) \{\oplus \mathbf{L}_i^\top \mathbf{h}_i(\mathbf{t})^\top\} \\
&= \{\oplus \mathbf{h}_i(\mathbf{t}) \mathbf{L}_i\}(\boldsymbol{\Sigma} \otimes \mathbf{I}_n) \{\oplus \mathbf{L}_i^\top \mathbf{h}_i(\mathbf{t})^\top\} + \mathbf{D}(\mathbf{t}, \mathbf{t}) \boldsymbol{\Sigma} \mathbf{D}(\mathbf{t}, \mathbf{t}) - \\
&\quad - \{\oplus \mathbf{h}_i(\mathbf{t}) \mathbf{L}_i\}(\boldsymbol{\Sigma} \otimes \mathbf{I}_n) \{\oplus \mathbf{L}_i^\top \mathbf{h}_i(\mathbf{t})^\top\} \\
&= \mathbf{D}(\mathbf{t}, \mathbf{t}) \boldsymbol{\Sigma} \mathbf{D}(\mathbf{t}, \mathbf{t}) = \mathbf{D}(\mathbf{t}, \mathbf{t}) \mathbf{A} \mathbf{A}^\top \mathbf{D}(\mathbf{t}, \mathbf{t})
\end{aligned}$$

□

**Proposition 12.**  $p(\mathbf{y}_m(\mathbf{t}) \mid \mathbf{y}_o(\mathbf{t}), \mathbf{y}) = N(\mathbf{y}_m(\mathbf{t}); \mathbf{h}_{m|o}, \mathbf{R}_{m|o}(\mathbf{t}))$ , where  $\mathbf{h}_{m|o} = \mathbf{H}_m(\mathbf{t})\mathbf{y} + \mathbf{H}_{m|o}(\mathbf{t})(\mathbf{y}_o(\mathbf{t}) - \mathbf{H}_o(\mathbf{t})\mathbf{y})$ ,  $\mathbf{H}_o(\mathbf{t})$  is the submatrix of  $\mathbf{H}(\mathbf{t})$  where we take the rows corresponding to  $o$  (similarly  $\mathbf{H}_m(\mathbf{t})$  with rows  $m$ ), and

$$\begin{aligned}
\mathbf{H}_{m|o}(\mathbf{t}) &= \mathbf{D}_m(\mathbf{t}, \mathbf{t}) \boldsymbol{\Sigma}_{m,o} \boldsymbol{\Sigma}_o^{-1} \mathbf{D}_o^{-1}(\mathbf{t}, \mathbf{t}) = -\mathbf{D}_m(\mathbf{t}, \mathbf{t}) \mathbf{Q}_m^{-1} \mathbf{Q}_{m,o} \mathbf{D}_o^{-1}(\mathbf{t}, \mathbf{t}) \\
\mathbf{R}_{m|o}(\mathbf{t}) &= \mathbf{D}_m(\mathbf{t}, \mathbf{t}) (\boldsymbol{\Sigma}_m - \boldsymbol{\Sigma}_{m,o} \boldsymbol{\Sigma}_o^{-1} \boldsymbol{\Sigma}_{o,m}) \mathbf{D}_m(\mathbf{t}, \mathbf{t}) = \mathbf{D}_m(\mathbf{t}, \mathbf{t}) \mathbf{Q}_m^{-1} \mathbf{D}_m(\mathbf{t}, \mathbf{t}),
\end{aligned}$$

where  $\boldsymbol{\Sigma}_{m,o}$  subsets  $\boldsymbol{\Sigma}$  to its  $m$  rows and  $o$  columns, and similarly for  $\mathbf{Q}$ .

*Proof of Proposition 12.* All the results are a consequence of the properties of multivariate Gaussians and Proposition 11. □

## B Section 1: *Introduction*

### B.1 Details on Figure 2

The figure displays a 4-outcome multivariate GP with IOX cross-covariance with the following settings:

$$\Sigma = \begin{bmatrix} 1 & -0.9 & 0.7 & 0.8 \\ -0.9 & 1 & -0.5 & -0.7 \\ 0.7 & -0.5 & 1 & 0.8 \\ 0.8 & -0.7 & 0.8 & 1 \end{bmatrix} \quad \begin{aligned} \rho_1(\boldsymbol{\ell}, \boldsymbol{\ell}') &= \mathcal{M}_{\nu=1}(\boldsymbol{\ell}, \boldsymbol{\ell}'; \phi_1 = 15) \\ \rho_2(\boldsymbol{\ell}, \boldsymbol{\ell}') &= \exp\{-15 \cdot \|\boldsymbol{\ell} - \boldsymbol{\ell}'\|\} \cos\{14.9 \cdot \|\boldsymbol{\ell} - \boldsymbol{\ell}'\|\} \\ \rho_3(\boldsymbol{\ell}, \boldsymbol{\ell}') &= \mathcal{M}_{\nu_3=1.5}(\tilde{\boldsymbol{\ell}}, \tilde{\boldsymbol{\ell}}'; \phi_3 = 15) \quad \text{where } \tilde{\boldsymbol{\ell}} = \boldsymbol{\ell} + \mathbf{u}(\boldsymbol{\ell}) \\ \rho_4(\boldsymbol{\ell}, \boldsymbol{\ell}') &= |1 + v(\boldsymbol{\ell})| |1 + v(\boldsymbol{\ell}')| \mathcal{M}_{\nu_4=1.5}(\boldsymbol{\ell}, \boldsymbol{\ell}'; \phi_4 = 15), \end{aligned}$$

where  $\mathbf{u}(\cdot) = (u_1(\cdot), u_2(\cdot))^\top$  is a bivariate GP with independent Matérn margins with parameters  $\sigma^2 = 0.03$ ,  $\phi = 1$ ,  $\nu = 1$ , and  $v(\cdot)$  is a Matérn GP with parameters  $\sigma^2 = 0.5$ ,  $\phi = 30$ ,  $\nu = 1.5$ . We generate data at a regular grid of 40,000 locations after applying a Vecchia approximation of each univariate GP using  $m = 40$  neighbors.

### B.2 Comparison with multivariate Matérn

The multivariate Matérn model (Gneiting et al. 2010) defines each  $C_{ij}(\cdot, \cdot)$  to be a Matérn function parametrized via  $\sigma_{ij}, \phi_{ij}, \nu_{ij}$ , with the possible addition of nugget effects. The fact that  $C_{ij}(\cdot, \cdot)$  are valid univariate covariance functions for each  $i, j$  does not guarantee that the resulting cross-covariance matrix function will also be valid. The validity of the latter depends on the values of the entire set of parameters  $\sigma_{ij}, \phi_{ij}, \nu_{ij}$  for  $i, j = 1, \dots, q$  in non-trivial ways. Finding the least restrictive constraints on the parameters is an active research area, see, e.g., (Apanasovich et al. 2012, Emery et al. 2022). An additional problem is that if each  $C_{ij}(\cdot, \cdot)$  has  $m$  free parameters, then the total number of parameters to be estimated from the data is  $m q(q + 1)/2$  and the constraints on them become increasingly cumbersome to satisfy. The parsimonious Matérn model of Gneiting et al. (2010) resolves

this issue by proposing to restrict the parameter space to guarantee the validity of the resulting cross-covariance matrix function. One defines the cross-covariances as

$$C_{ij}(\boldsymbol{\ell}, \boldsymbol{\ell}') = \sigma_{ij} S(\nu_i, \nu_j, d) M_{\frac{1}{2}(\nu_i + \nu_j)}(\boldsymbol{\ell}, \boldsymbol{\ell}'; \phi),$$

$$\text{where } S(\nu_i, \nu_j, d) = \frac{\Gamma(\nu_i + d/2)^{\frac{1}{2}} \Gamma(\nu_j + d/2)^{\frac{1}{2}}}{\Gamma(\nu_i)^{\frac{1}{2}} \Gamma(\nu_j)^{\frac{1}{2}}} \frac{\Gamma(\frac{1}{2}(\nu_i + \nu_j))}{\Gamma(\frac{1}{2}(\nu_i + \nu_j) + d/2)}, \quad (9)$$

and  $M_\nu(\boldsymbol{\ell}, \boldsymbol{\ell}'; \phi)$  is the Matérn correlation function with smoothness  $\nu$  and range  $1/\phi$  and  $\boldsymbol{\Sigma} = (\sigma_{ij})_{ij}$  is a covariance matrix. In other words, the parsimonious Matérn forces the cross-covariances to have smoothness equal to the average smoothness of the variables they refer to, and all covariances (marginal and cross) to share a single range parameter. Furthermore, the scaling factor  $0 < S(\nu_i, \nu_j, d) \leq 1$  operates to ensure validity of the cross-covariance matrix function. Like in IOX,  $\sigma_{ij}$  is the upper bound of  $C_{ij}(\boldsymbol{\ell}, \boldsymbol{\ell})$  which is achieved if  $\nu_i = \nu_j$ . Also similar to IOX is the fact that the smoothness of  $C_{ij}$  cannot be chosen freely. However, while IOX allows different ranges, the multivariate Matérn requires additional constraints to be imposed on other parameters to achieve the same result. The validity of IOX is derived directly from the validity of the component correlation functions, whereas one needs to perform further checks in multivariate Matérn models. This makes IOX advantageous when implementing multivariate extensions of non-stationary correlations.

Finally, IOX is advantageous in leading to a structured sample covariance matrix which we take advantage of in developing the models appearing in the main article. The multivariate Matérn does not lead to similar structure.

### B.3 Comparison with LMCs

We provide a summary of how IOX compares with LMCs. The LMC does not allow outcome specific smoothness, flexible nuggets, or easy-to-interpret range parameters. For the same



reasons, LMCs do not allow to construct Vecchia approximations with outcome-specific neighbor sets or DAGs.

Prior sampling from LMCs is very similar to IOX, with the only difference being that in LMCs, one introduces spatial dependence first, and then multivariate dependence, whereas the order of these operations is inverted in IOX. In Table 4 we outline prior sampling for IOX and LMCs in a way that clarifies this point visually. Figure 8 visualizes the resulting sample covariances. Appendix E.1 provides more details on prior sampling for IOX, including at non-reference locations.

Step	IOX	Separable model	LMC
1	$\mathcal{S}$ sample locations	$\mathcal{S}$ sample locations	$\mathcal{S}$ sample locations
2	$L_j = \text{chol}(\rho_j(\mathcal{S}))$ for $j = 1, \dots, q$ .	$L = \text{chol}(\rho(\mathcal{S}))$	$L_j = \text{chol}(\rho_j(\mathcal{S}))$ for $j = 1, \dots, q$ .
3	$\mathbf{V} \sim MN(\mathbf{0}, \mathbf{I}_n, \mathbf{I}_q)$ .	$\mathbf{V} \sim MN(\mathbf{0}, \mathbf{I}_n, \mathbf{I}_q)$	$\mathbf{V} \sim MN(\mathbf{0}, \mathbf{I}_n, \mathbf{I}_q)$ .
4	$\mathbf{w} = (\mathbf{A} \otimes \mathbf{I}_n) \text{vec}(\mathbf{V})$	$\mathbf{Y} = \mathbf{L} \mathbf{V} \mathbf{A}^\top$	$\mathbf{w} = \{\oplus L_j\} \text{vec}(\mathbf{V})$
5	$\mathbf{y} = \{\oplus L_j\} \mathbf{w}$	$\mathbf{y} = \text{vec}(\mathbf{Y})$	$\mathbf{y} = (\mathbf{A} \otimes \mathbf{I}_n) \mathbf{w}$ .
6	$\mathbf{y} \sim N(\mathbf{0}, \{\oplus L_j\} (\boldsymbol{\Sigma} \otimes \mathbf{I}_n) \{\oplus L_j^\top\})$	$\mathbf{y} \sim N(\mathbf{0}, \boldsymbol{\Sigma} \otimes \rho(\mathcal{S}))$	$\mathbf{y} \sim N(\mathbf{0}, (\mathbf{A} \otimes \mathbf{I}_n) \{\oplus \rho_j(\mathcal{S})\} (\mathbf{A}^\top \otimes \mathbf{I}_n))$

Table 4: Comparison of prior sampling of IOX and LMCs. We color code the spatial components of the sample cross-covariance matrix in **pink**, the multivariate components in **emerald**.

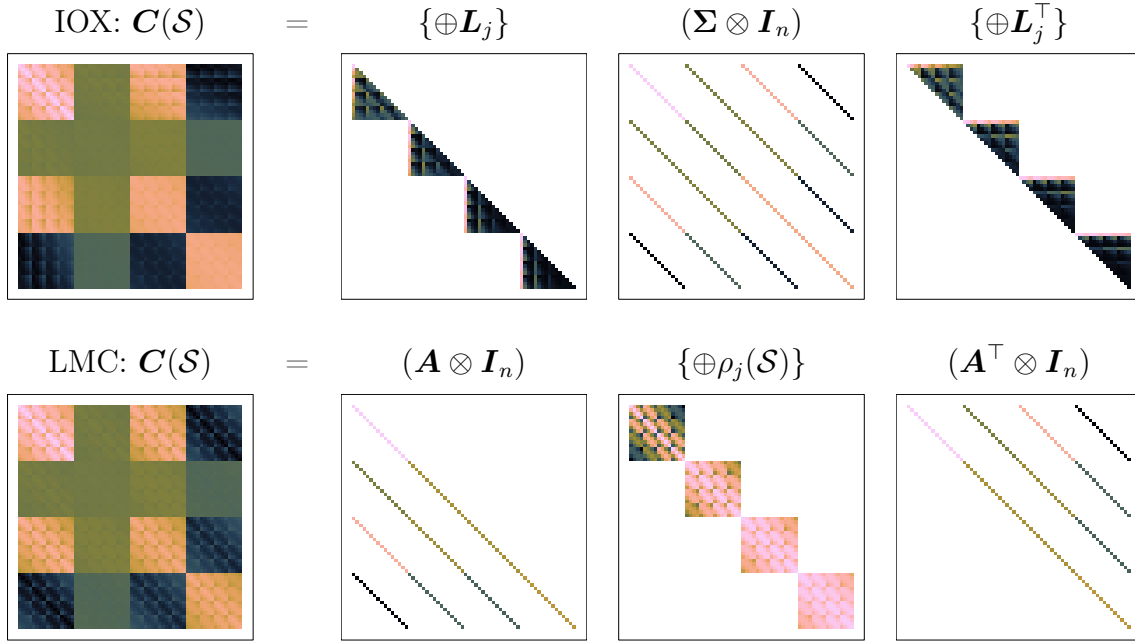


Figure 8: Visualization of IOX and LMC sample covariance matrices and the sparsity patterns of their components.

## C Section 2: *Inside-out cross-covariance*

### C.1 Additional considerations on $C_{ij}(\cdot, \cdot), i \neq j$

Our IOX cross-covariance matrix function is built on the idea that, in practice, we aim to primarily infer about  $C_{ii}(\cdot, \cdot)$  while *accounting* for cross-variable spatial dependence, without the latter being the primary inferential target. In IOX the cross-covariance  $C_{ij}(\cdot, \cdot)$  is not as directly interpretable as  $C_{ii}(\cdot, \cdot)$ . Here, we provide details on (1) how to interpret  $C_{ij}(\cdot, \cdot)$  and (2) how to model  $C_{ij}(\cdot, \cdot)$  more flexibly when explicit parametric models are needed.

For a given  $\mathcal{S}$  and a set of  $\rho_i(\cdot, \cdot)$  and associated parameters, let  $\mathcal{T}$  be a set of  $m$  test

locations, and  $\mathbf{h} = (h_x, h_y)$ . Then, compute

$$\tilde{C}_{ij}(\mathbf{h}) = \frac{1}{mn_a} \sum_{a=1}^{n_a} \sum_{\ell \in \mathcal{T}} C_{ij}(\ell, \ell + \mathbf{h}_\alpha), \quad \text{where } \mathbf{h}_\alpha = \begin{bmatrix} h_x \cos(2\pi a/n_a) \\ h_y \sin(2\pi a/n_a) \end{bmatrix}. \quad (10)$$

In particular, we may be interested in computing  $\tilde{C}_{ij}(\mathbf{0})$ , which reduces (10) to

$$\tilde{C}_{ij}(\mathbf{0}) = \frac{1}{mn_a} \sum_{a=1}^{n_a} \sum_{\ell \in \mathcal{T}} C_{ij}(\ell, \ell). \quad (11)$$

IOX includes a scaling factor which as we showed in the main article results in  $C_{ij}(\ell, \ell') < \sigma_{ij}$  for any  $i, j$  such that  $\rho_i(\cdot, \cdot) \neq \rho_j(\cdot, \cdot)$ . This is unsurprising; suppose  $\mathbf{y}_1$  and  $\mathbf{y}_2$  are two noise-free, jointly IOX variables at  $\mathcal{S}$ . The limit case  $\sigma_{12} \rightarrow 1$  implies near-collinearity of the spatially uncorrelated matrix-normal matrix  $\mathbf{V}$  used to generate  $\mathbf{Y}$  (see Appendix E.1), not of  $\mathbf{Y}$  itself.

Our method restricts the cross-covariances  $C_{ij}(\cdot, \cdot)$  through a product of the marginal Cholesky factors. Consequently,  $C_{ij}(\cdot, \cdot)$  is parametrized directly via  $\sigma_{ij}$  but implicitly on  $\rho_i(\cdot, \cdot)$  and  $\rho_j(\cdot, \cdot)$  and their parameters. For example, if  $\rho_j(\cdot, \cdot)$  is Matérn for all  $j$ ,  $C_{ij}(\cdot, \cdot)$  in IOX is not Matérn and is also not explicitly parametrized via range and smoothness parameters—it depends indirectly on  $1/\phi_i, 1/\phi_j, \nu_i, \nu_j$ . In a bivariate Matérn, on the other hand,  $C_{ij}(\cdot, \cdot)$  is Matérn with smoothness  $\nu_{ij}$  and range  $1/\phi_{ij}$ . We note that these parameters must be chosen carefully to ensure validity of the resulting cross-covariance matrix function (Emery et al. 2022), and interpreting them is also not straightforward (Kleiber 2017). Refer to the discussion at Section B.2 comparing IOX to multivariate Matérns.

In situations in which it is desirable to model  $C_{ij}(\cdot, \cdot)$  flexibly for some  $i, j$ , perhaps as a Matérn, we can straightforwardly generalize IOX. Without loss of generality, let  $\xi = \{1, 2\}$  be the pair of outcomes we wish to model more flexibly and  $\boldsymbol{\rho}_\xi(\cdot, \cdot)$  the marginal cross-correlation matrix function for the  $\xi$  variables.  $\boldsymbol{\rho}_\xi(\cdot, \cdot)$  must be a valid cross-correlation matrix function with  $\rho_{11}(\cdot, \cdot)$ ,  $\rho_{12}(\cdot, \cdot)$  and  $\rho_{22}(\cdot, \cdot)$  margins. Let  $\mathbf{L}_\xi$  the  $2n \times 2n$  lower

Cholesky factor of  $\boldsymbol{\rho}_\xi(\mathcal{S})$ , and let  $\mathbf{h}_\xi(\boldsymbol{\ell}) = \boldsymbol{\rho}_\xi(\boldsymbol{\ell}, \mathcal{S})\boldsymbol{\rho}_\xi(\mathcal{S})^{-1}$ ,  $\mathbf{r}_\xi(\boldsymbol{\ell}) = \boldsymbol{\rho}_\xi(\boldsymbol{\ell}, \boldsymbol{\ell}) - \mathbf{h}_\xi(\boldsymbol{\ell})\boldsymbol{\rho}_\xi(\mathcal{S}, \boldsymbol{\ell})$ .

Finally, let

$$\mathbf{D}_\xi(\boldsymbol{\ell}, \boldsymbol{\ell}') = \mathbb{1}_{\{\boldsymbol{\ell}=\boldsymbol{\ell}'\}} \begin{bmatrix} \text{chol}(\mathbf{r}_\xi(\boldsymbol{\ell})) & & & \\ & \sqrt{r_3(\boldsymbol{\ell})} & & \\ & & \ddots & \\ & & & \sqrt{r_q(\boldsymbol{\ell})} \end{bmatrix}.$$

Then, we can define the IOX cross-covariance matrix function as

$$\begin{aligned} \mathbf{C}(\boldsymbol{\ell}, \boldsymbol{\ell}') &= (\mathbf{h}_\xi(\boldsymbol{\ell})\mathbf{L}_\xi \oplus \{\oplus_{j>2} \mathbf{h}_j(\boldsymbol{\ell})\mathbf{L}_j\}) (\boldsymbol{\Sigma} \otimes \mathbf{I}_n) (\mathbf{L}_\xi^\top \mathbf{h}_\xi(\boldsymbol{\ell})^\top \oplus \{\oplus_{j>2} \mathbf{L}_j^\top \mathbf{h}_j(\boldsymbol{\ell})^\top\}) + \\ &\quad + \mathbf{D}_\xi(\boldsymbol{\ell}, \boldsymbol{\ell}') \boldsymbol{\Sigma} \mathbf{D}_\xi^\top(\boldsymbol{\ell}, \boldsymbol{\ell}') \\ &= \begin{bmatrix} \mathbf{h}_\xi(\boldsymbol{\ell})\mathbf{L}_\xi & & & \\ & \mathbf{h}_3(\boldsymbol{\ell})\mathbf{L}_3 & & \\ & & \ddots & \\ & & & \mathbf{h}_q(\boldsymbol{\ell})\mathbf{L}_q \end{bmatrix} (\boldsymbol{\Sigma} \otimes \mathbf{I}_n) \begin{bmatrix} \mathbf{L}_\xi^\top \mathbf{h}_\xi(\boldsymbol{\ell})^\top & & & \\ & \mathbf{L}_3^\top \mathbf{h}_3(\boldsymbol{\ell})^\top & & \\ & & \ddots & \\ & & & \mathbf{L}_q^\top \mathbf{h}_q(\boldsymbol{\ell})^\top \end{bmatrix} + \\ &\quad + \mathbf{D}_\xi(\boldsymbol{\ell}, \boldsymbol{\ell}') \boldsymbol{\Sigma} \mathbf{D}_\xi^\top(\boldsymbol{\ell}, \boldsymbol{\ell}'), \end{aligned}$$

where we essentially treat  $\xi$  as a grouped variable. The computationally convenient structure of IOX is lost at  $\xi$  but retained for all other variables. Following Proposition 2 in the main article, the marginal cross-covariance of  $\xi$  will be a function of  $\boldsymbol{\rho}_\xi(\cdot, \cdot)$  as desired. We can extend this further to allow explicit models of any groups of variables, at additional computational costs.

## C.2 Covariance-based definition of IOX

We have defined IOX on the basis of  $q$  univariate correlation functions in the main article, but we can equivalently define IOX on a given list of  $q$  covariance functions. Let  $\boldsymbol{\Sigma} = (\sigma_{ij})_{i,j=1}^q$  be a non-negative definite matrix,  $K_i(\cdot, \cdot) = s_i^2 \rho_i(\cdot, \cdot)$  for  $i = 1, \dots, q$ , where  $\rho_i(\cdot, \cdot)$

is a univariate correlation function and let  $\mathcal{S}$  be the reference set. Then, we define IOX as

$$C_{ij}(\boldsymbol{\ell}, \boldsymbol{\ell}') = \sigma_{ij} s_i s_j [\mathbf{h}_i(\boldsymbol{\ell}) \mathbf{L}_i \mathbf{L}_j^\top \mathbf{h}_j(\boldsymbol{\ell}') + \varepsilon(\boldsymbol{\ell}, \boldsymbol{\ell}')],$$

where  $s_j > 0$  for all  $j$ ,  $\mathbf{h}_i(\boldsymbol{\ell}) = \rho_i(\boldsymbol{\ell}, \mathcal{S}) \rho_i(\mathcal{S})^{-1}$ ,  $\mathbf{L}_i$  is the lower Cholesky factor of  $\rho_i(\mathcal{S})$ ,  $\varepsilon(\boldsymbol{\ell}, \boldsymbol{\ell}') = \mathbb{1}_{\{\boldsymbol{\ell}=\boldsymbol{\ell}'\}} \sqrt{r_i(\boldsymbol{\ell}) r_j(\boldsymbol{\ell}')}$ , and  $r_i(\boldsymbol{\ell}) = \rho_i(\boldsymbol{\ell}, \boldsymbol{\ell}) - \mathbf{h}_i(\boldsymbol{\ell}) \rho_i(\mathcal{S}, \boldsymbol{\ell})$ . The validity of the resulting IOX model is verified straightforwardly following the main article. The only change here is that we use  $\boldsymbol{\Sigma}^* = \mathbf{D}_s \boldsymbol{\Sigma} \mathbf{D}_s$ , where  $\mathbf{D}_s = \text{diag}\{s_i\}_{i=1}^q$ , rather than  $\boldsymbol{\Sigma}$ . Clearly,  $\boldsymbol{\Sigma}^*$  is non-negative definite if  $\boldsymbol{\Sigma}$  is. All other components of the model remain the same. In the above model,  $\mathbf{D}_s$  and  $\boldsymbol{\Sigma}$  are not identifiable, but  $\boldsymbol{\Sigma}^*$  is. Therefore, we can use the above setup as a parameter expansion strategy which may improve the efficiency of posterior sampling algorithms; see, e.g., [Peruzzi et al. \(2021\)](#).

## D Section 3: IOX Gaussian process models

### D.1 Latent factor models for the large $q$ case

In addition to reducing dimension by only allowing  $k_1$  distinct correlation functions, IOX can operate dimension reduction by assuming  $\boldsymbol{\Sigma}$  is low rank, i.e.,  $\boldsymbol{\Sigma} = \mathbf{A} \mathbf{A}^\top$  where  $\mathbf{A}$  is a  $q \times k_2$  matrix of full column rank. Changing  $k_2$  has no impact on the marginal properties of IOX because Proposition 2 does not depend on  $k_2$ . Let  $\tilde{\mathbf{y}} = \{\oplus \mathbf{L}_j^{-1}\}(\mathbf{y} - \mathbf{X}_q \boldsymbol{\beta})$  and  $\tilde{\boldsymbol{\varepsilon}} = \{\oplus \mathbf{L}_j^{-1}\} \boldsymbol{\varepsilon}$ . We can rewrite (7) as

$$\tilde{\mathbf{y}} = \mathbf{v} + \tilde{\boldsymbol{\varepsilon}}, \quad \mathbf{v} \sim N(\mathbf{0}, \boldsymbol{\Sigma} \otimes \mathbf{I}_n), \quad \tilde{\boldsymbol{\varepsilon}} \sim N(\mathbf{0}, \mathbf{B}), \quad (12)$$

where  $\mathbf{B}$  is a block-diagonal matrix whose  $j$ th block is  $\mathbf{L}_i^{-1} \mathbf{L}_i^{-\top}$ . Then, letting  $\mathbf{u}(\boldsymbol{\ell}) \stackrel{iid}{\sim} N(\mathbf{0}, \mathbf{I}_{k_2})$  we have  $\mathbf{v}(\boldsymbol{\ell}) = \mathbf{A} \mathbf{u}(\boldsymbol{\ell})$ . In matrix form,  $\tilde{\mathbf{Y}} = \mathbf{U} \mathbf{A}^\top + \tilde{\mathbf{E}}$ , where  $\mathbf{U} \sim MN(\mathbf{0}, \mathbf{I}_n, \mathbf{I}_{k_2})$  and  $\tilde{\mathbf{E}} \sim MN(\mathbf{0}, \mathbf{B}, \mathbf{I}_q)$ . A low-rank  $\boldsymbol{\Sigma}$  leads to computational savings in sampling  $\mathbf{w}$ . We

obtain

$$\begin{aligned}
\mathbf{M}_{w|y}^{-1} &= \{\oplus \mathbf{L}_i^{-\top}\}(\boldsymbol{\Sigma}^{-1} \otimes \mathbf{I}_n)\{\oplus \mathbf{L}_i^{-1}\} + (\boldsymbol{\Delta}^{-1} \otimes \mathbf{I}_n) \\
&= \{\oplus \mathbf{L}_i^{-\top}\}(\mathbf{A}^{+\top} \otimes \mathbf{I}_n)(\mathbf{A}^+ \otimes \mathbf{I}_n)\{\oplus \mathbf{L}_i^{-1}\} + (\boldsymbol{\Delta}^{-1} \otimes \mathbf{I}_n) \\
&= \mathbf{K}\mathbf{K}^\top + (\boldsymbol{\Delta}^{-1} \otimes \mathbf{I}_n)
\end{aligned}$$

where  $\mathbf{K} = \{\oplus \mathbf{L}_i^{-\top}\}(\mathbf{A}^{+\top} \otimes \mathbf{I}_n)$  is a  $nq \times nk_2$  matrix, and  $\mathbf{A}^+$  is the  $k_2 \times q$  Moore-Penrose pseudoinverse of  $\mathbf{A}$ . Although the prior on  $\mathbf{w}$  is singular if  $k_2 < q$ , the posterior is well-defined, since  $\mathbf{M}_{w|y}$  is full rank. We can then take advantage of the Woodbury matrix identity in sampling  $\mathbf{w}$  a posteriori to make the cost for sampling  $\mathbf{w}$  depend on  $k_2$  rather than  $q$ . Finally, to update  $\mathbf{A}$  we first deterministically compute  $\mathbf{u} = \mathbf{A}^+\{\oplus \mathbf{L}_i^{-1}\}\mathbf{w}$ , then, since  $\tilde{\mathbf{y}}_i = \mathbf{U}\mathbf{A}[i, :]^\top + \tilde{\boldsymbol{\varepsilon}}_i$ , we update each row of  $\mathbf{A}$  in parallel. Under a Gaussian prior on  $\mathbf{A}[i, :]^\top$  with prior covariance  $\mathbf{M}_A$ , the full conditional distribution is Gaussian with precision matrix  $\mathbf{U}^\top \mathbf{L}_i^\top \mathbf{L}_i \mathbf{U} + \mathbf{M}_A^{-1}$ . Here, computing  $\mathbf{L}_i \mathbf{U}$  involves solving the linear system  $\mathbf{L}_i^{-1} \boldsymbol{\alpha} = \mathbf{U}$ , which is cheap because  $\mathbf{L}_i^{-1}$  is triangular.

Due to the dimension of  $\mathbf{M}_{w|y}$ , single block updates of  $\mathbf{w}$  may be computationally prohibitive in large  $n$  settings, even if we assume a sparse DAG,  $k_2$  is relatively small, and we use sparse Cholesky (Chen et al. 2008) or preconditioned conjugate gradient methods (Nishimura & Suchard 2023). Instead of block sampling, we can take advantage of an assumed sparse DAG GP as in Section 5 and sample from the full conditional distributions at DAG nodes. The Appendix includes an in-depth discussion on a single-site sequential sampler for GP-IOX, where we outline the computational advantages of assuming  $k_2 \ll q$  in the large  $q$  setting.

## E Section 4: *Computations with GP-IOX models*

### E.1 Prior sampling

Let  $\mathcal{T}$  be sample locations. We consider two scenarios. The first is  $\mathcal{S} = \mathcal{T}$ , the second is  $\mathcal{T} \subset \mathcal{S}^c$ .

For the scenario  $\mathcal{S} = \mathcal{T}$ , from  $\rho_j(\cdot, \cdot)$ , compute  $\mathbf{L}_j$  for  $j = 1, \dots, q$ . For all  $\ell_i \in \mathcal{T}$  let  $\mathbf{v}(\ell_i) \stackrel{iid}{\sim} N(\mathbf{0}, \Sigma)$ . Denote  $\mathbf{V} = [\mathbf{v}(\ell_1) \cdots \mathbf{v}(\ell_n)]^\top$ —therefore,  $\mathbf{V}$  is a matrix-normal random matrix  $\mathbf{V} \sim MN(\mathbf{0}, \mathbf{I}_n, \Sigma)$ . Then,  $\mathbf{y} = \{\oplus \mathbf{L}_j\} \text{vec}(\mathbf{V})$  is  $\mathbf{y} \sim N(\mathbf{0}, \{\oplus \mathbf{L}_j\}(\Sigma \otimes \mathbf{I}_n)\{\oplus \mathbf{L}_j^\top\})$  as desired. Figure 1 shows an example in which we generate 3 spatially correlated outcomes with different smoothness via IOX. If only  $\mathbf{L}_i^{-1}$  is available for  $i = 1, \dots, q$ , then from  $\mathbf{v}_j$  (the  $j$ th column of  $\mathbf{V}$ ), one obtains  $\mathbf{y}_j = \text{solve}(\mathbf{L}_j^{-1}, \mathbf{v}_j)$  without needing to compute  $\mathbf{L}_i$  directly.

For the second scenario, let  $\mathcal{T} = \{\mathbf{t}_1, \dots, \mathbf{t}_N\}$  be sample locations and  $\mathcal{S} = \{\ell_1, \dots, \ell_n\}$ . We assume  $\mathcal{T} \subset \mathcal{S}^c$ . From  $\rho_j(\cdot, \cdot)$ , compute  $\mathbf{L}_j = \text{chol}(\rho_j(\mathcal{S}))$  for  $j = 1, \dots, q$ . For all  $\ell_i \in \mathcal{S}$  let  $\mathbf{v}(\ell_i) \stackrel{iid}{\sim} N(\mathbf{0}, \Sigma)$ . Denote  $\mathbf{V} = [\mathbf{v}(\ell_1) \cdots \mathbf{v}(\ell_n)]^\top$ —therefore,  $\mathbf{V}$  is a matrix-normal random matrix  $\mathbf{V} \sim MN(\mathbf{0}, \mathbf{I}_n, \Sigma)$ . Then,  $\mathbf{y}_\mathcal{S} = \{\oplus \mathbf{L}_j\} \text{vec}(\mathbf{V})$  is  $\mathbf{y} \sim N(\mathbf{0}, \{\oplus \mathbf{L}_j\}(\Sigma \otimes \mathbf{I}_n)\{\oplus \mathbf{L}_j^\top\})$  as desired. Finally, for each  $\mathbf{t} \in \mathcal{T}$  sample from  $N(\mathbf{y}(\mathbf{t}); \mathbf{m}_y(\mathbf{t}), \mathbf{R}(\mathbf{t}))$ , where  $\mathbf{m}_y(\mathbf{t}) = \mathbf{H}(\mathbf{t})\mathbf{y}_\mathcal{S}$ ,  $\mathbf{H}(\mathbf{t}) = \{\oplus \mathbf{h}_j(\mathbf{t})\}$  and  $\mathbf{R}(\mathbf{t}) = \mathbf{D}(\mathbf{t}, \mathbf{t})\Sigma\mathbf{D}(\mathbf{t}, \mathbf{t})$ . We take  $\mathcal{S}$  as a  $100 \times 100$  regular grid in  $\mathcal{D} = [0, 1]^2$  and sample a noise-free trivariate GP-IOX at a regular grid of dimension  $200 \times 200$  using the same parameter settings as in Figure 1. Figure 9 shows the resulting maps.

We outline an equivalent method for prior sampling. Call  $\mathcal{G}_\mathcal{S}$  the DAG at  $\mathcal{S}$  and let the DAG for  $\mathcal{S} \cup \mathcal{T}$ ,  $\mathcal{G}$ , be such that each node from  $\mathcal{T}$  has  $\mathcal{S}$  as its set of parents. For Vecchia-GP models, the set of parents for  $\mathbf{t} \in \mathcal{T}$  is restricted to the nearest neighbors within  $\mathcal{S}$ . Based on

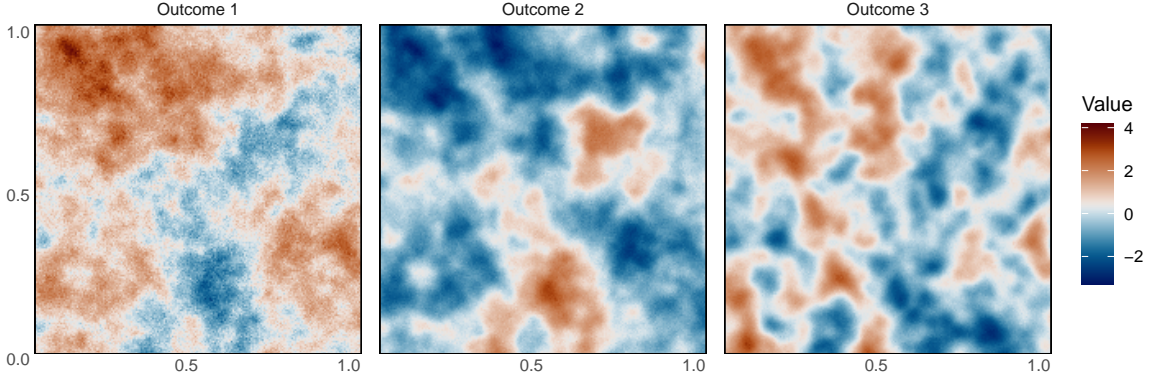


Figure 9: Three spatially correlated outcomes generated via GP-IOX at  $n = 40,000$  gridded locations from a reference set of size  $n_S = 2,500$ . We let  $\sigma_{ii} = 1$  for  $i \in \{1, 2, 3\}$  and  $\sigma_{12} = -0.9, \sigma_{13} = 0.7, \sigma_{23} = -0.5$  and choose  $\rho_i(\cdot, \cdot)$  as Matérn (Vecchia-approximated with  $m = 50$  neighbors) with range  $1/5, 1/15, 1/30$  and smoothness  $0.5, 1.2, 1.9$ , respectively.

the DAG, compute  $\mathbf{L}_j^{-1}$  from  $j = 1, \dots, q$ . The elements of  $\mathbf{L}_j^{-1}$  can be directly computed in the following way. Let  $\mathbf{h}_l = \rho_i(\boldsymbol{\ell}_l, \boldsymbol{\ell}_{[l]})\rho_i(\boldsymbol{\ell}_{[l]})^{-1}$ ,  $\mathbf{r}_l = \rho_i(\boldsymbol{\ell}_l, \boldsymbol{\ell}_l) - \mathbf{h}_l\rho_i(\boldsymbol{\ell}_{[l]}, \boldsymbol{\ell}_l)$ , where  $[l]$  denotes the set of parents of node  $l$  in the graph  $\mathcal{G}$ . Then, the diagonal elements of  $\mathbf{L}_j^{-1}$  are  $1/\sqrt{\mathbf{r}_\ell}$  for  $\boldsymbol{\ell} \in \mathcal{S} \cup \mathcal{T}$ . The non-zero elements of row  $a$  are  $-\mathbf{h}_a/\sqrt{\mathbf{r}_a}$ . Moving on, for all  $\boldsymbol{\ell} \in \mathcal{S} \cup \mathcal{T}$ , let  $\mathbf{v}(\boldsymbol{\ell}) \stackrel{iid}{\sim} N(\mathbf{0}, \boldsymbol{\Sigma})$ . Denote  $\mathbf{V} = [\mathbf{v}(\boldsymbol{\ell}_1) \cdots \mathbf{v}(\boldsymbol{\ell}_n), \mathbf{v}(\boldsymbol{t}_1), \dots, \mathbf{v}(\boldsymbol{t}_N)]^\top$ —therefore,  $\mathbf{V}$  is a matrix-normal random matrix  $\mathbf{V} \sim MN(\mathbf{0}, \mathbf{I}_{n+N}, \boldsymbol{\Sigma})$ . Then, let  $\mathbf{y} = \{\oplus \mathbf{L}_j\} \text{vec}(\mathbf{V})$  and build the  $(n + N) \times q$  matrix  $\mathbf{Y}$  from  $\mathbf{y}$  in column-major ordering. The last  $N$  rows of  $\mathbf{Y}$  have the desired marginal distribution.

## E.2 Posterior sampling: response model

We outline the remainder of the Gibbs sampler for the model in Section 3.1. For  $\boldsymbol{\beta}$ , we have  $p(\boldsymbol{\beta} \mid \mathbf{y}, \boldsymbol{\theta}, \boldsymbol{\Sigma}) = N(\mathbf{m}_{\boldsymbol{\beta}|\mathbf{y}}, \mathbf{M}_{\boldsymbol{\beta}|\mathbf{y}})$ , where

$$\mathbf{M}_{\boldsymbol{\beta}|\mathbf{y}}^{-1} = \mathbf{M}_{\boldsymbol{\beta}}^{-1} + \mathbf{X}_q^\top \mathbf{C}^{-1} \mathbf{X}_q \quad \text{and} \quad \mathbf{M}_{\boldsymbol{\beta}|\mathbf{y}}^{-1} \mathbf{m}_{\boldsymbol{\beta}|\mathbf{y}} = \mathbf{V}_{\boldsymbol{\beta}}^{-1} \mathbf{m}_{\boldsymbol{\beta}} + \mathbf{X}_q^\top \mathbf{C}^{-1} \mathbf{y}.$$



For updating  $\Sigma$ , first compute  $\mathbf{U} = \mathbf{Y} - \mathbf{X}\mathbf{B}$ , where  $\mathbf{B}$  is the  $p \times q$  matrix of regression coefficients. Then, compute the  $nq$ -dimensional vector  $\mathbf{v} = \{\oplus \mathbf{L}_i^{-1}\} \text{vec}(\mathbf{U})$ , where dependence on  $\boldsymbol{\theta}$  is through  $\mathbf{L}_i$ ,  $i = 1, \dots, q$ . Then build the  $n \times q$  matrix  $\mathbf{V}$  such that  $\text{vec}(\mathbf{V}) = \mathbf{v}$ . Notice that  $\mathbf{V}$  is the centered and spatially “whitened” version of  $\mathbf{Y}$ , and according to our model,  $\mathbf{V} \sim MN(\mathbf{0}, \mathbf{I}_n, \Sigma)$ . Then, with the prior  $p(\Sigma) \propto \det(\Sigma)^{-\frac{\nu_\Sigma + q + 1}{2}} \exp\{-\frac{\text{tr}(\Psi \Sigma^{-1})}{2}\}$ , i.e.,  $\Sigma \sim \mathcal{W}^{-1}(\nu_\Sigma, \Psi^{-1})$ , the conditional posterior is  $p(\Sigma \mid \mathbf{y}, \boldsymbol{\theta}, \boldsymbol{\beta}) = \mathcal{W}^{-1}(\nu_{\Sigma|y}, \Psi_{\Sigma|y}^{-1})$ , where  $\nu_{\Sigma|y} = \nu_\Sigma + n$  and  $\Psi_{\Sigma|y} = \Psi + \mathbf{V}^\top \mathbf{V}$ .

### E.3 Posterior sampling: latent model

We outline the remainder of the Gibbs sampler for the model in Section 3.2. For  $\boldsymbol{\beta}$ , we have  $p(\boldsymbol{\beta} \mid \mathbf{y}, \mathbf{w}, \Delta) = N(\mathbf{m}_{\boldsymbol{\beta}|y}, \mathbf{M}_{\boldsymbol{\beta}|y})$ , where

$$\mathbf{M}_{\boldsymbol{\beta}|y}^{-1} = \mathbf{M}_{\boldsymbol{\beta}}^{-1} + \mathbf{X}_q^\top (\Delta^{-1} \otimes \mathbf{I}_n) \mathbf{X}_q \quad \text{and} \quad \mathbf{M}_{\boldsymbol{\beta}|y}^{-1} \mathbf{m}_{\boldsymbol{\beta}|y} = \mathbf{M}_{\boldsymbol{\beta}}^{-1} \mathbf{m}_{\boldsymbol{\beta}} + \mathbf{X}_q^\top (\Delta^{-1} \otimes \mathbf{I}_n) (\mathbf{y} - \mathbf{w}).$$

For  $\Sigma$ , the Bayesian DAG implies  $p(\Sigma \mid \mathbf{y}, \boldsymbol{\beta}, \mathbf{w}, \Delta, \boldsymbol{\theta}) = p(\Sigma \mid \mathbf{w}, \boldsymbol{\theta})$ . We again let  $\Sigma \sim \mathcal{W}^{-1}(\nu_\Sigma, \Psi^{-1})$ . Compute the  $nq$ -dimensional vector  $\mathbf{v} = \{\oplus \mathbf{L}_i^{-1}\} \text{vec}(\mathbf{W})$ , where dependence on  $\boldsymbol{\theta}$  is through  $\mathbf{L}_i$ ,  $i = 1, \dots, q$ . Then build the  $n \times q$  matrix  $\mathbf{V}$  such that  $\text{vec}(\mathbf{V}) = \mathbf{v}$ . Then,  $p(\Sigma \mid \mathbf{w}) = \mathcal{W}^{-1}(\nu_{\Sigma|w}, \Psi_{\Sigma|w}^{-1})$ , where  $\nu_{\Sigma|w} = \nu_\Sigma + n$  and  $\Psi_{\Sigma|w}^{-1} = \Psi + \mathbf{V}^\top \mathbf{V}$ . Finally, we update  $\Delta = \text{diag}\{\delta_{ii}\}_{i=1, \dots, q}$ . For each  $j$ , we sample  $\delta_{jj} \mid \mathbf{y}_j, \boldsymbol{\beta}_j, \mathbf{w}_j$  from an Inverse Gamma distribution with parameters  $a_{d|y} = a_d + n/2$  and  $b_{d|y} = b_d + \frac{1}{2} \tilde{\mathbf{y}}_j^\top \tilde{\mathbf{y}}_j$ , where  $\tilde{\mathbf{y}}_j = \mathbf{y}_j - \mathbf{X} \boldsymbol{\beta}_j - \mathbf{w}_j$ .

### E.4 Sequential single-site sampler for sparse latent models

Suppose we build IOX with a Vecchia-approximated  $\tilde{\rho}_j(\cdot, \cdot)$  for each  $i = 1, \dots, q$ . As a consequence,  $\tilde{\rho}_j(\mathcal{S})^{-1} = \tilde{\mathbf{L}}_j^{-1} \tilde{\mathbf{L}}_j^{-1}$  where  $\tilde{\mathbf{L}}_j^{-1}$  is sparse. Moving forward, we will denote  $\mathbf{L}_i = \tilde{\mathbf{L}}_i$  to reduce the burden of notation and similarly for  $\tilde{\rho}_j(\cdot, \cdot)$ . A consequence of our

sparsity assumption is that we want to work with  $\mathbf{L}_j^{-1}$  and  $\rho_j(\mathcal{S})^{-1}$ , and *not* with  $\mathbf{L}_j$  and  $\rho_i(\mathcal{S})$ , because the former pair are sparse, whereas the latter are high dimensional and dense even when the DAG is sparse.

Without loss of generality, we assume a single sparse DAG for each  $j = 1, \dots, q$ , resulting in  $\mathbf{L}_j^{-1}$  having the same sparsity pattern for all  $j$ . Assume a nearest-neighbor DAG for simplicity, so the first  $m$  nodes in the DAG have  $0, 1, \dots, m - 1$  parents, respectively, and all remaining ones have  $m$  parents. In this DAG, there is one node for each location of  $\mathcal{S}$ . At  $\mathcal{S}$ , the latent model is

$$\begin{aligned} \mathbf{w} &\sim N(\mathbf{0}, \mathbf{C}) & \mathbf{C} &= \{\oplus \mathbf{L}_i\}(\boldsymbol{\Sigma} \otimes \mathbf{I}_n)\{\oplus \mathbf{L}_i^\top\} \\ \mathbf{y} &= \mathbf{w} + \boldsymbol{\varepsilon} & \boldsymbol{\varepsilon} &\sim N(\mathbf{0}, \boldsymbol{\Delta} \otimes \mathbf{I}_n). \end{aligned}$$

We have discussed block-updating  $\mathbf{w}$  in the main article. Here, we target sequential single-site updates. Let  $[i]$  denote the set of parent nodes of  $i$ . For simplicity, consider a location  $\ell_i$  corresponding to node  $i$  with  $m$  parents. In this section we let  $\mathbf{y}_i = \mathbf{y}(\ell_i) - (\mathbf{I}_q \otimes \mathbf{x}^\top(\ell_i))\boldsymbol{\beta}$  and  $\mathbf{w}_i = \mathbf{w}(\ell_i)$ ,  $\boldsymbol{\varepsilon}_i = \boldsymbol{\varepsilon}(\ell_i)$  to simplify notation. The single-site hierarchical model is

$$\begin{aligned} \mathbf{w}_i &= \mathbf{H}_i \mathbf{w}_{[i]} + \boldsymbol{\eta}_i & \boldsymbol{\eta}_i &\sim N(\mathbf{0}, \mathbf{R}_i) \\ \mathbf{y}_i &= \mathbf{w}_i + \boldsymbol{\varepsilon}_i & \boldsymbol{\varepsilon}_i &\sim N(\mathbf{0}, \boldsymbol{\Delta}) \end{aligned}$$

where  $\ell_{[i]} = \{\ell_j \in \mathcal{S} : j \rightarrow i\}$ ,  $\mathbf{w}_{[i]}$  is a  $qm \times 1$  vector storing the values of the latent effects at  $\ell_{[i]}$ , and  $\mathbf{H}_i = \mathbf{C}(i, [i])\mathbf{C}([i])^{-1}$  and  $\mathbf{R}_i = \mathbf{C}(i, i) - \mathbf{H}_i \mathbf{C}(i, [i])^\top$ , where we let  $\mathbf{C}(i, [i]) = \mathbf{C}(\ell_i, \ell_{[i]})$ . Here, we refer to  $\mathbf{C}$  as the sample cross-covariance matrix as well as the IOX cross-covariance matrix function since  $\mathbf{C}(i, [i])$  is the cross-covariance computed at  $\ell_i$  against  $\ell_{[i]}$  and, equivalently, the  $q \times mq$  matrix reading the rows and columns of  $\mathbf{C}$  corresponding to  $i$  and  $[i]$ , respectively.

Single-site updates generally proceed by sequentially updating  $\mathbf{w}_i$  conditional on  $\mathbf{w}_{i^c}$ ,

i.e., the value of  $\mathbf{w}$  at  $\mathcal{S} \setminus \{i\}$ . Let the  $nq \times nq$  precision matrix be  $\mathbf{P} = \mathbf{C}^{-1}$  and let  $i^c = \mathcal{S} \setminus \{i\}$ . The properties of block matrix inverses imply that we can define

$$\begin{aligned} \mathbf{B}_i &:= (\mathbf{C}(i, i) - \mathbf{C}(i, i^c)\mathbf{C}(i^c)^{-1}\mathbf{C}(i, i^c)^\top)^{-1} = \mathbf{P}(i, i) \\ \mathbf{b}_i &:= \mathbf{C}(i, i^c)\mathbf{C}(i^c)^{-1} = -\mathbf{P}(i, i)^{-1}\mathbf{P}(i, i^c), \end{aligned} \tag{13}$$

where  $\mathbf{P}(i, i)$  is a  $q \times q$  and  $\mathbf{P}(i, i^c)$  a  $q \times (n-1)q$  submatrix of  $\mathbf{P}$ , which is sparse. Then, let  $\mathbf{w}_{i^c}$  be the vector of  $\mathbf{w}$  at  $\mathcal{S} \setminus \{i\}$ . The full conditional update for  $\mathbf{w}_i$  is  $p(\mathbf{w}_i \mid \mathbf{w}_{i^c}, \mathbf{y}_i) = N(\mathbf{g}_i, \mathbf{G}_i)$ , where, after seeing that  $\mathbf{B}_i\mathbf{b}_i = -\mathbf{P}(i, i^c)$ , we have

$$\mathbf{G}_i = \mathbf{P}(i, i) + \mathbf{\Delta}^{-1}, \quad \mathbf{G}_i^{-1}\mathbf{g}_i = -\mathbf{P}(i, i^c)\mathbf{w}_{i^c} + \mathbf{\Delta}^{-1}\mathbf{y}_i. \tag{14}$$

This result follows from a conjugate update of the Gaussian ‘‘prior’’  $N(\mathbf{w}_i; \mathbf{b}_i\mathbf{w}_{i^c}, \mathbf{B}_i)$  on the Gaussian likelihood  $N(\mathbf{y}_i; \mathbf{w}_i, \mathbf{\Delta})$ .

Without sparsity assumptions on the DAG, single-site updates are as costly if not more costly than block updates, due to the size of  $i^c$  which leads to large costs in computing and sampling from each  $p(\mathbf{w}_i \mid \mathbf{w}_{i^c})$ . But because we assume a sparse DAG on  $\mathbf{w}$ , we can write  $p(\mathbf{w}_i \mid \mathbf{w}_{i^c}) = p(\mathbf{w}_i \mid \mathbf{w}_{b_i})$ , where  $b_i$  is the Markov blanket of  $i$  in the DAG. The Markov blanket of  $i$  is the set of nodes (locations)  $j$  such that  $j$  is either (1) a parent of  $i$ , that is  $j \rightarrow i$  in the DAG, (2) a child of  $i$ :  $i \rightarrow j$ , or (3) a co-parent of  $i$ : there is  $r$  such that  $i \rightarrow r$  and  $j \rightarrow r$ . Based on the precision matrix  $\rho_r(\mathcal{S})^{-1}$ , we find  $b_i$  as the list of non-zero indices of its  $i$ th column (or row), minus  $i$  itself. Then, (13) simplifies with  $\mathbf{b}_i = -\mathbf{P}(i, i)^{-1}\mathbf{P}(i, b_i)$  and similarly in (14) where we replace  $\mathbf{P}(i, i^c)$  with  $\mathbf{P}(i, b_i)$ .

Further, we can avoid calculating  $\mathbf{P}$  and instead directly use  $\mathbf{L}_j^{-1}$  for each  $j = 1, \dots, q$  for all computations. Denote as  $\mathbf{\Gamma}_j[:, i]$  the  $i$ th column of  $\mathbf{\Gamma}_j = \mathbf{L}_j^{-1}$ . Then,

$$\begin{aligned} \mathbf{P}(i, i) &= \{\oplus \mathbf{\Gamma}_j[:, i]^\top\}(\mathbf{\Sigma}^{-1} \otimes \mathbf{I}_n)\{\oplus \mathbf{\Gamma}_j[:, i]\} = \mathbf{\Sigma}^{-1} \odot \left[ \mathbf{\Gamma}_r[:, i]^\top \mathbf{\Gamma}_s[:, i] \right]_{r,s=1,\dots,q} \\ \mathbf{P}(i, b_i) &= \{\oplus \mathbf{\Gamma}_j[:, i]^\top\}(\mathbf{\Sigma}^{-1} \otimes \mathbf{I}_n)\{\oplus \mathbf{\Gamma}_j[:, b_i]\} = (\mathbf{\Sigma}^{-1} \odot \mathbf{1}_{1,|b_i|}) \left[ \mathbf{\Gamma}_r[:, i]^\top \mathbf{\Gamma}_s[:, b_i] \right]_{r,s=1,\dots,q}, \end{aligned} \tag{15}$$

where  $|b_i|$  is the dimension of  $b_i$  and we use a similar argument to Proposition 4 in the first row to express  $\mathbf{P}(i, i)$  as a Hadamard product. Computing (15) for each  $i = 1, \dots, n$  as well as  $\mathbf{G}_i$  (and its Cholesky factor) in (14) can be performed in parallel.

If  $q$  is large and we factorize  $\Sigma = \mathbf{A}\mathbf{A}^\top$  where  $\mathbf{A}$  has  $k_2 \ll q$  columns, then we have shown in the main article how we can achieve speedups in the block sampler via the Woodbury matrix identity. We can do something similar here. First, denote  $c_i = \{i\} \cup \{j : i \rightarrow j\}$ , i.e., the set of children of  $i$  along with  $i$  itself; the dimension of  $c_i$  is  $|c_i|$ . Then, we can write

$$\mathbf{P}(i, i) = \{\oplus \mathbf{\Gamma}_j[c_i, i]^\top\}(\Sigma^{-1} \otimes \mathbf{I}_{|c_i|})\{\oplus \mathbf{\Gamma}_j[c_i, i]\}$$

which is useful in reducing the inner matrix dimension. Then,  $\Sigma^{-1}$  does not exist, but the unique pseudoinverse  $\Sigma^+ = \mathbf{A}^{+\top} \mathbf{A}^+$  does, and is such that  $\mathbf{A}^+$  is of dimension  $k_2 \times q$ . Then, in (14) we find

$$\begin{aligned} \mathbf{G}_i^{-1} &= (\mathbf{P}(i, i) + \Delta^{-1})^{-1} = (\{\oplus \mathbf{\Gamma}_j[c_i, i]^\top\}(\mathbf{A}^{+\top} \otimes \mathbf{I}_{|c_i|})(\mathbf{A}^+ \otimes \mathbf{I}_{|c_i|})\{\oplus \mathbf{\Gamma}_j[c_i, i]\} + \Delta^{-1})^{-1} \\ &= (\mathbf{J}\mathbf{J}^\top + \Delta^{-1})^{-1} = \Delta - \Delta\mathbf{J}(\mathbf{I}_{|c_i|k_2} + \mathbf{J}^\top \Delta \mathbf{J})^{-1} \mathbf{J}^\top \Delta, \end{aligned} \tag{16}$$

where we let  $\mathbf{J} = \{\oplus \mathbf{\Gamma}_j[c_i, i]^\top\}(\mathbf{A}^{+\top} \otimes \mathbf{I}_{|c_i|})$ , which is of dimension  $|c_i|q \times |c_i|k_2$  and we use the Woodbury matrix identity to find the last equality. The required inverse is of dimension  $|c_i|k_2$ , meaning that for (16) to be advantageous compared to (15), we need  $|c_i|k_2 < q$ . In nearest-neighbor DAGs, one controls the number of parents  $m$  whereas the number of children varies across locations and may be large. For this reason, the radial neighbors DAG (Zhu et al. 2024) may be a convenient choice in this case; in a radial neighbors DAG, all neighbors of  $\ell_i$  within radius  $r$  are either parents or children of  $i$  in the DAG. Consequently,  $r$  indirectly bounds  $|c_i| \leq |\{\ell \in \mathcal{S} : |\ell - \ell_i| \leq r\}|$ .

What we have just shown is that the structure induced by IOX leads to computations of the conditional mean and covariance of  $p(\mathbf{w}_i | \mathbf{w}_{b_i}, \mathbf{y}_i)$  by either reading elements of the

precision matrix  $\mathbf{P}$ , or via simple dot products between columns of the sparse matrices  $\mathbf{\Gamma}_j = \mathbf{L}_j^{-1}$  and without ever directly computing  $\mathbf{L}_i$  or  $\rho_i(\mathcal{S})$ .

## E.5 Compute cost of proposed scalable algorithms

We detail the computational complexity of the scalable algorithms outlined in the main article. Our assumption here is that  $n$  is very large and  $n \gg q$ , leading to computational cost being dominated by operations along the spatial sites. We also assume a sparse DAG GP using  $m$  nearest neighbors. We compute  $\mathbf{L}_i$  at  $O(nm^3)$  flops for each  $i = 1, \dots, q$ , for a total of  $O(qnm^3)$ . With clustering of the correlation functions into  $k_1$  groups, this operation reduces to  $O(k_1nm^3)$ . Determinant and inverse of  $\mathbf{\Sigma}$  are cheap to compute in requiring  $O(q^3)$  flops, independent of  $n$ .

In the block sampler for the latent model  $\mathbf{M}_{w|y}$  is a  $nq \times nq$  sparse matrix. One can use iterative matrix solvers such as conjugate gradient (CG); at each iteration, CG performs a matrix-vector multiplication (cost  $O(n_{\text{nz}})$ ), for a total number of iterations that is guaranteed to be less than  $nq$  and can be reduced via preconditioning. The cost for solving  $\mathbf{M}_{w|y}$  is in the order of  $O(n_{\text{nz}}c)$  where  $n_{\text{nz}}$  is the number of nonzeros of  $\mathbf{C}^{-1}$ , and  $c$  is the condition number of  $\mathbf{M}_{w|y}$ .

## F Software and applications

All the code to generate figures and simulations is available at [github.com/mkln/spiox](https://github.com/mkln/spiox) along with the R package for running the response model and the three algorithms we outlined for the latent model (block,  $q$  sequential,  $n$  sequential). The R package is implemented in C++ using the Armadillo library (Sanderson & Curtin 2016) via RcppArmadillo (Eddelbuettel & Sanderson 2014). Parallel operations are performed via OpenMP

(Dagum & Menon 1998). For fast linear algebra, we recommend to link R with efficient BLAS/LAPACK libraries (Anderson et al. 1999) such as OpenBLAS (Zhang 2020). All our analyses are run on a workstation equipped with a 16-core AMD Ryzen 9 7950X3D CPU, 192GB memory, using Intel Math Kernel Library version 2024.2 (Intel Corporation 2024) for fast linear algebra and SuperLU (Li 2005) as a sparse solver.

## References

- Albert, J. H. & Chib, S. (1993), ‘Bayesian analysis of binary and polychotomous response data’, *Journal of the American Statistical Association* **88**(422), 669–679. [doi:10.2307/2290350](https://doi.org/10.2307/2290350). 15
- Alie, R., Stephens, D. A. & Schmidt, A. M. (2024), ‘Computational considerations for the linear model of coregionalization’. [arXiv:2402.08877](https://arxiv.org/abs/2402.08877). 3
- Álvarez, M. A. & Lawrence, N. D. (2011), ‘Computationally efficient convolved multiple output Gaussian processes’, *Journal of Machine Learning Research* **12**(41), 1459–1500. <http://jmlr.org/papers/v12/alvarez11a.html>. 3
- Anderson, E., Bai, Z., Bischof, C., Blackford, S., Demmel, J., Dongarra, J., Du Croz, J., Greenbaum, A., Hammarling, S., McKenney, A. & Sorensen, D. (1999), *LAPACK Users’ Guide*, third edn, Society for Industrial and Applied Mathematics, Philadelphia, PA. 54
- Apanasovich, T. V. & Genton, M. G. (2010), ‘Cross-covariance functions for multivariate random fields based on latent dimensions’, *Biometrika* **97**, 15–30. [doi:10.1093/biomet/asp078](https://doi.org/10.1093/biomet/asp078). 4
- Apanasovich, T. V., Genton, M. G. & Sun, Y. (2012), ‘A valid Matérn class of cross-covariance functions for multivariate random fields with any number of

- components’, *Journal of the American Statistical Association* **107**(497), 180–193.  
[doi:10.1080/01621459.2011.643197](https://doi.org/10.1080/01621459.2011.643197). 4, 39
- Banerjee, S., Finley, A. O., Waldmann, P. & Ericsson, T. (2010), ‘Hierarchical spatial process models for multiple traits in large genetic trials’, *Journal of American Statistical Association* **105**(490), 506–521. [doi:10.1198/jasa.2009.ap09068](https://doi.org/10.1198/jasa.2009.ap09068). 7
- Banerjee, S., Gelfand, A. E., Finley, A. O. & Sang, H. (2008), ‘Gaussian predictive process models for large spatial data sets’, *Journal of the Royal Statistical Society, Series B* **70**, 825–848. [doi:10.1111/j.1467-9868.2008.00663.x](https://doi.org/10.1111/j.1467-9868.2008.00663.x). 7, 9
- Berrocal, V., Gelfand, A. E. & Holland, D. M. (2010), ‘A bivariate space–time downscaler under space and time misalignment’, *The Annals of Applied Statistics* **4**(4), 1942–1975.  
3
- Chandra, N. K., Mueller, P. & Sarkar, A. (2022), ‘Bayesian scalable precision factor analysis for massive sparse gaussian graphical models’. [arXiv:2107.11316](https://arxiv.org/abs/2107.11316). 30
- Chattopadhyay, S., Zhang, A. R. & Dunson, D. B. (2024), ‘Blessing of dimension in Bayesian inference on covariance matrices’. [arXiv:2404.03805](https://arxiv.org/abs/2404.03805). 30
- Chen, Y., Davis, T. A., Hager, W. W. & Rajamanickam, S. (2008), ‘Algorithm 887: CHOLMOD, supernodal sparse Cholesky factorization and update/downdate’, *ACM Trans. Math. Softw.* **35**(3). [doi:10.1145/1391989.1391995](https://doi.org/10.1145/1391989.1391995). 46
- Dagum, L. & Menon, R. (1998), ‘OpenMP: an industry standard api for shared-memory programming’, *Computational Science & Engineering, IEEE* **5**(1), 46–55. 54
- Datta, A., Banerjee, S., Finley, A. O. & Gelfand, A. E. (2016), ‘Hierarchical nearest-

- neighbor Gaussian process models for large geostatistical datasets’, *Journal of the American Statistical Association* **111**, 800–812. doi:10.1080/01621459.2015.1044091. 7, 19
- De Iaco, S., Palma, M. & Posa, D. (2019), ‘Choosing suitable linear coregionalization models for spatio-temporal data’, *Stochastic Environmental Research and Risk Assessment* **33**, 1419–1434. doi:10.1007/s00477-019-01701-2. 3
- Dey, D., Datta, A. & Banerjee, S. (2022), ‘Graphical Gaussian process models for highly multivariate spatial data’, *Biometrika* **109**(4), 993–1014. doi:doi.org/10.1093/biomet/asab061. 5
- Eddelbuettel, D. & Sanderson, C. (2014), ‘RcppArmadillo: Accelerating R with high-performance C++ linear algebra’, *Computational Statistics and Data Analysis* **71**, 1054–1063. doi:10.1016/j.csda.2013.02.005. 53
- Emery, X., Porcu, E. & White, P. (2022), ‘New validity conditions for the multivariate Matérn coregionalization model, with an application to exploration geochemistry’, *Mathematical Geosciences* **54**(6), 1043–1068. 4, 22, 29, 39, 43
- Fahmy, Y. & Guinness, J. (2022), ‘Vecchia approximations and optimization for multivariate Matérn models’, *Journal of Data Science* **20**(4), 475–492. doi:10.6339/22-JDS1074. 22
- Finazzi, F. & Fassò, A. (2014), ‘D-STEM: A software for the analysis and mapping of environmental space-time variables’, *Journal of Statistical Software* **62**(6), 1–29. doi:10.18637/jss.v062.i06. 3
- Finley, A. O., Banerjee, S. & E.Gelfand, A. (2015), ‘spBayes for large univariate and mul-



- tivariate point-referenced spatio-temporal data models', *Journal of Statistical Software* **63**(13), 1–28. doi:[10.18637/jss.v063.i13](https://doi.org/10.18637/jss.v063.i13). 3
- Finley, A. O., Banerjee, S., Ek, A. R. & McRoberts, R. E. (2008), 'Bayesian multivariate process modeling for prediction of forest attributes', *Journal of Agricultural, Biological, and Environmental Statistics* **13**, 60. doi:[10.1198/108571108X273160](https://doi.org/10.1198/108571108X273160). 3
- Finley, A. O., Datta, A. & Banerjee, S. (2020), 'R package for nearest neighbor Gaussian process models'. [arXiv:2001.09111](https://arxiv.org/abs/2001.09111). 26
- Finley, A. O., Datta, A., Cook, B. D., Morton, D. C., Andersen, H. E. & Banerjee, S. (2019), 'Efficient algorithms for Bayesian nearest neighbor Gaussian processes', *Journal of Computational and Graphical Statistics* **28**, 401–414. doi:[10.1080/10618600.2018.1537924](https://doi.org/10.1080/10618600.2018.1537924). 4
- Finley, A. O., Sang, H., Banerjee, S. & Gelfand, A. E. (2009), 'Improving the performance of predictive process modeling for large datasets', *Computational Statistics and Data Analysis* **53**, 2873–2884. doi:[10.1016/j.csda.2008.09.008](https://doi.org/10.1016/j.csda.2008.09.008). 7
- Fricker, T. E., Oakley, J. E. & Urban, N. M. (2013), 'Multivariate Gaussian process emulators with nonseparable covariance structures', *Technometrics* **55**(1), 47–56. 3
- Gaspari, G. & Cohn, S. E. (1999), 'Construction of correlation functions in two and three dimensions', *Quarterly Journal of the Royal Meteorological Society* **125**(554), 723–757. doi:[10.1002/qj.4971255417](https://doi.org/10.1002/qj.4971255417). 5
- Gelfand, A. E., Kim, H. J., Sirmans, C. F. & Banerjee, S. (2003), 'Spatial modeling with spatially varying coefficient processes', *Journal of the American Statistical Association* **98**(462), 387–396. doi:[10.1198/016214503000170](https://doi.org/10.1198/016214503000170). 3

- Gelfand, A., Schmidt, A., Banerjee, S. & Sirmans, C. F. (2004), ‘Nonstationary multivariate process modeling through spatially varying coregionalization’, *Test* **13**(2), 263–312. [doi:10.1007/BF02595775](https://doi.org/10.1007/BF02595775). 3
- Genton, M. G. & Kleiber, W. (2015), ‘Cross-covariance functions for multivariate geostatistics’, *Statistical Science* **30**, 147–163. [doi:10.1214/14-STS487](https://doi.org/10.1214/14-STS487). 3, 4, 34
- Girolami, M. & Calderhead, B. (2011), ‘Riemann manifold Langevin and Hamiltonian Monte Carlo methods’, *Journal of the Royal Statistical Society: Series B* **73**(2), 123–214. [doi:10.1111/j.1467-9868.2010.00765.x](https://doi.org/10.1111/j.1467-9868.2010.00765.x). 15
- Gneiting, T., Kleiber, W. & Schlather, M. (2010), ‘Matérn cross-covariance functions for multivariate random fields’, *Journal of the American Statistical Association* **105**(491), 1167–1177. [doi:10.1198/jasa.2010.tm09420](https://doi.org/10.1198/jasa.2010.tm09420). 4, 6, 22, 39
- Heaton, M. J., Datta, A., Finley, A. O., Furrer, R., Guinness, J., Guhaniyogi, R., Gerber, F., Gramacy, R. B., Hammerling, D., Katzfuss, M., Lindgren, F., Nychka, D. W., Sun, F. & Zammit-Mangion, A. (2019), ‘A case study competition among methods for analyzing large spatial data’, *Journal of Agricultural, Biological and Environmental Statistics* **24**(3), 398–425. [doi:10.1007/s13253-018-00348-w](https://doi.org/10.1007/s13253-018-00348-w). 7
- Intel Corporation (2024), *Intel Math Kernel Library*. Version 2024-2, Software available at <https://software.intel.com/content/www/us/en/develop/tools/math-kernel-library.html>. 54
- Jin, B., Peruzzi, M. & Dunson, D. B. (2024), ‘Bag of DAGs: Inferring directional dependence in spatiotemporal processes’. [arXiv:2112.11870](https://arxiv.org/abs/2112.11870). 19
- Katzfuss, M. (2017), ‘A multi-resolution approximation for massive spatial datasets’, *Journal of the American Statistical Association* **112**, 201–214. [doi:10.1080/01621459.2015.1123632](https://doi.org/10.1080/01621459.2015.1123632). 7

- Katzfuss, M. & Gong, W. (2019), ‘A class of multi-resolution approximations for large spatial datasets’, *Statistica Sinica* **30**, 2203–2226. doi:10.5705/ss.202018.0285. 7
- Katzfuss, M. & Guinness, J. (2021), ‘A general framework for Vecchia approximations of Gaussian processes’, *Statistical Science* **36**(1), 124–141. doi:10.1214/19-STS755. 19
- Kleiber, W. (2017), ‘Coherence for multivariate random fields’, *Statistica Sinica* **27**(4), 1675–1697. doi:10.5705/ss.202015.0309. 43
- Krainski, E. T., Gómez-Rubio, V., Bakka, H., Lenzi, A., Castro-Camilo, D., Simpson, D., Lindgren, F. & Rue, H. (2019), *Advanced Spatial Modeling with Stochastic Partial Differential Equations Using R and INLA*, Chapman & Hall/CRC Press, Boca Raton, FL. 3
- Li, X. S. (2005), ‘An overview of SuperLU: Algorithms, implementation, and user interface’, *ACM Transactions on Mathematical Software* **31**(3), 302–325. 54
- Liu, H., Ding, J., Xie, X., Jiang, X., Zhao, Y. & Wang, X. (2022), ‘Scalable multi-task Gaussian processes with neural embedding of coregionalization’, *Knowledge-Based Systems* **247**, 108775. doi:10.1016/j.knosys.2022.108775.  
**URL:** <https://www.sciencedirect.com/science/article/pii/S0950705122003641> 3
- Majumdar, A. & Gelfand, A. E. (2007), ‘Multivariate spatial modeling for geostatistical data using convolved covariance functions’, *Mathematical Geology* **39**(2), 225–245. doi:10.1007/s11004-006-9072-6. 5
- Matheron, G. (1982), ‘Pour une analyse krigéante des données régionalisées’, *Technical report N.732, Centre de Géostatistique* . 3

- Moreno-Muñoz, P., Artés, A. & Álvarez, M. (2018), Heterogeneous multi-output gaussian process prediction, *in* S. Bengio, H. Wallach, H. Larochelle, K. Grauman, N. Cesa-Bianchi & R. Garnett, eds, ‘Advances in Neural Information Processing Systems’, Vol. 31, Curran Associates, Inc. [https://proceedings.neurips.cc/paper\\_files/paper/2018/file/165a59f7cf3b5c4396ba65953d679f17-Paper.pdf](https://proceedings.neurips.cc/paper_files/paper/2018/file/165a59f7cf3b5c4396ba65953d679f17-Paper.pdf). 3
- Nishimura, A. & Suchard, M. A. (2023), ‘Prior-preconditioned conjugate gradient method for accelerated Gibbs sampling in “large n, large p” Bayesian sparse regression’, *Journal of the American Statistical Association* **118**(544), 2468–2481. [doi:10.1080/01621459.2022.2057859](https://doi.org/10.1080/01621459.2022.2057859). 46
- Pebesma, E. J. (2004), ‘Multivariable geostatistics in S: the gstat package’, *Computers & Geosciences* **30**(7), 683–691. 3
- Peruzzi, M. (2022), *meshed: Bayesian Regression with Meshed Gaussian Processes*. R package.  
**URL:** <https://CRAN.R-project.org/package=meshed> 3, 22
- Peruzzi, M., Banerjee, S., Dunson, D. B. & Finley, A. O. (2021), ‘Grid-Parametrize-Split (GriPS) for improved scalable inference in spatial big data analysis’. [arXiv:2101.03579](https://arxiv.org/abs/2101.03579). 4, 45
- Peruzzi, M., Banerjee, S. & Finley, A. O. (2022), ‘Highly scalable Bayesian geostatistical modeling via meshed Gaussian processes on partitioned domains’, *Journal of the American Statistical Association* **117**(538), 969–982. [doi:10.1080/01621459.2020.1833889](https://doi.org/10.1080/01621459.2020.1833889). 7, 19
- Peruzzi, M. & Dunson, D. B. (2022), ‘Spatial multivariate trees for big data Bayesian regression’, *Journal of Machine Learning Research* **23**(17), 1–40. <http://jmlr.org/papers/v23/20-1361.html>. 5

- Peruzzi, M. & Dunson, D. B. (2024), ‘Spatial meshing for general Bayesian multivariate models’, *Journal of Machine Learning Research* **25**(87), 1–49. <http://jmlr.org/papers/v25/22-0083.html>. 3, 15
- Polson, N. G., Scott, J. G. & Windle, J. (2013), ‘Bayesian inference for logistic models using Polya-Gamma latent variables’, *Journal of the American Statistical Association* **108**, 1339–1349. [doi:10.1080/01621459.2013.829001](https://doi.org/10.1080/01621459.2013.829001). 15
- Quiroz, Z. C., Prates, M. O., Dey, D. K. & Rue, H. (2021), ‘Fast Bayesian inference of block nearest neighbor Gaussian process for large data’. [arXiv:1604.08403](https://arxiv.org/abs/1604.08403). 7
- Reich, B. J., Fuentes, M., Herring, A. H. & Evenson, K. R. (2010), ‘Bayesian variable selection for multivariate spatially varying coefficient regression’, *Biometrics* **66**(3), 772–782. [doi:10.1111/j.1541-0420.2009.01333.x](https://doi.org/10.1111/j.1541-0420.2009.01333.x). 3
- Sampson, P. D. & Guttorp, P. (1992), ‘Nonparametric estimation of nonstationary spatial covariance structure’, *Journal of the American Statistical Association* **87**(417), 108–119. [doi:10.1080/01621459.1992.10475181](https://doi.org/10.1080/01621459.1992.10475181). 6, 30
- Sanderson, C. & Curtin, R. (2016), ‘Armadillo: a template-based C++ library for linear algebra’, *Journal of Open Source Software* **1**, 26. 53
- Schmidt, A. M. & Gelfand, A. E. (2003), ‘A Bayesian coregionalization approach for multivariate pollutant data’, *Journal of Geophysical Research* **108**, D24. [doi:10.1029/2002JD002905](https://doi.org/10.1029/2002JD002905). 3, 4
- Schürch, C. M., Bhate, S. S., Barlow, G. L., Phillips, D. J., Noti, L., Zlobec, I., Chu, P., Black, S., Demeter, J., McIlwain, D. R., Kinoshita, S., Samusik, N., Goltsev, Y. & Nolan, G. P. (2020), ‘Coordinated cellular neighborhoods orchestrate antitu-

- moral immunity at the colorectal cancer invasive front’, *Cell* **182**(5), 1341–1359.e19.  
[doi:10.1016/j.cell.2020.07.005](https://doi.org/10.1016/j.cell.2020.07.005). 27
- Schäfer, F., Katzfuss, M. & Owhadi, H. (2024), ‘Sparse Cholesky factorization by Kullback–Leibler minimization’, *SIAM Journal on Scientific Computing*. [doi:10.1137/20M1336254](https://doi.org/10.1137/20M1336254).  
7
- Shirota, S., Finley, A. O., Cook, B. D. & Banerjee, S. (2019), ‘Conjugate nearest neighbor Gaussian process models for efficient statistical interpolation of large spatial data’.  
[arXiv:1907.10109](https://arxiv.org/abs/1907.10109). 7, 21
- Stein, M. (1990), ‘Uniform asymptotic optimality of linear predictions of a random field using an incorrect second-order structure’, *The Annals of Statistics* **18**(2), 850–872.  
[doi:10.1214/aos/1176347629](https://doi.org/10.1214/aos/1176347629). 4
- Stein, M. L., Chi, Z. & Welty, L. J. (2004), ‘Approximating likelihoods for large spatial data sets’, *Journal of the Royal Statistical Society, Series B* **66**, 275–296.  
[doi:10.1046/j.1369-7412.2003.05512.x](https://doi.org/10.1046/j.1369-7412.2003.05512.x). 19
- Taylor-Rodriguez, D., Finley, A. O., Datta, A., Babcock, C., Andersen, H. E., Cook, B. D., Morton, D. C. & Banerjee, S. (2019), ‘Spatial factor models for high-dimensional and large spatial data: An application in forest variable mapping’, *Statistica Sinica* **29**(3), 1155–1180. [doi:10.5705/ss.202018.0005](https://doi.org/10.5705/ss.202018.0005). 3
- Teh, Y. W., Seeger, M. & Jordan, M. I. (2005), Semiparametric latent factor models, *in* R. G. Cowell & Z. Ghahramani, eds, ‘Proceedings of the Tenth International Workshop on Artificial Intelligence and Statistics’, Society for Artificial Intelligence and Statistics, pp. 333–340. <http://proceedings.mlr.press/r5/teh05a/teh05a.pdf>. 3

- Tikhonov, G., Opedal, O. H., Abrego, N., Lehtikoinen, A., de Jonge, M. M. J., Oksanen, J. & Ovaskainen, O. (2020), ‘Joint species distribution modelling with the R-package hmsc’, *Methods in Ecology and Evolution* **11**(3), 442–447. doi:10.1111/2041-210X.13345. 3
- Townes, F. W. & Engelhardt, B. E. (2023), ‘Nonnegative spatial factorization applied to spatial genomics’, *Nature Methods* **20**, 229–238. doi:10.1038/s41592-022-01687-w. 3
- Vecchia, A. V. (1988), ‘Estimation and model identification for continuous spatial processes’, *Journal of the Royal Statistical Society, Series B* **50**, 297–312. doi:10.1111/j.2517-6161.1988.tb01729.x. 7, 18
- Velandia, D., Bachoc, F., Bevilacqua, M., Gendre, X. & Loubes, J.-M. (2017), ‘Maximum likelihood estimation for a bivariate Gaussian process under fixed domain asymptotics’, *Electronic Journal of Statistics* **11**(2), 2978 – 3007. doi:10.1214/17-EJS1298. 4
- Wackernagel, H. (2003), *Multivariate Geostatistics: An Introduction with Applications*, Springer, Berlin. doi:10.1007/978-3-662-05294-5. 3
- Yarger, D., Stoev, S. & Hsing, T. (2024), ‘Multivariate Matérn models – a spectral approach’. arXiv:2309.02584. 4
- Zhang, H. (2004), ‘Inconsistent estimation and asymptotically equal interpolations in model-based geostatistics’, *Journal of the American Statistical Association* **99**(465), 250–261. doi:10.1198/016214504000000241. 4
- Zhang, H. (2007), ‘Environmetrics’, *Environmetrics* **18**(2), 125–139. doi:10.1002/env.807. 4
- Zhang, L. & Banerjee, S. (2022), ‘Spatial factor modeling: A Bayesian matrix-normal

approach for misaligned data', *Biometrics* **78**(2), 560–573. doi:[10.1111/biom.13452](https://doi.org/10.1111/biom.13452). 3, 21

Zhang, L., Banerjee, S. & Finley, A. O. (2021), 'High-dimensional multivariate geostatistics: A bayesian matrix-normal approach', *Environmetrics* **32**(4), e2675. doi:[10.1002/env.2675](https://doi.org/10.1002/env.2675). 21

Zhang, X. (2020), *An Optimized BLAS Library Based on GotoBLAS2*.

**URL:** <https://github.com/xianyi/OpenBLAS/> 54

Zheng, X., Kottas, A. & Sansó, B. (2023), 'Nearest-neighbor mixture models for non-Gaussian spatial processes', *Bayesian Analysis* **18**(4), 1191–1222. doi:[10.1214/23-BA1405](https://doi.org/10.1214/23-BA1405). 19

Zhu, Y., Peruzzi, M., Li, C. & Dunson, D. B. (2024), 'Radial neighbours for provably accurate scalable approximations of Gaussian processes', *Biometrika* . doi:[10.1093/biomet/asae029](https://doi.org/10.1093/biomet/asae029). 7, 52